

INFORMATION TO USERS

This dissertation was produced from a microfilm copy of the original document. While the most advanced technological means to photograph and reproduce this document have been used, the quality is heavily dependent upon the quality of the original submitted.

The following explanation of techniques is provided to help you understand markings or patterns which may appear on this reproduction.

1. The sign or "target" for pages apparently lacking from the document photographed is "Missing Page(s)". If it was possible to obtain the missing page(s) or section, they are spliced into the film along with adjacent pages. This may have necessitated cutting thru an image and duplicating adjacent pages to insure you complete continuity.
2. When an image on the film is obliterated with a large round black mark, it is an indication that the photographer suspected that the copy may have moved during exposure and thus cause a blurred image. You will find a good image of the page in the adjacent frame.
3. When a map, drawing or chart, etc., was part of the material being photographed the photographer followed a definite method in "sectioning" the material. It is customary to begin photoing at the upper left hand corner of a large sheet and to continue photoing from left to right in equal sections with a small overlap. If necessary, sectioning is continued again – beginning below the first row and continuing on until complete.
4. The majority of users indicate that the textual content is of greatest value, however, a somewhat higher quality reproduction could be made from "photographs" if essential to the understanding of the dissertation. Silver prints of "photographs" may be ordered at additional charge by writing the Order Department, giving the catalog number, title, author and specific pages you wish reproduced.

University Microfilms

300 North Zeeb Road
Ann Arbor, Michigan 48106
A Xerox Education Company

73-4951

MICKISH, Roger Alan, 1945-
ELECTRON IMPACT EXCITATION AND COLLISIONAL
PERTURBATION STUDIES IN HYDROGEN.

The University of Oklahoma, Ph.D., 1972
Physics, general

University Microfilms, A XEROX Company, Ann Arbor, Michigan

© 1972

ROGER ALAN MICKISH

ALL RIGHTS RESERVED

THE UNIVERSITY OF OKLAHOMA

GRADUATE COLLEGE

ELECTRON IMPACT EXCITATION AND COLLISIONAL
PERTURBATION STUDIES IN HYDROGEN

A DISSERTATION

SUBMITTED TO THE GRADUATE FACULTY

in partial fulfillment of the requirements for the

degree of

DOCTOR OF PHILOSOPHY

By

ROGER ALAN MICKISH

Norman, Oklahoma

1972

ELECTRON IMPACT EXCITATION AND COLLISIONAL
PERTURBATION STUDIES IN HYDROGEN

APPROVED BY

Robert M. St. John

S. E. Babh Jr.

R. G. Fowler

William N. Huff

Dennis Slay

DISSERTATION COMMITTEE

PLEASE NOTE:

Some pages may have

indistinct print.

Filmed as received.

University Microfilms, A Xerox Education Company

ACKNOWLEDGMENTS

I would like to express my appreciation to the entire faculty and staff of the Physics Department at the University of Oklahoma. Special thanks goes to fellow researchers, Max Lake, Bob Twist, and Jack Martin, and especially Carl Bush. Without their support, this work would have never been completed. Others to whom I am indebted are Mary Lou Stokes, Gene Scott, Cleve Christian and Woody Porter.

There is no adequate way to thank Ron Stermer for the many times he patiently reconstructed the glassware of the flow system after numerous breakdowns.

This research has been conducted under the direction of Dr. Robert M. St. John, to whom I am deeply indebted for his support and for use of his excellent research facilities.

Appreciation is expressed for the financial support of the Air Force Office of Scientific Research, and for the support and interest of Dr. Ralph E. Kelley, Scientific Advisor for that Agency.

Finally, I would like to thank my parents and wife, Andrea and her parents who helped immensely throughout this effort. Andrea's encouragement, understanding, and help have been invaluable. The successful conclusion of this work is as much a result of her efforts as mine.

TABLE OF CONTENTS

ACKNOWLEDGMENTS	iii
LIST OF TABLES.	
LIST OF ILLUSTRATIONS	
Chapter	
I. INTRODUCTION.	1
II. HYDROGEN BALMER STUDIES IN A STATIC SYSTEM.	6
Introduction.	6
Experimental Procedure.	7
Calculations.	15
Optical Cross Sections	15
Excited Atom-Atom (Molecule) Collisions.	20
Excited Atom-Electron Collisions	26
Excited Atom-Ion Collisions.	27
Electron Gun Characteristics	30
Discussion of H_{α} and H_{β} Optical Cross Sections from Electron- H_2 Collisions	33
III. THEORY OF HYDROGEN BALMER STUDIES IN A FLOW SYSTEM.	42
Background.	42
The Degeneracy Problem.	42
Defining the Electron Impact Cross Sections for A Single Level	45
Hydrogen Balmer Crossed Beam Cross Section Measurement.	48
Theoretical Calculations.	54
IV. HYDROGEN BALMER STUDIES IN A FLOW SYSTEM.	60
Introduction.	60
Basic Considerations in Atomic Hydrogen Measurement	61
Molecular Hydrogen Studies.	78
Experimental Apparatus.	82
Atomic Hydrogen Cross Sections.	90
Molecular Nitrogen Excitation Functions	95

TABLE OF CONTENTS (Cont'd.)

Chapter	Page
V. LIFETIME MEASURING SYSTEM	98
Introduction.	98
The Basic System.	98
BIBLIOGRAPHY.	104
APPENDIX I.	108

LIST OF TABLES

Table	Page
1. Hydrogen Balmer Absolute Excitation Cross Sections by Electron-H ₂ Molecule Collisions.	18
2. Typical Values of Balmer Optical Cross Sections and the Measureable Parameters of the Collision Chamber, Light Detection and Processing Equipment, and Standardization System	19
3. A Table of Values for the Critical Pressure n_0 , the Experimentally Determined Lifetimes τ of the Relevant Excited Balmer States, and Theoretical and Experimental Collisions Cross Sections	24
4. Optical Cross Sections Calculated from the Theoretical Results of Vainshtein Ref. 55, $Q(n\ell \text{ to } 2\ell)10^{-3}\pi a_0^2$. .	56
5. Branching Ratios and Transition Probabilities from Condon and Shortley [50]	59

LIST OF ILLUSTRATIONS

Figure	Page
1. Schematic of the electron gun, light detection and processing equipment. Included are the radius of the electron beam at the collision chamber slit and the radius of the chamber itself. For more details see Walker [15]	8
2. Radiation from the collision chamber was monitored as a function of chamber current at 0.5 mtorr pressure. The non-linearity is a consequence of geometry, ionization energy of the gas and cathode temperature	9
3. An intensity vs pressure curve of H_{β} . The non-linearity occurred at pressures unique to the transitions studied	11
4. Non-linear output of H_{γ} radiation from the collision chamber due to current dependent phenomena.	13
5. Electron gun characteristics composite. The linear regions of radiation intensity I response with current change are shown. The upper limit of linear response at a particular pressure is indicated by a solid line.	14
6. Hydrogen Balmer H_{α} (n=3 to 2) absolute excitation cross section by electron-H molecule collisions.	16
7. Hydrogen Balmer (n=4 to 2) absolute excitation cross section via electron- H_2 molecule collisions	17
8. At low pressures spontaneous emission accounts for essentially all depopulation of the excited state, and emerging radiation changes linearly with pressure.	21
9. At higher pressures an alternate depopulation channel becomes significant. The depopulation channel opened alters the previous scheme and causes non-linear changes in radiation with respect to pressure change.	21
10. The inverse of the experimentally determined collision cross section vs respective principal quantum numbers. This graph indicates $\sigma \propto n^3$ is a good approximation	25

LIST OF ILLUSTRATIONS (Cont'd.)

Figure	Page
11. Potential-energy curves for H_2^- , H_2 and H_2^+	36
12. Potential-energy curves for H_2 and H_2^+ (expanded scale) .	37
13. Optical excitation cross sections of the 4634 Å G to B transition in molecular hydrogen. The upper curve was taken at 9.7 mtorr pressure and the lower was obtained at 30 mtorr pressure	39
14. The three transitions that produce Balmer alpha radiation	44
15. Balmer alpha radiation resulting from three distinct transitions is unresolved in this detection system.	44
16. Theoretical optical cross section components that comprise the Balmer H_α total optical cross section . .	58
17. Theoretical optical cross section components that comprise the Balmer H_β total optical cross section . .	58
18. Theoretical optical cross section components that comprise the Balmer H_γ total optical cross section . .	58
19. Theoretical optical cross section components that comprise the Balmer H_δ total optical cross section . .	58
20. Optical excitation functions of the 4554 Å k to a molecular transition with the Wood tube cathode close to the nozzle arm	63
21. Optical excitation cross sections of the 4634 Å G to B transition in molecular hydrogen. These functions were obtained on the same equipment in the same manner and at the same time as the data reported by Walker in Ref. 14.	66
22. Composite of the flow system electron gun characteristics. The linear regions of radiation intensity I response with current change are shown. The upper limit of linear response at a particular pressure is indicated by a solid line. The dotted vertical lines at the bottom of the graph indicate onset of the excitation at that pressure. ON and OFF refer to the Wood tube ON and OFF	67

LIST OF ILLUSTRATIONS (Cont'd.)

Figure	Page
23. Optical excitation functions change when Wood tube currents change.	69
24. Optical excitation functions change when the pressure is changed.	69
25. Below onset an electron beam of high energy electrons exists in the collision chamber. It produces the non-zero below onset radiation shown. Its intensity is controlled by grid number two.	73
26. Potential was applied to two 3cm long probes in the nozzle arm of the Wood tube. This current vs applied voltage curve resulted.	76
27a. Molecular hydrogen energy level diagram of the singlet spectrum. Data taken from Dickie [62] and Sharp [41].	80
27b. Molecular hydrogen energy level diagram of the triplet spectrum. Data taken from Dickie [62] and Sharp [41].	81
28. Crossed beam flow system	84
29. The time dependence of the H_{β} excitation function with the Wood tube on.	88
30. Molecular hydrogen optical excitation functions.	89
31. Hydrogen Balmer excitation functions	91
32. Comparison of the experimental total Balmer alpha optical cross section with theory	92
33. Comparison of the experimental total Balmer beta optical cross section with theory	92
34. Comparison of the experimental total Balmer gamma optical cross section with theory	92
35. Comparison of the experimental total Balmer delta optical cross section with theory	92

LIST OF ILLUSTRATIONS (Cont'd.)

Figure	Page
36. Cross section ($1s, H_{\alpha}$) of atomic hydrogen as a function of the electron energy (3×rms error plus estimated systematic error). The solid curve represents the theoretical results of Morrison and Rudge [69]. . . .	94
37. The optical excitation cross section for population of the $B^2\Sigma_u^+$ state.	96
38. Schematic of a system to be used for lifetime measurements in the 2000 Å to 7800 Å range	100

CHAPTER I

INTRODUCTION

This work, consisting of two projects, and one literature survey encompasses studies in three active areas of atomic and molecular physics that are closely related. These fields are atomic and molecular lifetimes, electron impact excitation of atoms and molecules, and excited atom perturbations. Results from studies in these areas are important in applied fields such as gas discharge, laser, and atmospheric work besides being necessary for testing and improving existing theories and methods of basic physics. The literature survey was in the area of atomic and molecular lifetimes. It consists only of the design of a system suitable for measuring lifetimes of hydrogen atomic and molecular states.

In the last few years much progress has been made in lifetime studies. See, for example, Ref. 1. There are a number of methods employed. At the University of Oklahoma a hot hollow cathode arrangement with a pulsed positive grid nestled within is used as an excitation source. A square wave voltage pulse is applied and the radiation decay after the pulse cutoff reveals information about the lifetime of the states from which the radiation originates.

Holzberlein [2], Johnson [3], Copeland [4], Schaefer [5], Skwerski [6], Mickish [7] and Thompson [8] have elaborated on the techniques involved in degree publications monitored by R. G. Fowler.

The reader is referred to these sources for details.

Another method is to modulate an electron beam of a mono-energetic electron gun by a square voltage pulse on one of the plates to produce an excitation source. Lawrence [9] and Weaver and Hughes [10] have used this method to study lifetimes. We initially hoped to set up a lifetime system using an electron gun ourselves; however, we ran into financial difficulties and had to abandon the project at least for the present. To help those who eventually pursue this goal, a state of the art system planned for our work is described in Chapter V.

Experimental measurements of electron impact excitation cross sections to upper levels in hydrogen by electron-H atom collisions has proved to be very difficult. In a review article on electron impact excitation of atoms, Moiseiwitsch and Smith [11] discuss the difficulties of measuring electron impact on atomic hydrogen cross sections. They suggest that the biggest problem has been obtaining sufficiently large density of hydrogen atoms to bombard with electrons. Progress in this area has been difficult and time consuming. As a result only a few excitation measurements have appeared. They go on to discuss these measurements often praising the investigators for their efforts. However, the problems have been so great and often so overwhelming that they conclude:

"There remains a need for additional work to confirm the measurements now in the literature, and to extend the range of information available. There is also a need for more detailed and quantitative treatment of errors, so the limitations of a given measurement are well defined. A measurement is complete only if the reliability and accuracy of the results are stated quantitatively. Systematic geometrical and physical errors should be identified and evaluated. The statistical errors should be treated separately in well defined terms. The statement of a statistically determined

probable error coupled with quantitative estimates of the magnitudes of systematic errors is valuable. A presentation of error bars two or three times the statistical probable error in the expectation that it covers a host of vaguely defined systematic effects provides little information.

There have been no accurate absolute measurements of hydrogen atom excitation cross sections."

Thus, in spite of the fact that excitation of atomic hydrogen has received much attention by theoretical physicists due to its relative simplicity, little is really known experimentally. With this in mind, James D. Walker, Jr. initiated research five years ago in this direction under the guidance of his advising professor Robert M. St. John. These initial efforts are reported in Walker's Ph.D. dissertation [12]. Setting up the system proved to be very difficult. A couple of atomic hydrogen sources were tried without success. Then finally Walker hit on a slightly modified design of the Wood tube (glow discharge) that produced what he considered as an adequate atomic hydrogen density. He then crossed the gas flowing from the wood tube with an electron beam from an electron gun much the same way as Ornstein and Lindeman did in an earlier experiment [13].

In his initial attempt to obtain atomic hydrogen Balmer electron impact cross sections Walker reported [12] the electron gun would not work for low voltage electrons. Thus, his dissertation contained only the high energy portions of what he considered the cross Balmer sections. But due to the malfunctioning electron gun and possibly other effects, these cross sections rate a low confidence level.

In a second effort Walker made major changes in the hydrogen flow system in an attempt to eliminate back streaming of diffusion pump

oil. The changes he made will be discussed further in Chapter IV. With this second system Walker reported obtaining atomic H_{α} , H_{β} , H_{γ} , H_{δ} , and H_{ϵ} optical excitation functions from 0--450 eV [14]. Since then, it was decided that further work should be carried out to determine better the limitations of the experiment and to obtain a more accurate knowledge of the errors described by Moiseiwitsch and Smith [11]. The other two projects reported herein are an attempt to determine these errors and limitations.

In the first experiment we set out to measure the effect of electron beam current and pressure on excited Balmer-radiating hydrogen atoms that were created by electron- H_2 molecule collision. We carried out this experiment on a proven static system used by K. Walker [15]. This work is reported in Chapter II.

In the second experiment we set out to measure any effect the Wood tube discharge might have on the hydrogen Balmer excitation functions obtained using the flow system and also check the pressure dependence of radiating hydrogen atoms in hydrogen gas. These and other efforts are reported in Chapter IV.

Absolute standardization of cross sections is the ultimate objective of our lab. For the past ten years, a number of graduate students along with their director, Robert M. St. John, have firmly established a standardization procedure here at the University of Oklahoma. In the past, dissertations contained derivations of the standardization formulation. The interested reader is referred to the excellent presentation of Sharpton [16] for this information.

In Chapter III, the mathematical procedure behind extracting

hydrogen Balmer-optical excitation cross sections from the flow system is presented. The important parameters are discussed and elaborated on. Although investigation of the hydrogen molecule was not a primary goal, we had to work with it a good deal. Information about the molecule resulting from this work is concentrated in Chapter II and IV.

CHAPTER II

HYDROGEN BALMER STUDIES IN A STATIC SYSTEM

Introduction

Discrepancies exist in the shape and absolute values of pioneer and recent experimental hydrogen Balmer optical excitation cross sections obtained from electron-H₂ molecule collisions [10, 12, 17-22]. These discrepancies are a consequence of such phenomena as excited atom-molecule collisions, excited atom-ion collisions, impurity and molecular background, properties of the electron gun, and standardization procedures.

The excitation cross sections measured and reported herein result from observations made at an angle of 90° relative to the electron beam. These are classified as optical cross sections and differ from level cross sections. The latter are obtained from the former by taking into consideration (a) cascade into the level from higher states, (b) the availability of several channels from radiative decay, and (c) the anisotropic property of the radiation pattern.

A conventional electron gun [23], high vacuum system, and data acquisition system [24] were used to determine experimental conditions that perturbed hydrogen Balmer radiating atoms in the collision chamber. Then, operating under conditions absent of significant perturbation, the absolute excitation cross sections of H_α and H_β due to electron-H₂ molecule collisions were obtained. In this paper we will compare these

cross sections to the results obtained in other laboratories. In addition, order of magnitude calculations will be carried out to show that excited atom-H₂ molecule collision cross sections for these lines are possibly as large as 10^{-13}cm^2 and possibly proportional to n^3 , where n is the principal quantum number of the corresponding Balmer transition. Also, significant excited atom-ion perturbations occur only at relatively high pressures and current densities.

Experimental Procedure

The apparatus used in this investigation is discussed elsewhere [15,25,26] and shown in Fig. 1. The electron gun and its supporting system are shown with the radiation detection and recording system. Important parameters measured in the experiment are indicated by the symbols representing them. These symbols I_{CC} , I_e , and D_{CC} stand for the current in the photomultiplier tube caused by the radiation from the collision chamber, the magnitude of the electron current that passes through the first four grids and into the collision chamber, and the diameter of the stop of the lens, respectively. These measurements and parameters will be discussed and applied below.

A detailed study of the radiation emerging from the collision chamber as a function of pressure and electron density was carried out on H_α , H_β , H_γ , H_δ and the $4634\text{\AA } 3d\sigma G^1\Sigma_g^+ \rightarrow 2p\sigma B^1\Sigma_u^+$ molecule transition. First, the pressure monitored by an MKS Baratron type 90 capacitance manometer, was set at 0.50 mtorr. At this pressure an intensity vs. current curve was run, and the current at which the radiation emitted became non-linear, if at all, was noted. Figure 2 illustrates this type observation. Although it might seem that the non-linearity of

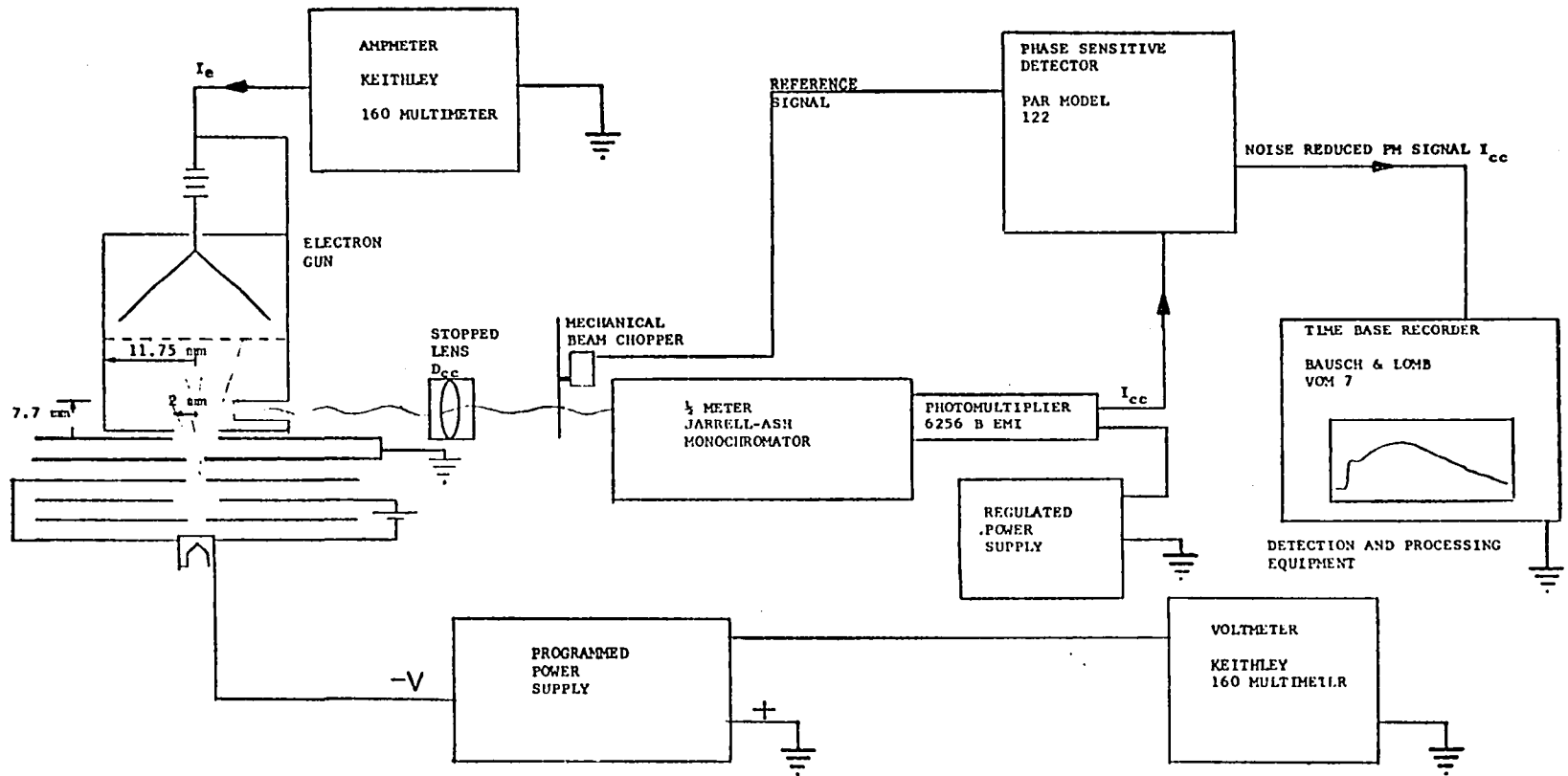


Figure 1. Schematic of the electron gun, light detection and processing equipment. Included are the radius of the electron beam at the collision chamber slit and the radius of the chamber itself. For more details see Walker.¹⁵

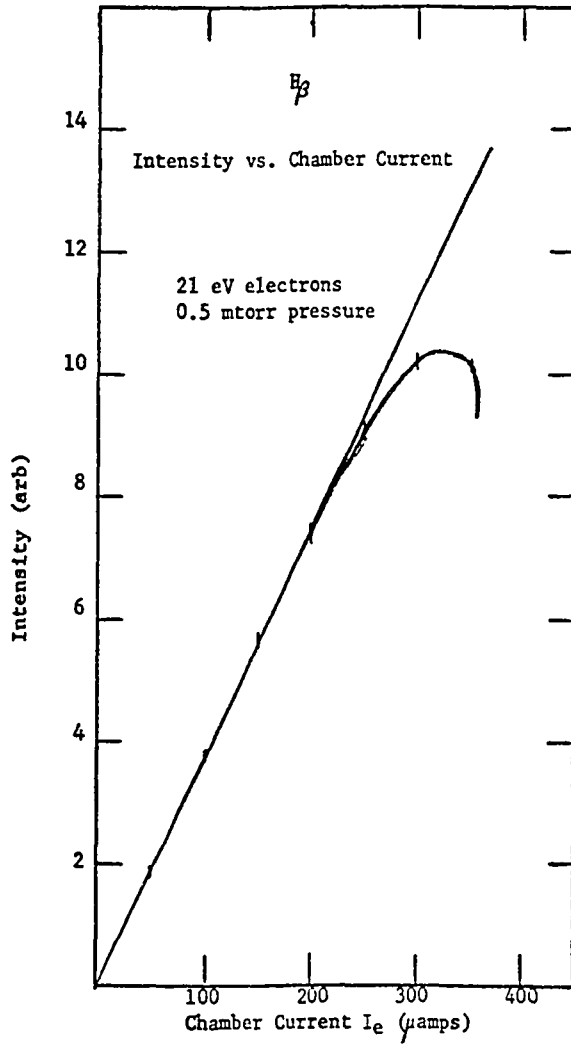


Figure 2. Radiation from the collision chamber was monitored as a function of chamber current at 0.5 mtorr pressure. The non-linearity is a consequence of geometry, ionization energy of the gas and cathode temperature.

this curve was due to the electric field of the electron beam, we found that as the pressure in the chamber was increased, or the electron energy was increased, the intensity vs. current curve remained linear to the limit of the electron gun current of 1 ma. We thus attribute the non-linearity shown in Fig. 2 to the geometry of the gun and the interaction of electrons at or before the virtual cathode.

Next, with a variation in reproducibility ranging from approximately 10% for H_{α} to 50% for H_{δ} we found that a non-linearity appears in the intensity vs pressure curve at a pressure unique to each transition studied and independent of electron energy 35 to 500 eV and current density. Figure 3 illustrates this for the H_{β} transition. The currents were taken from the linear regions of curves such as that in Fig. 2. The critical pressures, where non-linearity begins, were found to be 5.25 ± 0.5 , 4.00 ± 0.4 , 1.10 ± 0.30 , 0.35 ± 0.15 and 10.0 ± 1.0 mtorr for H_{α} (n=3 to 2), H_{β} (n=4 to 2), H_{γ} (n=5 to 2), H_{δ} (n=6 to 20), and the H_2 4634 Å G to B transition respectively.

A final experiment was performed to check again for current dependence. We monitored the radiation of each of the transitions at a pressure of 10 mtorr and plotted intensity vs current for 100 eV electrons. As expected, in every case the light emitted was linear with respect to current to the current limit of the electron gun. This linearity with current indicates that the pressure induced non-linearity is due to collisions of the excited atoms with molecules and not with ions or electrons. Collisions of excited atoms with molecules is the source of collision broadening of spectral lines.

Ionic interactions should definitely be a function of the electron beam current. Such a current dependence appears in our studies at higher

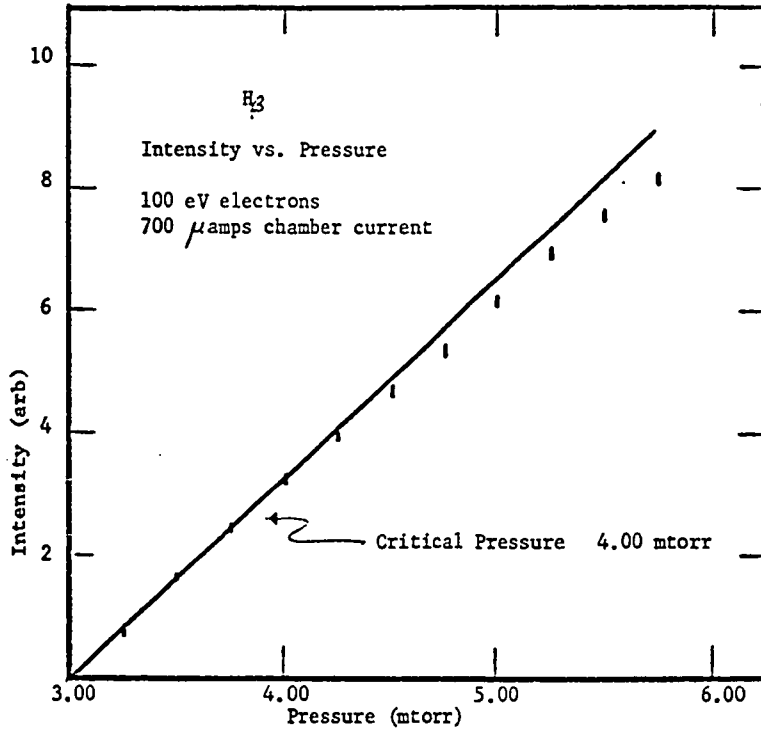


Figure 3. An Intensity vs. Pressure curve of H_3 . The non-linearity occurred at pressures unique to the transitions studied.

pressures. For example, the chamber pressure was set at 100 mtorr and the electron energy at 100 eV while H_γ radiation was monitored as a function of current. The results plotted in Fig. 4 show the non-linearity occurring at an electron beam current of approximately 400 μ A. We feel that this perturbation could possibly be due to collisions of excited atoms with positive ions or to the geometry of the electron gun and the interaction of electrons at or before the virtual cathode. The arguments against excited atom-electron collisions are given below.

Figure 5 is a composite of regions of linear emission of radiation from the excitation chamber as a function of electron energy, electron current, and gas pressure. Similar composites occur for other gases. The composite for a given gas differs with the operating temperature of the cathode. A variation in the cathode temperature will also shift onset voltages and change shapes of the onset portions of the excitation functions acquired while working in the linear regions of Fig. 5. Thus, we find that for this electron gun the onset portion of the excitation functions is sensitive to electron current, geometry, and cathode temperature. The difference between electron gun determined onset voltage and the spectroscopically determined value is termed the potential shift of the electron gun and will be discussed in detail in Chapter IV. As the cathode temperature is increased the potential shift decreases. Its observed value for Balmer excitation functions usually less than 3 eV.

The absolute hydrogen Balmer H_α and H_β optical excitation cross sections due to electron- H_2 molecule collisions were obtained under

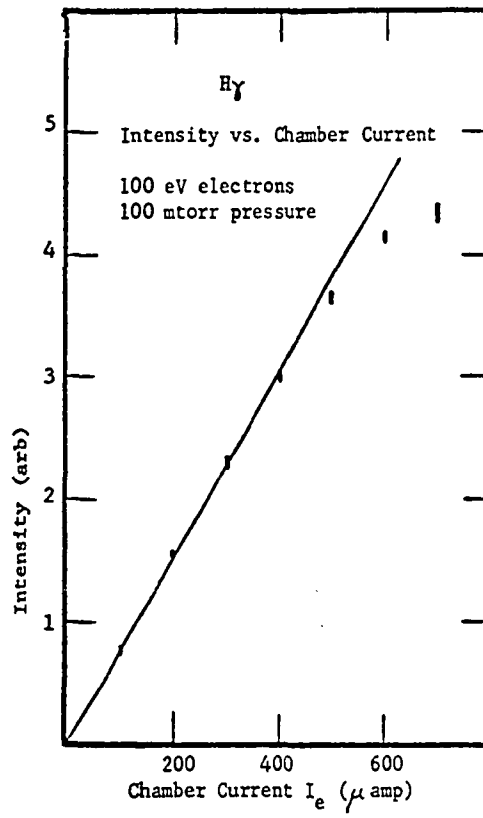
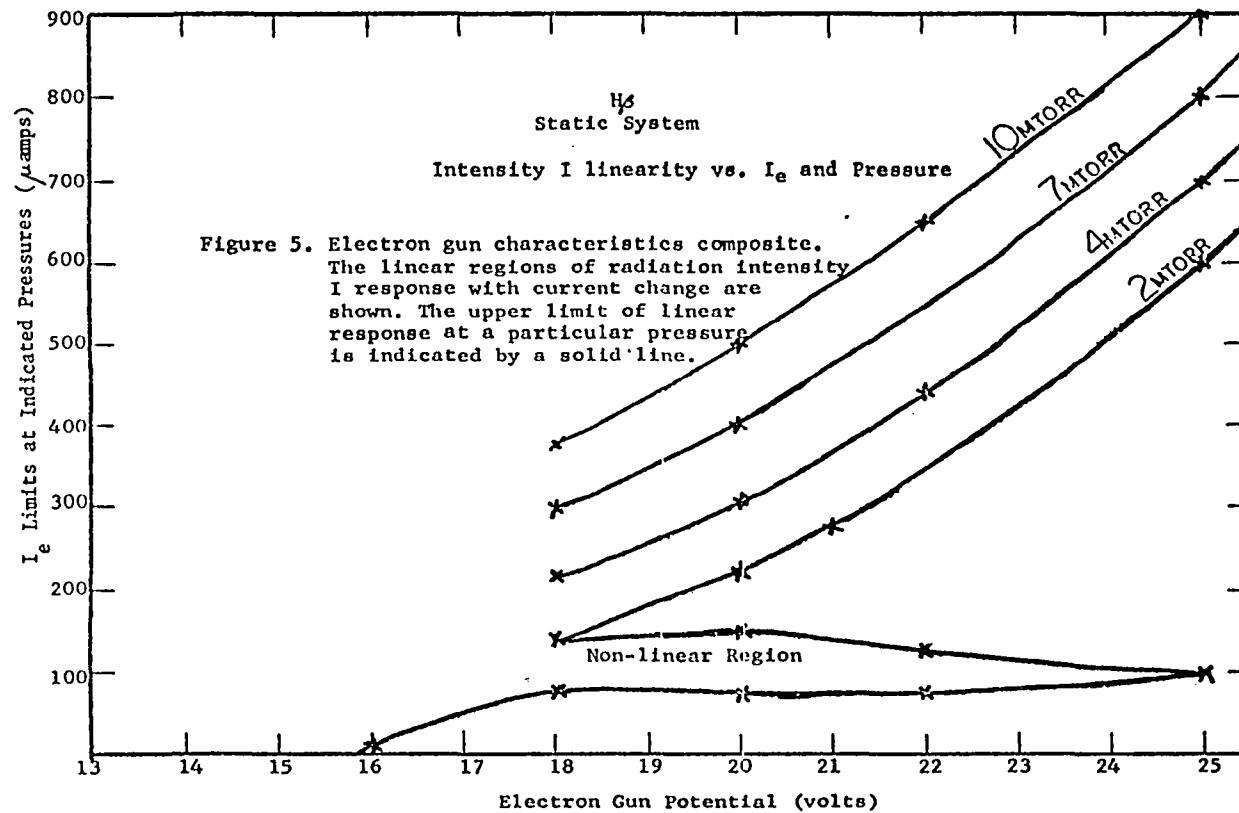


Figure 4. Non-linear output of H γ radiation from the collision chamber due to current dependent phenomena.



linear current conditions and at the critical pressures discussed above in order to avoid significant excited atom-molecule interactions. The absolute calibration of these cross sections were performed as described in other papers [25,27] and below. These functions appear in Figs. 6 and 7. In Table 1 numerical values are presented.

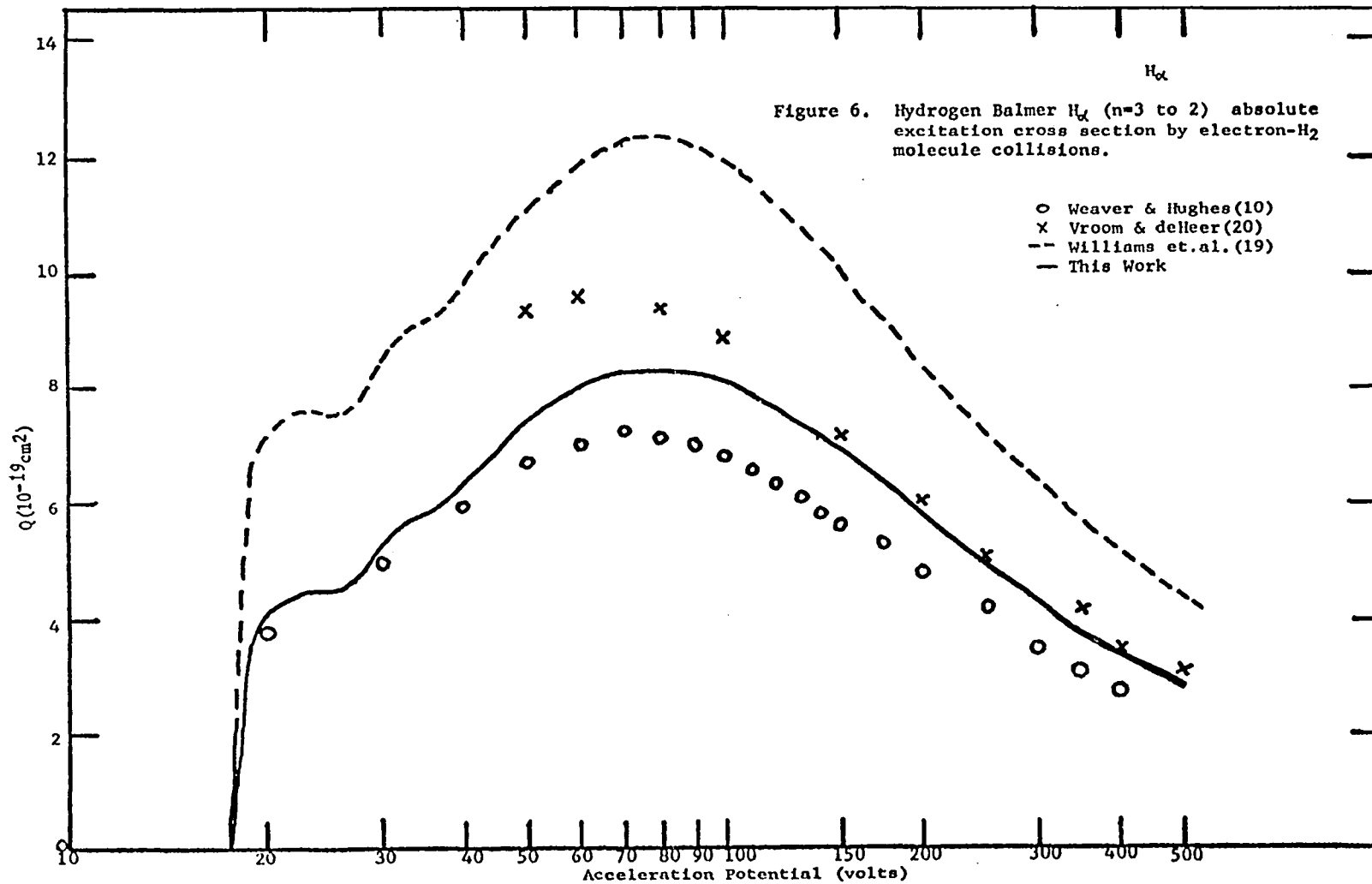
Calculations

Optical Cross Sections

The relationship between the optical cross section Q and the measurable parameters of the collision chamber, light detection and processing equipment, and standardization system is given by Sharpton *et al.* [25] and St. John [27] as

$$Q = \frac{4\pi e H D_{SL}^2 I_{cc} (1.05) 10^{-13}}{3.22 p D_{cc}^2 I_e I_{SL}} \left(\frac{\Delta\lambda P_{16}}{16} \right) \quad (1)$$

where e is the charge of an electron (Coulombs), H is the height of the monochromator entrance slit (cm), p is the pressure in mtorr, D_{SL} and D_{cc} are the diameters of aperture stops used when viewing the standard lamp and collision chamber respectively, I_{cc} and I_{SL} are photomultiplier currents due to radiation from the collision chamber and standard lamp respectively, I_e is the electron current passing through the collision chamber (amps), $\Delta\lambda(\text{\AA})$ is the band pass of the monochromator and $P_{16}/16$ is the number of photons per unit Angstrom band pass which are emitted by the standard lamp and which subsequently are transmitted through the monochromator per second, per square centimeter of ribbon area, per solid angle subtended by the same. In Table 2 typical values for these parameters are listed.



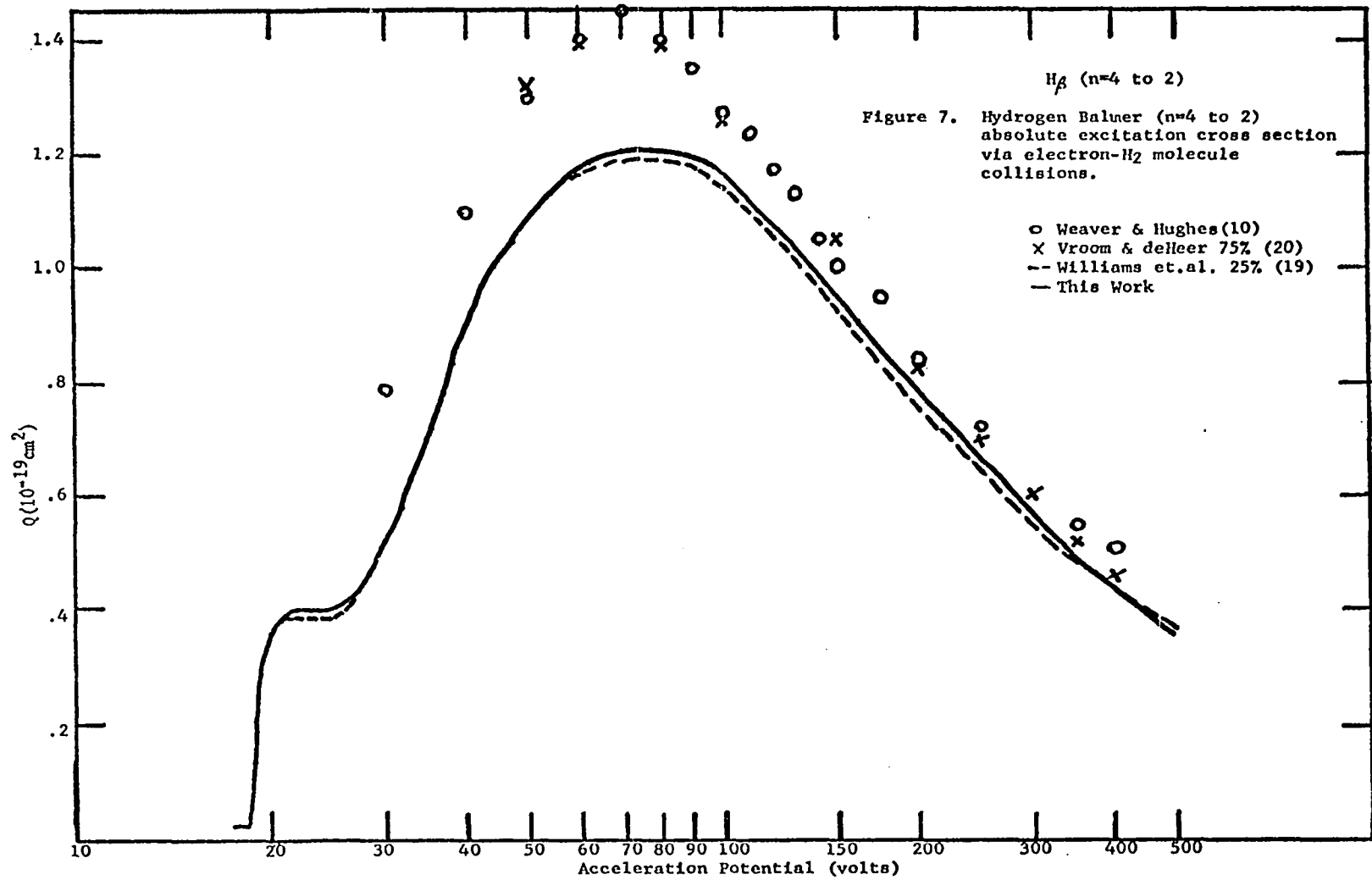


Table 1

Hydrogen Balmer Absolute Excitation Cross Sections By Electron-
H₂ Molecule Collisions

H _α				H _β			
Acc. Pot.	Cross Section	Acc. Pot.	Cross Section	Acc. Pot.	Cross Section	Acc. Pot.	Cross Section
(volts)	(10 ⁻¹⁹ cm ²)	(volts)	(10 ⁻¹⁹ cm ²)	(volts)	(10 ⁻¹⁹ cm ²)	(volts)	(10 ⁻¹⁹ cm ²)
17.50	0	59.0	7.96	18.75	0.128	52.5	1.108
17.75	0.37	60.0	8.00	19.0	0.238	55.0	1.138
18.00	1.01	62.5	8.07	19.5	0.333	57.5	1.159
18.25	1.81	65.0	8.15	20.0	0.360	60.0	1.176
18.50	2.62	67.5	8.22	21.0	0.388	65.0	1.193
18.75	3.31	70.0	8.26	22.0	0.400	70.0	1.202
19.00	3.59	72.5	8.30	23.0	0.400	75.0	1.210
19.25	3.80	75.0	8.30	24.0	0.400	80.0	1.202
19.50	3.97	77.5	8.34	25.0	0.408	85.0	1.202
19.75	4.00	80.0	8.30	26.0	0.415	90.0	1.197
20.0	4.11	82.5	8.30	27.0	0.435	95.0	1.189
20.5	4.11	85.0	8.30	28.0	0.455	100.0	1.168
21.0	4.26	87.5	8.30	29.0	0.485	105.0	1.138
21.5	4.34	90.0	8.30	30.0	0.525	110.0	1.125
22.0	4.40	92.5	8.22	31.0	0.565	120.0	1.083
22.5	4.37	95.0	8.19	32.0	0.599	130.0	1.036
23.0	4.45	97.5	8.15	33.0	0.645	140.0	1.002
23.5	4.50	100	8.11	34.0	0.688	150.0	0.943
24.0	4.50	105	8.00	35.0	0.723	160.0	0.913
24.5	4.50	110	7.88	36.0	0.756	170.0	0.883
25.0	4.50	115	7.81	37.0	0.794	180.0	0.841
26.0	4.55	120	7.62	38.0	0.841	190.0	0.815
27.0	4.62	125	7.47	39.0	0.875	200.0	0.781
28.0	4.74	130	7.35	40.0	0.909	225.0	0.722
29.0	5.03	135	7.24	41.0	0.943	250.0	0.662
30.0	5.27	140	7.16	42.0	0.968	275.0	0.611
31.0	5.42	145	6.97	43.0	0.976	300.0	0.569
32.0	5.50	150	6.94	44.0	0.998	325.0	0.526
33.0	5.69	160	6.67	45.0	1.020	350.0	0.484
34.0	5.72	170	6.44	47.5	1.053	400.0	0.437
35.0	5.80	180	6.25	50.0	1.087	500.0	0.352
36.0	5.87	190	5.99				
37.0	5.99	200	5.80				
38.0	6.18	220	5.46				
39.0	6.29	240	5.08				
40.0	6.41	260	4.85				
41.0	6.48	280	4.55				
42.0	6.59	300	4.24				
43.0	6.67	325	4.02				
44.0	6.78	350	3.75				
45.0	6.86	375	3.60				
47.5	7.16	400	3.45				
50.0	7.35	425	3.22				
52.5	7.58	450	3.11				
55.0	7.77	475	2.96				
57.0	7.85	500	2.84				
58.0	7.88						

TABLE 2

Typical values of Balmer optical cross sections and the measurable parameters of the collision chamber, light detection and processing equipment, and standardization system.

	H cm	D _{SL} cm	I _{cc}	$\Delta\lambda$ Å	T _{SL} K	P ₁₆ 10 ¹⁵	P mtorr	D _{cc} cm	I _e 10 ⁻⁴ amp	I _{SL}	Q 10 ⁻¹⁹ cm ²
H _α (filtered)	.0432	.2083	6.9	7.5	1800	1.18	5.25	.9056	6.00	218.8	8.30
H _β	.0432	.3034	3.9	1.1	2000	.297	4.00	.9056	6.00	87.3	1.21

Excited Atom-Atom (molecule) Collisions

The rate of change of population of the upper excited state * of a three-level atom (molecule) system during electron bombardment is given by the following rate equation at low gas densities.

$$\frac{dn^*}{dt} = n n_e v_e Q(v_e, n \text{ to } n^*) - n^* \left(\frac{1}{\tau} + n v \sigma \right) \quad (2)$$

Here, n^* is the number density of atoms in the excited state of the three level atom, n is the number density of atoms in the ground state, n_e is the number density of electrons bombarding the gas with a velocity v_e , τ is the lifetime of the excited state, v is the average velocity of the gas atoms and is given by $v = (8kT/m)^{\frac{1}{2}}$, σ is the cross section of perturbing excited atom-ground state atom (molecule) collisions, and Q is the absolute excitation cross section for population of the excited level by electron collisions.

The excited atom-ground state atom (molecule) interaction term $n^*n v \sigma$ is negligible at very low pressures. Under steady state conditions the intensity of the emerging radiation changes linearly with pressure changes in this range. See Fig. 8. At higher pressures there will be non-linear intensity of the radiation emitted in response to changes in pressure if the excited state channels of population or depopulation are altered. Figure 9 shows an additional depopulation channel.

In our studies we found the intensities hydrogen H_α , H_β , H_γ , H_δ and the 4634 Å molecular G to B transition became non-linear at pressures starting approximately at 5.25 ± 0.5 , 4.00 ± 0.4 , 1.10 ± 0.30 , 0.35 ± 0.15 and 10 ± 1.0 mtorr respectively. This non-linearity indicates

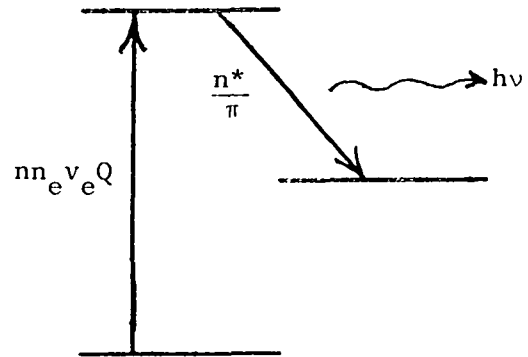


Figure 8. At low pressures spontaneous emission accounts for essentially all depopulation of the excited state, and emerging radiation changes linearly with pressure.

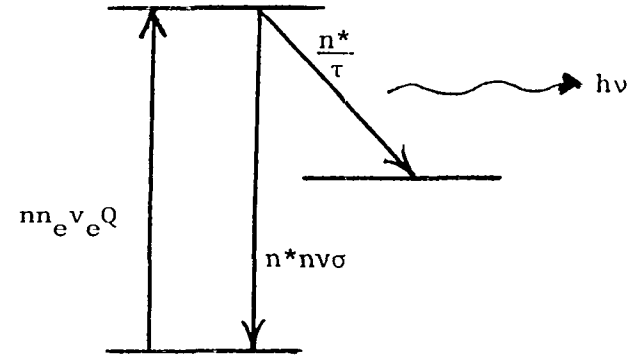


Figure 9. At higher pressures an alternate depopulation channel becomes significant. The depopulation channel opened alters the previous scheme and causes non-linear changes in radiation with respect to pressure change.

some alteration in the population or depopulation mechanisms of the appropriate excited states due to excited atom-ground state atom (molecule) interactions. Since hydrogen Balmer radiation is produced from three near degenerate ℓ -levels, the depopulation channels could be altered by collision induced transitions between them. Another possibility is that excited atoms could transfer their excitation energy to other atoms and molecules in the collision chamber. Whatever the mechanisms are, they are represented here by the collision cross section term σ in Eq. (2). It should be noted that at higher pressures excited atom-atom (molecule) interactions may alter population and depopulation channels in such a way that intensity of radiation emitted in response to changes in pressure will still be linear, but the measured lifetime of the state will have altered. This would happen in situations in which no additional channels are opened but in which transition probabilities are altered by collisions.

We have also made an order of magnitude estimate of each σ by assuming the hydrogen Balmer radiating system can be approximated by a three level model. This is considered a good assumption since some evidence indicates Balmer radiation obtained from electron- H_2 molecule collisions is primarily from the nd to $2p$ transition [7]. We also assumed that the breaking point in intensity vs pressure curves (Fig. 3) is the point where the altering collision term $n^*n\nu\sigma$ is 1% as large as the spontaneous emission term n^*/τ of Eq. (2). Letting the number density of the gas be n_0 at this breaking point which we call the critical pressure, the expression for σ obtained from Eq. (2) is

$$\sigma = \frac{.01}{n_0 \tau \nu} \quad (3)$$

Values for n_0 , τ , and σ are given in Table 3 for each transition of interest. The lifetime τ was taken from experimental work done by Mickish [7]. We found σ to be quite large and about the size of calculated elastic collision cross sections. In Table 3 $\sigma(295^\circ \text{ K})$ was calculated assuming the average velocity of the atoms in the excitation region was given by $v = (8kT/m)^{\frac{1}{2}}$. This is the cross section to be expected if the atoms excited by electron- H_2 molecule collisions still have the velocity of the parent molecule. Robisco [28] *et al.* has shown that at higher electron energies the resulting excited hydrogen atom could have a translational velocity of approximately 4.7 eV. We have also calculated the excited atom- H_2 molecule interaction cross section using this velocity and termed it $\sigma(4.7 \text{ eV})$. The argument of Robisco *et al.* [28] will be discussed more fully later. In Fig. 10, $n_0\tau$ is plotted vs the principal quantum number of the upper level of the corresponding Balmer transitions. This plot reveals that σ is approximately proportional to n^3 . The Bohr theory gives an electron orbit cross section as $\pi a_0 n^4$ where a_0 is the Bohr radius of $.51 \text{ \AA}$ and n is the principal quantum number. The Schrödinger formulation gives

$$\sigma_{\text{(Schrödinger)}} = \pi a_0^2 n^4 \left\{ 1 + \frac{3}{2} \left[1 - \frac{l(l+1) - 3/4}{n^2} \right] \right\} \quad (4)$$

These theoretical cross sections are included in Table 3. As suggested by Mickish [7] the d orbitals were assumed to be the major contributor to the Balmer radiation produced by electron- H_2 molecule collisions in the Schrödinger calculation. A more complete theoretical analysis of hydrogen excited to its $n = 3, 4, 5$ and 6 levels and interacting with either atoms or molecules is not presented in the literature at present.

Table 3. A table of values for the critical pressure n_0 , the experimentally determined lifetimes τ of the relevant excited Balmer states, and theoretical and experimental collision cross sections.

	(Ref. 7) 10^{-9} sec.	n_0 mtorr	$10^{-8} n_0 \tau$ sec.mtorr	$\sigma_{\text{EXP}}(295^\circ\text{K})$ 10^{-14}cm^2	σ_{Bohr} 10^{-14}cm^2	$\sigma_{\text{Schrodinger}}$ 10^{-14}cm^2	$\sigma_{\text{exp}}(4.7\text{eV})$ 10^{-15}cm^2
H $_{\alpha}$	63 \pm 6	5.25 \pm 0.5	33.1 \pm 6.3	5.23 \pm 0.99	.713	1.11	3.09 \pm 0.58
H $_{\beta}$	39 \pm 9	4.00 \pm 0.4	15.6 \pm 5.2	11.1 \pm 3.7	2.25	4.43	6.55 \pm 2.2
H $_{\gamma}$	71 \pm 10	1.10 \pm 0.3	7.8 \pm 3.2	22.1 \pm 9.1	5.50	11.9	13.0 \pm 5.4
H $_{\delta}$	105 \pm 21	.35 \pm 0.15	3.7 \pm 2.3	47.2 \pm 30	11.4	25.8	27.8 \pm 17.7

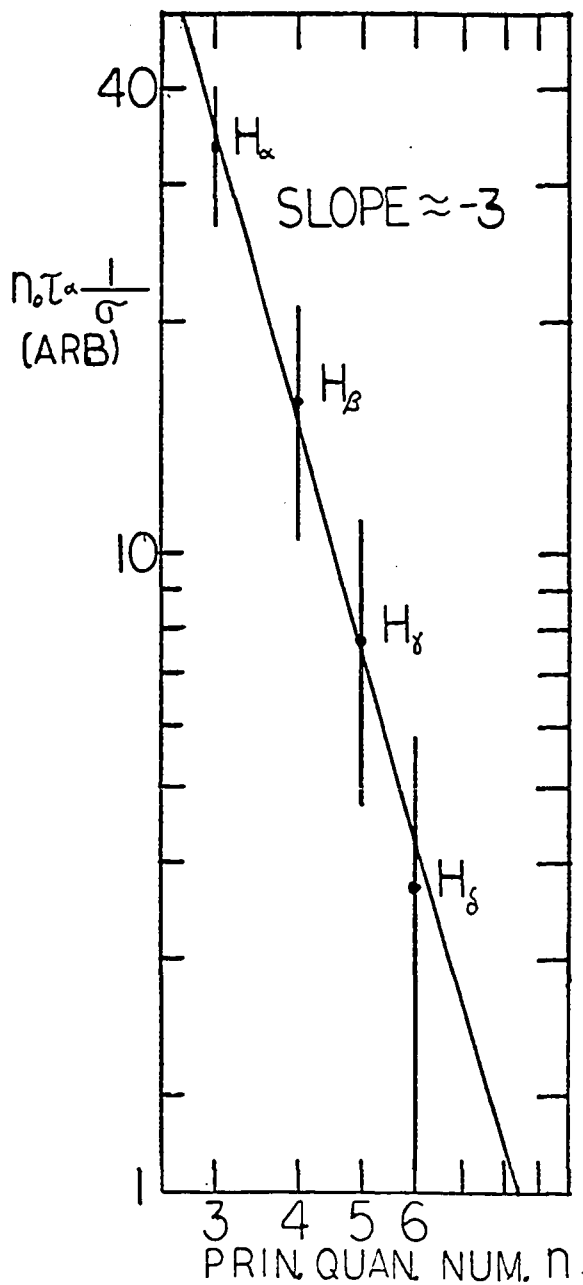


Figure 10. The inverse of the experimentally determined collision cross section vs. respective principal quantum numbers. This graph indicates $\sigma \propto n^3$ is a good approximation.

A number of authors do, however, discuss related phenomena and some are included in the bibliography [29-35]. Mott and Massey [35] best explain the procedure involved in carrying out transfer of excitation in slow collisions calculations.

Excited Atom-Electron Collisions

We can expect atom-molecule collisional effects to be independent of the electron beam density; but, we also expect that excited atom-electron collisional effects are current dependent. As shown in Fig. 4, we found that at higher pressures and current densities H_{γ} radiation responds nonlinearly to changes in current. If this perturbation is due to excited atom-electron collisions, then the rate equation is

$$\frac{dn^*}{dt} = n n_e v_e Q(v_e, n \rightarrow n^*) - n^* \left(\frac{1}{\tau} + n v \sigma + n_e v_e \sigma_e \right) . \quad (5)$$

Here, n^* is the excited state number density, n is the ground state number density, n_e is the electron beam number density with velocity v_e , τ is the lifetime of the excited state, v is the average velocity of gas atoms, σ is the cross section of perturbing excited atom-ground state atom collisions, Q is the absolute excitation cross section for population of the excited level by electron collisions, and σ_e is the cross section of perturbing electron-excited atom collisions. The expression is identical to Eq. (3) except for the addition of the electron-excited atom interaction term $n^* n_e v_e \sigma_e$. If for an electron beam number density n_e^0 this mechanism is 1 per cent as large as the other depopulation terms, then from Eq. (5)

$$\sigma_e = \frac{.01 \left(\frac{1}{\tau} + n v \sigma \right)}{n_e^0 v_e} . \quad (6)$$

An order of magnitude value for the H_{γ} electron-excited atom cross section was calculated from data obtained from Figs. 1 and 4 and Table 3. The resulting electron excited atom cross section would be

$$\sigma_e(H_{\gamma}) \simeq 4 \times 10^{10} \text{cm}^2.$$

Purcell [36] discusses the possibility of electrons inducing transitions between the near degenerate levels $2^2S_{1/2} \rightarrow 2^2P_{3/2}$ in the excited hydrogen atom from a different approach. He suggests that the field of the moving electrons and positive ions looks like a fluctuating field to the excited atom. Considering a certain number density of electrons and positive ions at a given temperature he concludes that the cross section for this process is quite large. His figures for the $2^2S_{1/2} \rightarrow 2^2P_{3/2}$ transition predict a cross section of approximately 10^{-12}cm^2 under the conditions obtained from Fig. 4. The cross sections for such an induced transition in the $n = 5$ level of hydrogen however has not been calculated although Wilcox and Lamb [21] have applied his treatment to the $3s$ state. In both the rate equation and the Purcell approach the results are unacceptably large, and we must look to the positive ions for a possible explanation.

Excited Atom-Ion Collisions

So far we have discussed and used the terminology of the impact approach of collisional and Stark broadening. This approach is reported to be valid when the perturbers interact with the excited atoms for a much shorter time than the lifetime of the relevant state. Thus, this approach is ideal for the electron-excited atom problem. The quasi-static broadening approach is an approximation of the other extreme. It is valid when the perturbers move slowly so that the

perturbation is practically constant over an interaction time which is of the order of the lifetime of the excited state. The quasi-static or statistical description is pursued by Holtsmark [29]. He found that the most probable electric field experienced at a single point in space due to the time average of fields of neighboring ions is given by

$$E = \frac{2.61}{4\pi\epsilon_0} e(n_i)^{2/3} \quad (7)$$

where E is in volts per meter and n_i is the number density of the ions. In the excitation chamber near the electron gun, space charge neutralization would cause the number density of positive ions to be equal to the number density of electrons in the beam. This is a consequence of Poisson's equation. Thus

$$n_i = n_e = \frac{I_e}{ev_e A} \quad (8)$$

where I_e is the electron current, v_e is the velocity of the electrons, and A is the area of the beam at the slit. We find the number density of both ions and electrons at 400 μ amps, regardless of the pressure, to be

$$n_i = n_e = 5.4 \times 10^6 \frac{\text{ions}}{\text{cm}^3} . \quad (9)$$

Substituting this number density into Eq. (6) we find a field strength $E \approx 1.2 \times 10^{-2}$ volts/cm. This field is possibly strong enough to cause some ℓ -level mixing such as Bethe and Salpeter discuss in their book [15], but, not the non-linear effect recorded in Fig. 4. We can not accept it as the cause, because, this field strength is independent of the pressure of the gas in the chamber. If this model were valid, non-linear effects would set in at 400 μ amps at any pressure. This is

not observed experimentally. At lower pressures the current reaches over 1 ma with no current dependent effects evident. The corresponding number density of ions and field strength at 1 ma are 13×10^6 ions/cm³ and 2.1×10^{-2} volts/cm respectively.

If we assume the ion density is not governed by space charge neutralization, the pressure dependent non-linearity can be explained. For an order of magnitude calculation, we write the rate equation governing the population of ions in the chamber:

$$\frac{dn_+}{dt} = nn_e v_e Q_+ (n \text{ to } n_+) + D \nabla^2 n_+ \quad (10)$$

where n_+ is the number density of positive ions, Q_+ is the cross section for production of ions from electron impact with neutrals n , n_e is the number density of electrons in the beam with velocity v_e , and D is the diffusion coefficient of hydrogen ions in hydrogen. Cylindrical coordinates can be used since the experiment was performed in a cylindrical collision chamber under steady state conditions. Assuming that n_+ is a function of r only, Eq. (10) becomes

$$\frac{r \partial^2 n_+}{\partial r^2} + \frac{\partial n_+}{\partial r} + r \left(\frac{nn_e v_e Q_+}{D} \right) = 0 \quad (11)$$

The solution is

$$n_+ = \frac{nn_e v_e Q_+ (R^2 - r^2)}{4D} \quad (12)$$

when the conditions

$$n_+ = 0 \text{ at } r = R \text{ the radius of the chamber}$$

$$n_+ = \text{finite at } r = 0$$

are imposed. Equation (12) reveals that the number density of positive

ions in the chamber is a function of pressure and current density, which is exactly what we have found in our data of H_γ , as shown in Fig. 4. In calculating n_+ we make use of more approximations. From kinetic theory the diffusion coefficient is

$$D = \frac{1}{3} v\lambda \approx \frac{v}{3n(4\pi a_0^2)} = 5.1 \times 10^4 \quad (13)$$

where $4\pi a_0^2$ is a reasonable cross section for atom-ion collisions [37], n is the number density of the gas atoms, v is the average velocity of the gas atoms, and λ is the mean free path for collisions in the gas. The cross section for ionization by electron- H_2 molecule collisions Q_+ is obtained from data compiled by Kieffer and Dunn.[38]. Finally, the electron number densities and the velocities of the electrons are obtained from the H_γ intensity vs current curve in Fig. 4 and the electron beam radius given in Fig. 1. The radius R of the chamber is 1.175 cm. Then from Eqs. (12) and (17) respectively, the maximum ion density and field strength is

$$n_+ \approx 6.2 \cdot 10^9 \text{ ions/cm}^3 \quad (14)$$

$$E \approx 1.3 \frac{\text{volts}}{\text{cm}} . \quad (15)$$

More than likely, the ion density and field strength is less than this since we ignored the loss of ions by collisions with the end walls of the chamber. This is of secondary importance as we have identified the positive ions as a possible source of the current and pressure dependent perturbation displayed in Fig. 4.

Electron Gun Characteristics

It is possible that the non-linearity of radiation intensity

with current shown in Fig. 4 is a characteristic of the electron gun in all gases and not confined to hydrogen. We have already shown in Figs. 2 and 5 that the electron gun manifests non-linear behavior when operated at low electron voltages. A similar phenomena is likely to occur in all gases at higher pressures. This is because more multiple electron collisions occur.

The ratio of current of colliding electrons I_e to the total current of electrons I in a monoenergetic electron beam is given by

$$\frac{I_{\text{coll.}}}{I} = n\Delta xQ \quad (16)$$

where n is the number density of gas particles, Δx is the distance traveled by the electrons in the gas at a particular velocity and Q is the summation of all possible inelastic cross sections of electrons whose velocity is that of the beam. By substituting values for n , Δx , and Q we can get an order of magnitude estimate of the per cent of electrons suffering multiple collisions. This percentage in turn suggests some limitations of the electron gun.

The derivation and consequences of Eq. (16) is as follows. The number of these atoms that suffer inelastic collisions per second per unit volume is given by the rate equation

$$\frac{dn}{dt} = n n_e v_e Q \quad (17)$$

where n_e is the number density of electrons in the beam and v_e is the velocity of the electrons. Since the number density of atoms suffering inelastic collisions per second must equal the number density of electrons suffering inelastic collisions per second and $I = n_e v_e A e$

where A is the cross sectional area of the electron beam and e is the charge of an electron, then Eq. (17) is

$$\frac{dn}{dt} = n n_e v_e Q = \frac{I_{\text{coll.}}}{V e} \quad (18)$$

where V is the volume of interest. Substituting current in the middle term and the volume of interest as $V = A \Delta x$ we have Eq. (16)

$$\frac{I_{\text{coll.}}}{I} = n \Delta x Q \quad (19)$$

For accurate experimental cross section work we wish to have 1 per cent or fewer electrons making inelastic collisions before entering the chamber viewing area. This assures a monoenergetic beam. Under this criteria

$$n \Delta x Q \leq .01 \quad (20)$$

For an order of magnitude calculation we assume that the total inelastic cross section is on the order of the total ionization cross section; this assumption is supported by experimental evidence. See, for example, Ref. 38. For electron guns operated at low pressures there is only one region where Δx is large enough for concern. That is the region between the first accelerating grid and viewing area. For hydrogen, Eq. (20) can be satisfied if the pressure of hydrogen atoms is kept at approximately 10 mtorr or below. At higher pressures a significant percentage of the beam electrons make multi-collisions. It might seem that at high pressures intensity vs current studies could be made and any non-linearity could be attributed to the gas under study and not the gun. Under these conditions all currents would seem to have the same percentage of electrons making multiple collisions in the region between the

first accelerating grid and the viewing area. This is probably not a safe conclusion because at higher pressures the region around the other grids becomes important.

The other grids in the electron gun are for current control. For current variation in an intensity vs pressure study, the voltage on grid number two must be changed. At low pressures nothing dramatic happens to the plasma around these plates due to few electron-atom interactions except at low accelerating potentials. At high pressures more interactions occur and even a large percentage of multiple electron collisions occur in this area. As the voltage on grid number two changes different percentages of electron collisions occur in this area. As the voltage on the grid changes different percentages of electrons are affecting the gas around these plates. The subsequent changes in plasma density around these plates alters the energy distribution of the electrons in the electron beam as a function of the grid number two voltage and consequently current density. As a result we can expect the electron gun to be non-linear at pressures somewhere above 10 mtorr depending on the gas.

Discussion of H_{α} and H_{β} Optical Cross Sections from Electron- H_2 Collisions

The excitation functions of H_{α} and H_{β} from 0 to 500 eV for electron impact on H_2 are shown in Figs. 6 and 7 respectively. The majority of the investigators have concentrated on the high energy portion of the function, but Williams *et al.* [19], Vroom and deHerr [20], Kruihof and Ornstein [22], and Wilcox and Lamb [21] have studied the onset. Williams *et al.*, Kruihof and Ornstein and Wilcox and Lamb report

onsets that look very much like the results of this work but, Vroom and deHeer report additional structure. This additional structure is probably due to molecular background. For H_{α} both the 1st order molecular background, scattered light and the 2nd order $2s\sigma a^3\Sigma_g^+ \rightarrow 2p\sigma b^3\Sigma_u^+$ continuum radiation must be eliminated. Our H_{α} excitation function was measured with the monochromator bandpass set at $\Delta\lambda = 14.1 \text{ \AA}$. The five molecular lines reported by Gale, Monk, and Lee [39] close enough to H_{α} to contribute radiation to the excitation function were too weak for detection. The detectable second order continuum radiation and scattered light was eliminated by a Oriel Model G-772-4750 long pass filter. Without a filter or with a larger bandpass the resulting excitation function has additional structure like that reported by Vroom and DeHeer [20]. The two molecular transitions $3d\sigma I_b^1\pi_g \rightarrow 2p\sigma B^1\Sigma_u^+$ 4861.74 \AA and $3d\sigma J_b^1\Delta_g \rightarrow 2p\sigma B^1\Sigma_g^+$ 4860.81 \AA contribute to the H_{β} excitation function [39,40]. That radiation is detectable, and the small non-zero cross section just below onset of H_{β} , Fig. 7, reveals the relative magnitude of their contribution.

The shape of the H_{α} and H_{β} excitation functions reported here agree well with work reported in other labs [10,19-21]. The absolute value of the excitation cross section, however, varies among these investigators. For H_{β} Weaver and Hughes [10] report an absolute excitation cross section approximately 20 per cent less than reported in this work. Williams *et al.* [19] report values 50 per cent greater than this work, and Vroom and deHeer [20] report values very close to those reported here for energies greater than 150 eV. They report values up to

25 per cent greater than found in this work for lower electron energies.

For H_{β} Weaver and Hughes report an absolute excitation cross section approximately 7 per cent greater than found in this work. Williams *et al.* report values very close to a factor of four greater than this work, and Vroom and deHeer report values 40 per cent greater than this work for energies greater than 150 eV. Vroom and deHeer's values are up to 60 per cent greater than found in this work for lower electron energies.

The hydrogen Balmer excitation functions H_{α} and H_{β} obtained in this study show interesting structure in the 16 to 45 eV range. We suspect that at the excitation onsets, and at approximately 25 eV and 35 eV, three different excitation mechanisms are activated. At the lower energies Robisco [28] *et al.* have suggested that H(2s) states are produced by excitation of molecular singlet and triplet bonding orbitals that vibrationally dissociate into one H(1s) and one H(2s) atom. The excellent potential energy curves for H_2 in Figs. 11 and 12 presented by Sharp [41] show that in general a dissociation onset into products H(nl) and H(1s) is given by:

$$18.0758 - \frac{13.5979}{n^2} \text{ eV} . \quad (21)$$

For the 25 eV inflection in our H_{α} and H_{β} excitation functions we also reference Robisco [28]. He suggests that anti-bonding doubly excited states of the molecule dissociate into high velocity (n ℓ) atoms. His data suggests that in creation of high velocity metastable H(2s) atoms, the molecule is excited to previously undetected doubly excited repulsive states that eventually end up as (1s) and (2s) atoms. The onset of this process for creating fast (1s) and (2 ℓ) atom is

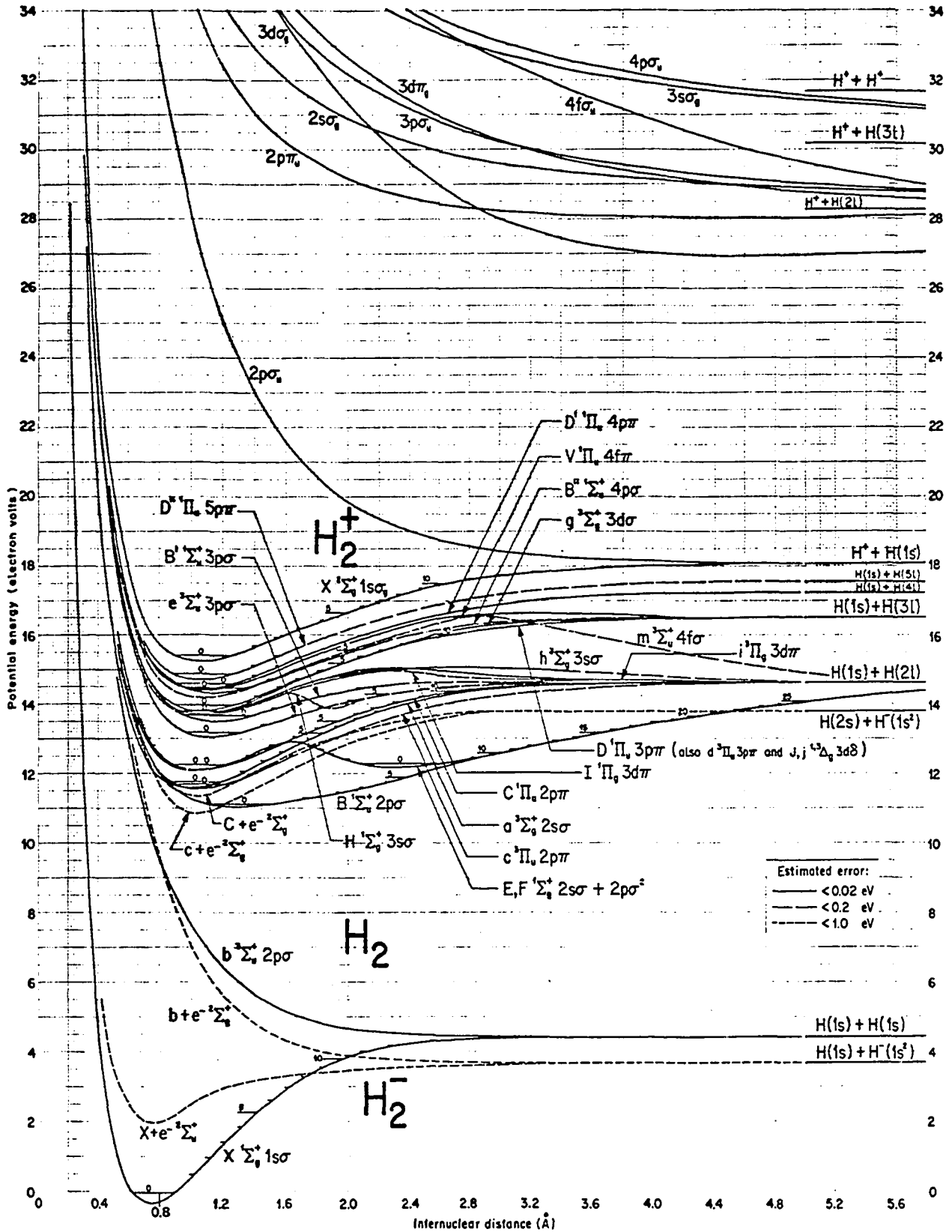


FIG. 11. Potential-Energy Curves for H_2^- , H_2 , and H_2^+
 From T. E. Sharp, reference 41.

approximately 10.1 eV above the process of producing slow (1s)+(2ℓ) atoms. The 10.1 eV extra excitation energy is converted to translational energy. That is why the latter atoms are fast. It is probable that there are other repulsive doubly excited states that are excited and end up as fast as H(1s) + H(nℓ) atoms.

Finally we get to the third inflection seen on the excitation functions at approximately 35 eV. Balmer radiation is probably produced by simultaneous excitation and ionization of the molecule. For producing such H⁺ and H(nℓ) atoms the electron energy must be at least:

$$31.6737 - \frac{13.5979}{n^2} \text{ eV} \quad (22)$$

For H_α this is approximately 5 eV less than revealed by our excitation function. Sharp's potential energy curves in Fig. 11 for H₂⁻, H₂ and H₂⁺ show that H⁺ + H(nℓ) atoms will not be produced until the electron energy is over 34 eV due to the Frank-Condon principle in accordance with our data. From Fig. 11, we can also expect the hydrogen atoms produced by this process to be of high velocity.

We have also concluded that the pressure dependence of the H₂ G to B 4634 Å optical excitation function for lack of a better explanation lends possible supporting evidence to the existence of high velocity H(nℓ) atoms. In Fig. 13, the optical excitation function is shown at two pressures. At the higher pressure the high energy portion of the function increases relative to the low energy portion. This increase is possibly due to molecular interaction with H(nℓ) atoms since they are preferentially populated at higher energies. The excited hydrogen atoms possibly release their energy to the ground state molecules

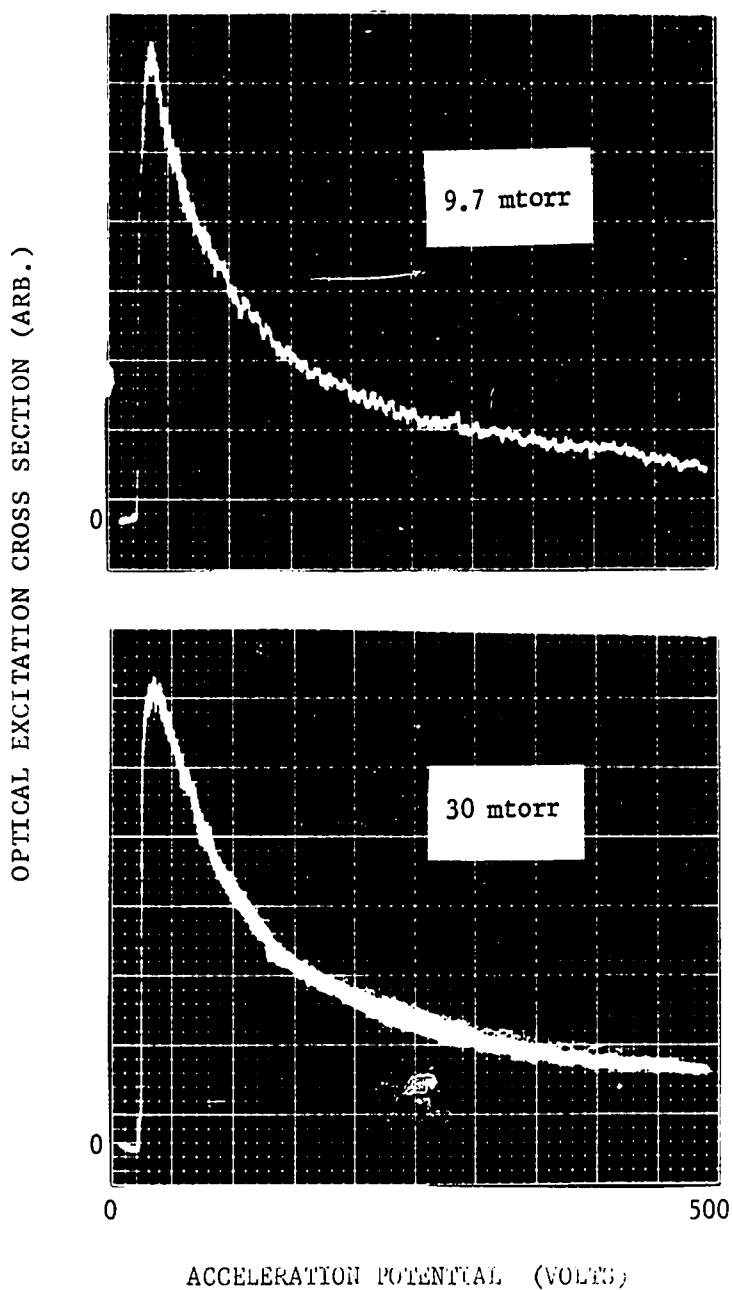


FIG. 13. Optical excitation cross sections of the 4634 Å G to B transition in molecular hydrogen. The upper curve was taken at 9.7 mtorr pressure and the lower was obtained at 30 mtorr pressure.

that eventually radiate (4634\AA) light. Since the G state lies approximately 4.5 eV above ground it is necessary that the $H(n\ell)$ atoms have approximately 4.5 eV kinetic energy. This we have already established as possible. This pressure dependence became apparent at approximately 10 mtorr of pressure. Other possibilities are resonance trapping and excited molecule-molecule collisions. Further studies will have to be carried out to determine the mechanism definitely.

In future work a good knowledge of the hydrogen molecular spectrum will be essential. Its spectrum is very complex. It is often referred to as the many line spectrum of hydrogen. When first encountering this spectrum, its comprehension appears impossible. In fact, historically, the spectrum defied analysis for many years. Today with the wavelength tables of Monk, Gale and Lee [39] together with the monograph on molecular hydrogen by Richardson [40] the spectrum is at least attackable. The wavelength tables give the wavelength and wave numbers of thousands of lines of the secondary spectrum of hydrogen which were obtained with high resolution apparatus. Along with these lines the relative intensities are also listed. Richardson has arranged these lines in an internally consistent scheme such that most reported lines are identified with a specific transition. His tables are arranged so that for a given transition particular wavelengths representing that transition can be found. However, if a wavelength is known it is difficult to find what transition it represents and what transitions its nearest neighbors in the molecular spectrum represent. In order to make such spectrum identification feasible wave numbers were taken from Richardson's monograph together with their relative intensities as is

given by Monk, Gale and Lee [39] and their assigned transitions. These wave numbers were then ordered by computer. The result is a table convenient for use in spectrum analysis. This table is presented in Appendix I.

Work is still continuing on the identification of the H₂ spectra. Since Richardson's work, Herzberg [45] has reviewed work on hydrogen and published a comprehensive table of the vibrational and rotational constants for the electronic states of H₂. Other review articles have appeared in the last few years and are discussed in the most recent review article written by Sharp [41].

CHAPTER III

THEORY OF HYDROGEN BALMER STUDIES IN A FLOW SYSTEM

Background

In the hydrogen atom each principle quantum number n has n states of differing l -values that are nearly degenerate in energy. These near degenerate l -levels are so close together that contributions from the different l -levels to hydrogen Balmer radiation has never been completely resolved by optical means. Series [42] reviews the work done in this area in his monograph *Spectrum of Atomic Hydrogen*. This book is a valuable, concise, and well written survey of many theoretical and experimental considerations published on the hydrogen atom. The reader is referred to this book for greater insight into the degeneracy problem. Kuhn [43] and Bethe and Salpeter [44] are also important in this respect.

Because of the degeneracy problem, only a sum of three hydrogen Balmer electron impact optical cross sections as defined on page 6 can be obtained with a system such as ours. We will show in this chapter why only this sum can be obtained. We will also obtain and exhibit optical excitation cross sections from theory for comparison.

The Degeneracy Problem

Experimentally some transitions in atoms and molecules occur more readily than others. In most instances these are "optically

allowed" transitions. See for example Refs. 42, 43, 45-47. Theoretically "selection rules" are arrived at in quantum mechanics for induced as well as spontaneous transitions which predict that these transitions are favorable. For the hydrogen atom see for example Refs. 44, 48-53. Hydrogen Balmer radiation results from transitions between principal quantum levels n and 2. In Fig. 14 the Balmer alpha H_{α} ($n=3$ to 2) transition is represented. Slanted lines represent experimentally and theoretically determined allowed transitions. In general only ns to $2p$, np to $2s$ and nd to $2p$ transition contribute to hydrogen Balmer radiation. A detector monitoring H_{α} radiation will collect the sum of photons created from these three transitions in which ℓ changes by unity.

In our experimental arrangement we monitor the radiation emitted by a large number of hydrogen atoms in an electron beam section of definite length. In Fig. 15 a model of such a system is drawn. Since the detector cannot resolve the three $\ell \rightarrow \ell \pm 1$ transition contributions, the output of the device is simply the sum of the photon contributions from all three transitions. Following Sharpton [16] we let $J(\ell, \ell \pm 1)$ represent the number of photons reaching the detector per centimeter and second of the electron beam with frequency corresponding to the particular $\ell \rightarrow \ell \pm 1$ transition. Then the total number of photons detected as H_{α} radiation per centimeter of the electron beam per second is

$$J(H_{\alpha}) = J(3s, 2p) + J(3p, 2s) + J(3d, 2p) \quad (23)$$

Without higher resolution equipment we can not determine experimentally how much each $\ell \rightarrow \ell \pm 1$ transition contributes. All we know is the sum. Because of this we can not calculate the level cross sections of

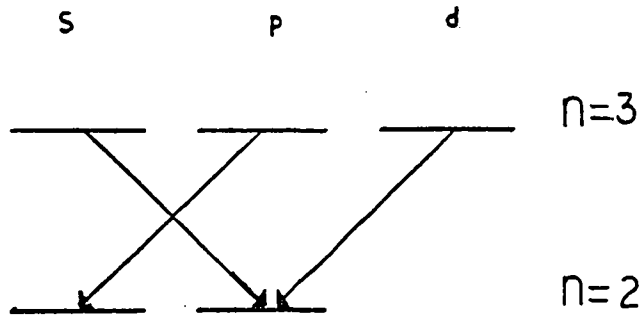


FIG. 14. The three transitions that produce Balmer alpha radiation.

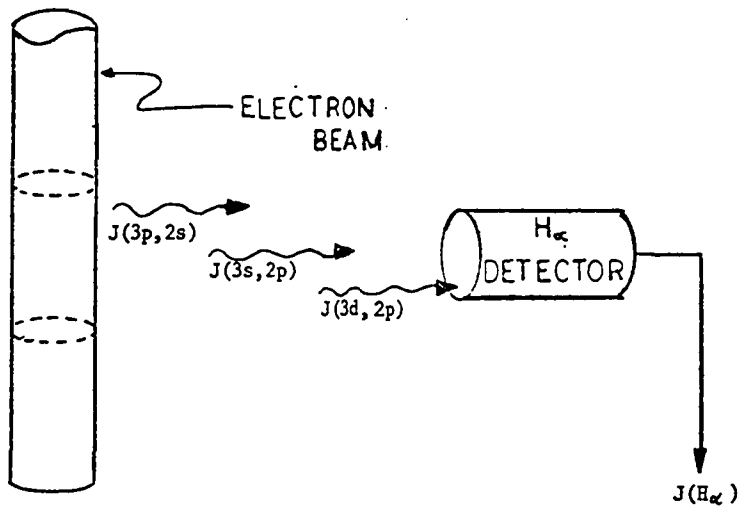


FIG. 15. Balmer alpha radiation resulting from three distinct transitions is unresolved in this detection system.

hydrogen with our system. We can only measure the sum of the three optical excitation cross sections representing transitions from s, p and d upper levels. In the following formulation we will attempt to make this clearer.

Defining the Electron Impact Cross Sections for A Single Level

First we must define the electron impact level excitation cross section in terms of experimentally measurable quantities. To do this we write down the rate equation for the production of a single excited state. In general the energy level diagram or scheme of the species we are interested in will have states (i) that lie above and states (k) that lie below the state (j) we are particularly interested in, as well as the ground state. Thus, letting n_j be the number of excited atoms produced per cubic centimeter by the electron beam, the population equation under the assumption of only single electron neutral ground state atom collisions become

$$\frac{dn_j}{dt} = n n_e v_e Q_j - n_j \sum_{k < j} A_{jk} + \sum_{i > j} A_{ij} n_i \quad (24)$$

$$\text{total rate} = \begin{array}{l} \text{direct} \\ \text{excitation} \\ \text{rate} \end{array} - \begin{array}{l} \text{spon-} \\ \text{taneous} \\ \text{emission} \\ \text{rate} \end{array} + \begin{array}{l} \text{cascade} \\ \text{rate} \end{array}$$

In this equation n_e is the number of electrons per cubic centimeter in the electron beam, v_e is the velocity of these electrons, Q_j is the level cross section for excitation to the j th level, n is the number of ground state atoms per cubic centimeter, and A_{ij} is the probability per second that an excited atomic electron will make a transition from the i th to the j th level. The A_{ij} 's are technically called the spontaneous Einstein transition probabilities. Some experimental conditions that

make it necessary to include other terms in the rate equation are discussed in Chapter II. We operate under experimental conditions such that other phenomena are negligible when possible and that the terms in Eq. (24) are the only ones that need to be considered.

At equilibrium $dn_j/dt = 0$ and the population of the j th state by direct electron impact excitation from the ground state and indirect population by cascades is equal to the depopulation due to spontaneous emission. Thus from Eq. (24)

$$n_j \sum_{k < j} A_{jk} = n n_e v_e Q_j + \sum_i A_{ij} n_i \quad (25)$$

spontaneous
direct
cascade
emission
excitation
rate
rate
rate

For each transition from an upper level to a lower level, whether it be from the k th state, to the j th state, or between any other state, a photon is emitted of a wavelength determined by the energy difference between the relevant states. Eq. (25) simply states that the total number of photons produced by spontaneous transitions out of the j th state to lower lying levels must add up to the total number of atoms put in the j th state by direct electron excitation and cascade. So, in order to determine Q_j we simply need to count all the photons that represent transitions out of and into the j th state and to measure n , n_e , and v_e . Equation (25) can be more clearly expressed in terms of photon flux J by letting the total number of photons emitted per centimeter per second from the electron beam with frequency corresponding to a single j to k transition be given by

$$J_{jk} = A_{jk} \int_A n_j dA \quad (26)$$

where A is the cross sectional area of the beam.

The electron beam current is given by

$$I_e = e \int_A n_e v_e dA$$

where e is the electronic charge.

Next we rewrite Eq. (25) as

$$n n_e v_e Q_j = n_j \left(\frac{A_{jk}}{A_{jk}} \right) \sum_{k < j} A_{ij} - \sum_{i > j} n_i A_{ij} \quad (27)$$

Then, multiply by the differential area dA and integrate. The result is

$$n \left(\frac{I_e}{e} \right) Q_j = J_{jk} \left(\frac{\sum_{k < j} A_{jk}}{A_{jk}} \right) - \sum_{i > j} J_{ij} \quad (28)$$

direct excitation rate = spontaneous emission rate - cascade rate

Thus Eq. (28) indicates that the total number of photons leaving the j th level per cm/sec in the electron beam can be determined by counting the number of photons emitted per cm/sec of the electron beam, with frequency corresponding to a single j to k transition and multiplying it by the physical constant $(\sum_{k < j} A_{jk} / A_{jk})$ characteristic of the atomic system under study. The quantity $(A_{jk} / \sum_{k < j} A_{jk})$ is defined as the branching ratio B_{jk} . Substituting the expression for the branching ratio into Eq. (28), we have

$$Q_j = \frac{J_{jk}}{n \left(\frac{I_e}{e} \right) B_{jk}} - \frac{\sum_{i > j} J_{ij}}{n \left(\frac{I_e}{e} \right)} \quad (29)$$

It is convenient to define the quantity

$$Q_{ij} = \frac{J_{jk}}{I \frac{e}{n}} \quad (30)$$

as the electron impact optical excitation cross section of the spectral line determined by the j to k transition. In general, it is the electron impact cross section for production of radiation of the frequency determined by the j to k transition no matter what the mechanisms. If Eq. (24) holds, we see that the optical excitation cross section will be a constant characteristic of the atomic system under study since it is normalized with respect to the number density of ground state atoms in the beam and the electron beam current.

Finally, in terms of the optical excitation cross sections, the electron impact level excitation cross section for direct population of the jth level is given by

$$Q_j = \frac{Q_{jk}}{B_{jk}} - \sum_{i>j} Q_{ij} . \quad (31)$$

The term Q_{jk}/B_{jk} is also defined as the apparent cross section of the jth level.

Hydrogen Balmer Crossed Beam Cross Section Measurement

The crossed beam system developed for obtaining hydrogen Balmer cross sections is shown in Fig. 28. The details of construction and operation are given by Walker [12] and in this work in Chapter IV. The source of hydrogen atoms is a glow discharge of the R. W. Wood [54] type. Hydrogen molecules are crossed with an electron beam from an operating electron gun when the Wood discharge tube is off. Then with the discharge tube on both hydrogen molecules and hydrogen atoms are

crossed with the electron beam. In principle, the absolute hydrogen Balmer optical excitation cross sections can be extracted from the resulting intensity vs electron voltage curves when (1) the mass flow is held constant, (2) the electron beam current is recorded in both cases, (3) the relative number of hydrogen molecules in the collision chamber when the Woods discharge tube is on and off is known, (4) and when the density of hydrogen molecules in the electron beam is known when the Wood tube is off. In the following formulation we will derive this relationship.

From the degeneracy problem section of this chapter we know that hydrogen Balmer radiation is composed of three near degenerate $\ell \rightarrow \ell \pm 1$ components. In the following formulation we will study one component and then generalize at the end. For the steady state rate equation representing population of the j th level of the atom in the cross beam experiment with the Wood tube off we have from Eq. (24)

$$\frac{dn_j}{dt} = n_{H_2} n_e v_e Q(H_2, j) + \sum_{i>j} A_{ij} n_i - n_j \sum_{k<j} A_{jk} \quad (32)$$

With the Wood tube on

$$\frac{dn'_j}{dt} = n'_{H_2} n_e v_e Q(H_2, j) + n_H n_e v_e Q(H, j) + \sum_{i>j} A_{ij} n'_i - n'_j \sum_{k<j} A_{jk} \quad (33)$$

Then substituting $Q(H_2, j)$ of Eq. (32) into Eq. (33) we get

$$n_H n_e v_e Q(H, j) = \left(n'_j - \frac{n'_{H_2}}{n_{H_2}} n_j \right) \sum_{k<j} A_{jk} - \sum_{i>j} A_{ij} \left(n'_i - \frac{n'_{H_2}}{n_{H_2}} n_i \right) \quad (34)$$

Expressing this relationship in terms of photon flux and branching ratios as in Eq. (29) we have

$$Q(H,j) = \frac{J'_{jk} - \frac{n'_{H2}}{n_{H2}} J_{jk}}{n_H \frac{I_e}{e} B_{jk}} - \frac{\sum_{i>j} (J'_{ij} - \frac{n'_{H2}}{n_{H2}} J_{ij})}{n_H \frac{I_e}{e}} \quad (35)$$

From Eq. (30) we identify the electron-hydrogen atom optical excitation cross section as

$$Q_{jk}(H) = \frac{J'_{ik} - \frac{n'_{H2}}{n_{H2}} J_{ij}}{n_H \frac{I_e}{e}} \quad (36)$$

Substituting this expression into Eq. (35) we have

$$Q(H,j) = \frac{Q_{jk}(H)}{B_{jk}} - \sum_{i>j} Q_{ij}(H) \quad (37)$$

which is the same as Eq. (31).

In hydrogen we have three near degenerate l levels that contribute to Balmer radiation. In the degeneracy problem section of this chapter we concluded that without high resolution equipment or some other resolution means we can not determine the specific contribution from any single transition, but only the total flux from all three levels. The expression for the total electron impact level excitation cross section obtained from all three contributing transitions, say for $n = 3$, would be from generalization of Eq. (37).

$$Q(H,3s) + Q(H,3p) + Q(H,3d) = \frac{Q_{3s,2p}(H)}{B_{3s,2p}} + \frac{Q_{3p,2s}(H)}{B_{3p,2s}} + \frac{Q_{3d,2p}(H)}{B_{3d,2p}} \\ - \sum_{\text{cascades}} [Q_{\text{upper},3s}(H) + Q_{\text{upper},3p}(H) + Q_{\text{upper},3d}(H)] \quad (38)$$

In our work we obtain the total number of photons detected as radiation per centimeter of the electron beam per second which contributes from all three near degenerate transitions and is generalized from Eq. (23).

$$J_{\text{HBalmer}} = J_{(ns,2p)} + J_{(np,2s)} + J_{(nd,2p)} \quad (39)$$

We obtain this radiation produced by electron hydrogen atom interaction by subtracting radiation emitted in the electron beam with the Wood tube on and off as is expressed in Eq. (36).

$$J_{\text{HBalmer}} = J_{\text{HBalmer}}^{\text{ON}} - \frac{n_{\text{H}_2}^{\text{ON}}}{n_{\text{H}_2}^{\text{OFF}}} J_{\text{HBalmer}}^{\text{OFF}} \quad (40)$$

Dividing Eq. (39) by $n_{\text{H}} I_e / e$ we get the sum of the three optical excitation cross sections

$$Q_{\text{HBalmer}}^{(\text{H})} = Q_{ns,2p}^{(\text{H})} + Q_{np,2s}^{(\text{H})} + Q_{nd,2p}^{(\text{H})} \quad (41)$$

as defined in Eq. (36).

Since we can not measure the individual contributions in Eq. (41) but only in the sum of them from Eq. (40), we can not determine the level cross sections in our experiment. What we measure is the total hydrogen Balmer electron impact optical excitation cross section given by Eqs. (36), (40) and (41) and rewritten as

$$Q_{\text{HBalmer}}^{(\text{H})} = \frac{J_{\text{HBalmer}}^{\text{ON}} - \frac{n_{\text{H}_2}^{\text{ON}}}{n_{\text{H}_2}^{\text{OFF}}} J_{\text{HBalmer}}^{\text{OFF}}}{n_{\text{H}} \frac{I_e}{e}} \quad (42)$$

In Eq. (42), the ratio $n_{H_2}^{ON}/n_{H_2}^{OFF}$ is obtained by monitoring a molecular band. The absolute number of photons are determined by comparing the radiation from the excitation chamber with a standard lamp. The reader is referred to Sharpton [16] for a complete discussion of this technique. The electron beam current I_e is monitored by a precision ammeter and n_H is obtained from mass conservation considerations and knowledge of the number density of hydrogen molecules in the electron beam when the Wood tube is off.

The argument that leads to a value of n_H follows. The flow rate \dot{N} of a gas in particles per second through a hole in the Wood tube wall is

$$\dot{N} = \frac{1}{4}n\langle v \rangle A \quad (43)$$

where n is the density of particles in the chamber, $\langle v \rangle$ is the average velocity of the particles in the chamber, and A is the area of the hole. When the Wood tube is off all particles in the gas are molecules. When the Wood tube is on, we have both hydrogen atoms and molecules. Applying conservation of hydrogen atoms to relate the two conditions we have

$$\dot{N}_{H_2} = \frac{1}{2}\dot{N}_H + \dot{N}'_{H_2} \quad (44)$$

Then by substituting Eq. (43) into Eq. (44) we have

$$\frac{1}{4}n_{H_2}\langle v_{H_2} \rangle = \frac{1}{8}n_H\langle v_H \rangle + \frac{1}{8}n'_{H_2}\langle v'_{H_2} \rangle \quad (45)$$

The atoms and molecules are in thermal equilibrium when the discharge tube is on so,

$$m_H\langle v_H^2 \rangle = m_{H_2}\langle v_{H_2}^2 \rangle \quad (46)$$

Thus,

$$v_H = \sqrt{2} v_{H_2}' \quad (47)$$

Then Eq. (45) becomes

$$n_{H_2} \frac{\langle v_{H_2} \rangle}{\langle v_H \rangle} = \frac{1}{2} n_H + \frac{n_{H_2}'}{\sqrt{2}} \quad (48)$$

so that

$$n_H = 2 \left[n_{H_2} \frac{\left(\frac{8kT_{\text{off}}}{\pi m_{H_2}} \right)^{\frac{1}{2}}}{\left(\frac{8kT_{\text{on}}}{\pi m_H} \right)^{\frac{1}{2}}} - \frac{n_{H_2}'}{\sqrt{2}} \right] \quad (49)$$

where T_{off} and T_{on} are the gas temperature with the Wood tube off and on respectively. Equation (49) simplifies to

$$n_H = \sqrt{2} \left[n_{H_2} \left(\frac{T_{\text{off}}}{T_{\text{on}}} \right)^{\frac{1}{2}} - n_{H_2}' \right] \quad (50)$$

In the region of the discharge tube where the sidearm is located, the temperature is at most approximately 40° C above room temperature. If there is diffuse scattering in the arm that is attached to the Wood tube, we would expect the temperature dependence in Eq. (50) to be reduced even further. Walker [12] presented a survey of the controversy still shrouding the question of whether or not reflection by Pyrex glass surfaces is diffuse or specular. His conclusion from his literature search was that the reflection is more apt to be diffuse than specular. Thus, if we assume that the temperature change in the discharge has no effect as Walker did, the number density of hydrogen in the electron beam can be approximated by the expression

$$n_H = \sqrt{2} [n_{H_2}^{off} - n_{H_2}^{on}] . \quad (51)$$

Implied in the above derivation is that the only particles that contribute to the hydrogen beam are either neutral atoms or molecules. A primary reason for carrying out the investigations in Chapter IV was to determine whether this assumption was valid. In a situation where it is not valid, the photon flux $J_{HBalmer}^{on}$ might contain enough radiation from electron-ion interactions to invalidate both the shape of the excitation function and the absolute value of the cross section. We also assume in the above derivation that the angular dispersion of the gas as it leaves the Wood tube nozzle is the same for when the tube is off and on. Combining Eq. (51) with the expression for the optical excitation cross section given by Eq. (42) we have

$$Q_{HBalmer}^{(H)} = \frac{J_{HBalmer}^{on} - \frac{n_{H_2}^{on}}{n_{H_2}^{off}} J_{HBalmer}^{off}}{\sqrt{2} n_{H_2}^{off} \left[1 - \frac{n_{H_2}^{on}}{n_{H_2}^{off}} \right] \frac{I_e}{e}} . \quad (52)$$

The density $n_{H_2}^{off}$ is measured by comparing the radiation from the collision chamber under static and flow conditions. The photon flux is obtained by comparing radiation from the collision chamber with a standard light source and the ratio $n_{H_2}^{on}/n_{H_2}^{off}$ is determined by monitoring molecular band intensity ratios.

Theoretical Calculations

Much theoretical work has been done on atomic hydrogen electron impact excitation cross sections. Much of it is reviewed by Moiseiwitch

and Smith [11]. Vainshtein [55] has calculated the level excitation cross sections for atomic hydrogen for the s, p, and d states using the Born approximation. These calculations are for $n = 2$ through 9 and for electron energies of 1.16 through 24.04 threshold units. Although there are other types of theoretical calculations, results for the upper hydrogen level excitation cross sections have not appeared in the literature. The reader is referred to Mott and Massey [35], Massey and Burhop [56], McDaniel [57], and Moiseiwitch and Smith [11] for more detailed information on these other methods of calculations. These authors analyze the relative merits of the different methods and give the reader insight into what to expect experimentally for the excitation cross sections for atomic hydrogen.

If we rewrite Eq. (31) we can obtain single theoretical optical excitation cross sections. We have for example

$$Q_{3s,2p} = B_{3s,2p} Q(H,3s) + B_{3s,2p} \sum_{\text{upper}} Q_{\text{upper},3s} \quad (53)$$

The first term on the right side of the equation is the contribution to the optical excitation function due to direct electron excitation of the 3s level. The second term is the contribution of radiation resulting from excitation of higher levels and subsequent cascade to the 3s level. In Table 4 we have tabulated the single optical cross sections obtained by evaluating equations such as Eq. (53) and used the data of Vainshtein [55]. Each total optical excitation cross section Q_{HBalmer} is the sum of three single optical excitation cross section $Q_{ns,2p}$, $Q_{np,2s}$, and $Q_{nd,2p}$, respectively. The branching ratios also needed for calculating the s, p and d optical excitation cross sections were

TABLE 4
OPTICAL CROSS SECTIONS CALCULATED FROM THE THEORETICAL RESULTS OF VAINSHTEIN REF 55.
 $Q(n\ell \text{ to } 2\ell) 10^{-3} \pi a_0^2$

Energy eV	Q _{3s,2p}			Q _{3p,2s}			Q _{3d,2p}			SUM		Q _{4s,2p}			Q _{4p,2s}			Q _{4d,2p}			SUM
	Direct Excit.	Direct Cascade	Total	Direct Excit.	Direct Cascade	Total	Direct Excit.	Direct Cascade	Total			Direct Excit.	Direct Cascade	Total	Direct Excit.	Direct Cascade	Total	Direct Excit.	Direct Cascade	Total	
13.93	39.3	3.051	42.34	16.64	1.458	18.1	15.0	0.339	15.3	75.74	14.79	8.256	0.401	8.66	.684	.035	7.193	5.267	.128	5.4	13.459
19.70	43.1	4.530	47.6	25.02	1.488	26.51	21.4	0.505	21.9	96.01	20.91	8.954	0.592	9.55	.893	.040	9.33	7.42	.189	7.61	17.895
29.30	33.7	4.587	38.3	25.72	1.392	27.11	19.9	0.510	20.4	85.81	31.11	6.977	0.597	7.57	.906	.032	9.39	6.79	.190	6.98	17.127
42.76	24.8	4.073	28.9	23.13	1.051	24.18	16.0	0.452	16.5	69.58	45.39	5.111	0.528	5.64	.806	.024	8.30	5.439	.168	5.61	14.474
60.05	18.3	3.472	21.8	19.94	0.789	20.73	12.5	0.386	12.9	55.43	63.75	3.767	0.450	4.22	.688	.018	7.06	4.217	.143	4.36	11.842
81.19	13.8	2.936	16.7	16.87	0.602	17.47	9.73	0.326	10.1	44.27	86.19	2.843	0.380	3.22	.582	.014	5.96	3.285	.121	3.41	9.692
135.0	8.51	2.128	10.6	12.39	0.375	12.77	6.20	0.237	6.4	29.77	143.3	1.750	0.274	2.02	.422	.009	4.31	2.086	.088	2.17	6.682
204.2	5.69	1.605	7.30	9.333	0.252	9.59	4.22	0.178	4.39	21.28	216.8	1.169	0.207	1.38	.317	.006	3.24	1.415	.066	1.48	4.858
288.7	4.05	1.242	5.29	7.292	0.180	7.47	3.03	0.139	3.17	15.93	306.5	0.831	0.160	0.99	.247	.004	2.51	1.013	.051	1.06	3.669
	Q _{5s,2p}			Q _{5p,2s}			Q _{5d,2p}			SUM		Q _{6s,2p}			Q _{6p,2s}			Q _{6d,2p}			SUM
	Direct Excit.	Direct Cascade	Total	Direct Excit.	Direct Cascade	Total	Direct Excit.	Direct Cascade	Total			Direct Excit.	Direct Cascade	Total	Direct Excit.	Direct Cascade	Total	Direct Excit.	Direct Cascade	Total	
15.15	3.113	.053	3.17	2.867	.056	2.92	2.469	.037	2.51	8.60	15.31	1.57	none	1.57	1.607	1.607	1.31	1.31	1.31	4.487	
21.42	3.365	.078	3.44	4.236	.064	4.30	3.449	.054	3.50	11.24	21.65	1.69	none	1.69	2.368	2.368	1.83	1.83	1.83	5.888	
31.87	2.613	.078	2.69	4.271	.052	4.32	3.145	.054	3.20	10.21	32.21	1.31	none	1.31	2.392	2.392	1.66	1.66	1.66	5.362	
46.49	1.912	.069	1.98	3.788	.039	3.83	2.509	.048	2.56	8.37	46.99	.958	none	.958	2.106	2.106	1.32	1.32	1.32	4.384	
65.30	1.408	.059	1.47	3.221	.029	3.25	1.940	.041	1.98	6.7	66.00	.705	none	.705	1.797	1.797	1.02	1.02	1.02	3.522	
88.29	1.059	.050	1.11	2.726	.022	2.75	1.509	.034	1.54	5.4	89.23	.531	none	.531	1.511	1.511	.793	.793	.793	2.835	
146.8	.651	.036	.687	1.971	.014	1.98	.960	.025	.985	3.652	148.4	.327	none	.327	1.096	1.096	.504	.504	.504	1.527	
222.0	.435	.027	.462	1.487	.009	1.50	.650	.019	.669	2.631	224.4	.219	none	.219	.822	.822	.342	.342	.342	1.383	
314.0	.310	.021	.33	1.152	.007	1.16	.466	.015	.480	1.97	317.3	.156	none	.156	.639	.639	.245	.245	.245	1.040	

obtained by using transition probabilities given by Condon and Shortley [50]. Only the direct excitation term, and the direct cascade terms were included in the calculation.

Both are listed in Table 5. Since Condon and Shortley list only transition probabilities for the first six n levels of the hydrogen atom, not all of Vainshtein's data could be used. Likewise, Vainshtein lists only s , p , and d -level excitation cross sections so not all of Condon and Shortley's data could be used. In Figs. 16-19 the component optical excitation cross sections taken from Table 4 are presented. Walker [12] has carried out similar calculations using different transition probabilities. The reader is referred to his work for calculations using all of Vainsthein's level cross section data. Branching ratios calculated from transition probabilities given by Condon and Shortley are listed in Table 5.

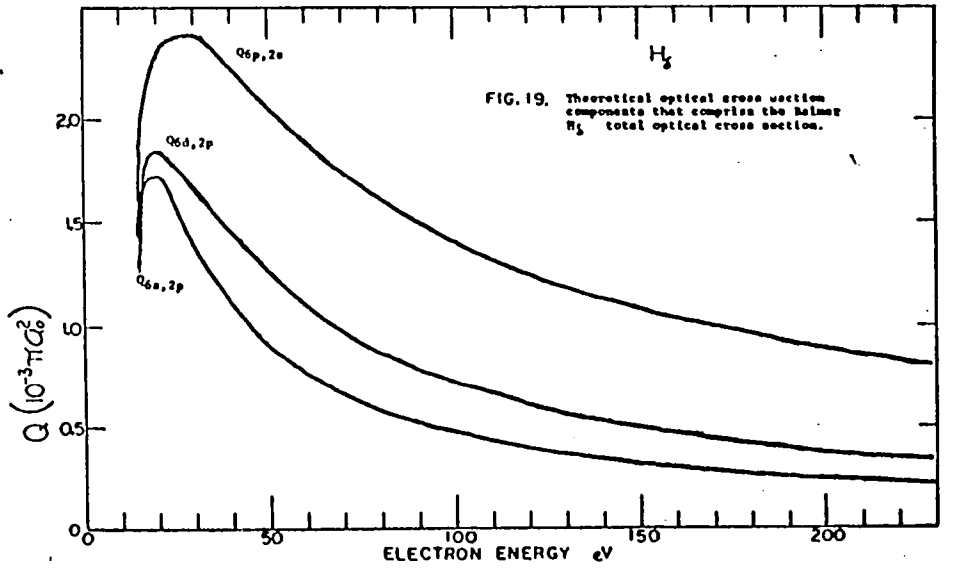
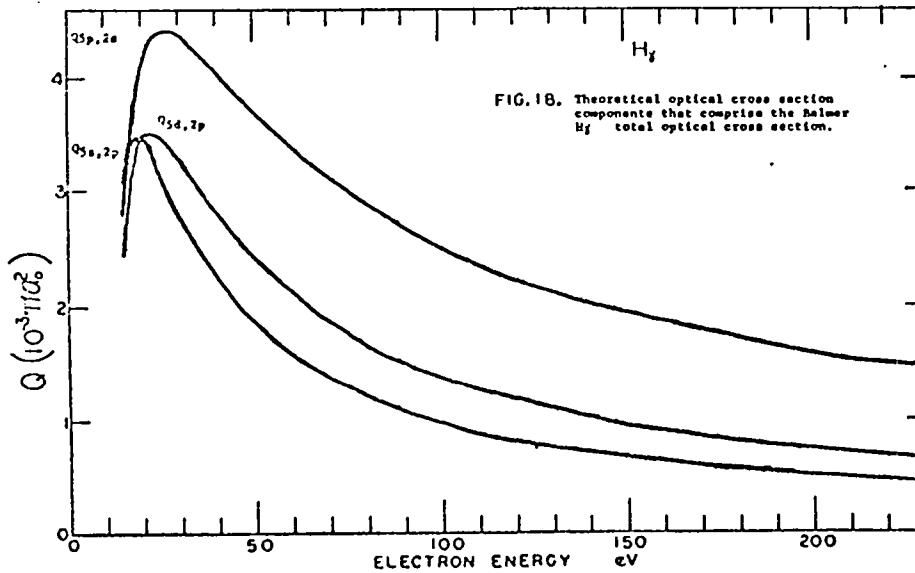
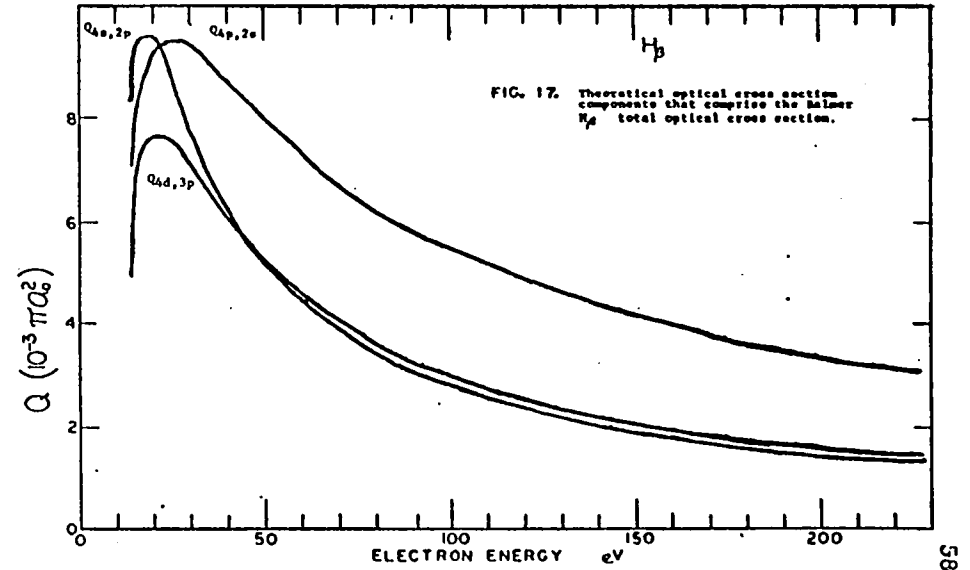
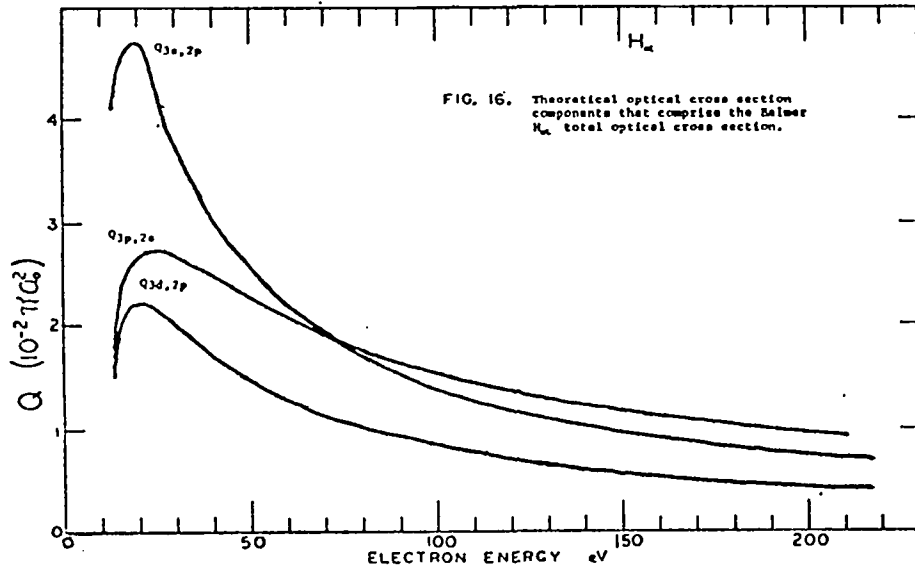


TABLE 5

BRANCHING RATIOS AND TRANSITION PROBABILITIES FROM CONDON + SHORTLEY⁵⁰

LOWER LEVEL CONFIGURATION $n'l'$ $n' < n$
 $l' = l \pm 1$

UPPER LEVEL CONFIGURATION $n'l$	$\sum_{n'l'} A_{n'l, n'l'} \cdot 10^{-8} \text{ sec}^{-1}$		* $A_{n'l, n'l'} \cdot 10^{-8} \text{ sec}^{-1}$		** $B_{n'l, n'l'}$		$A_{n'l, n'l'} \cdot 10^{-8} \text{ sec}^{-1}$		$B_{n'l, n'l'}$		$A_{n'l, n'l'} \cdot 10^{-8} \text{ sec}^{-1}$		$B_{n'l, n'l'}$	
	10^{-8} sec^{-1}	10^{-8} sec^{-1}	10^{-8} sec^{-1}	10^{-8} sec^{-1}	10^{-8} sec^{-1}	10^{-8} sec^{-1}	10^{-8} sec^{-1}	10^{-8} sec^{-1}	10^{-8} sec^{-1}	10^{-8} sec^{-1}	10^{-8} sec^{-1}	10^{-8} sec^{-1}	10^{-8} sec^{-1}	10^{-8} sec^{-1}
			2p		3p		4p		5p					
2s	0													
3s	.063	.063	100.00											
4s	.043	.025	58.14	.018	41.86									
5s	.027 ₇	.012 ₇	45.85	.008 ₅	30.69	.006 ₅	23.46							
6s	.017 ₆	.007 ₃	41.48	.005 ₁	28.98	.003 ₅	19.88	.0017	9.66					
			1s	2s	3s	3d	4s	4d	5s	5d				
2p	6.25	6.25	100.00											
3p	1.86	1.64	88.2	.22	11.8									
4p	.81	.68	84.2	.095	11.8	.030	3.71							
						.003	.4							
5p	.415	.34	81.7	.049	11.8	.016	3.8	.007 ₅	1.8					
						.001 ₅	.4	.002 ₅	.5					
6p	.243	.195	80.3	.029	11.9	.009 ₆	3.95	.004 ₅	1.85	.0021	.86			
						.0007	.29	.0009	.37	.0010	.41			
			2p	3p	4p	4f	5p	5f						
3d	.64	.64	100.00											
4d	.274	.204	74.5	.070	25.5									
5d	.142	.094	66.2	.034	23.9	.014	9.9							
						.000 ₅	.4							
6d	.080	.048	60.1	.0187	23.4	.008 ₆	10.8	.0040	5.0					
						.0002	.25	.0004	.5					
			3d	4d	5d	5f								
4f	.137	.137	100.00											
5f	.071	.045	63.4	.026	36.6									
6f	.0412	.021	50.9	.0129	31.3	.0072	17.4							
						.0001	.2							
			4f	5f										
5g	.042	.042 ₅	100.00											
6g	.0247	.0137	55.5	.0110	44.5									
			5g											
6h	.0154	.0154	100.00											

* $A_{n'l, n'l'}$ is the Einstein spontaneous transition probability from a single upper level $n'l$ to a single lower level $n'l'$.

** $B_{n'l, n'l'}$ is the branching ratio. It is the percentage of a large number of atoms in single excited state $n'l$ that will eventually make a transition to the specified single lower state $n'l'$. Expressed as a percentage it is

$$B_{n'l, n'l'} = \frac{A_{n'l, n'l'}}{\sum_{n'l'} A_{n'l, n'l'}} \times 100\%$$

CHAPTER IV

HYDROGEN BALMER STUDIES IN A FLOW SYSTEM

Introduction

The earliest reported work on the excitation cross sections of atomic hydrogen is that of Ornstein and Lindeman in 1933. They crossed an electron beam from an electron gun with atomic particles flowing from the positive column of a Wood tube. Since that time, a number of other atomic hydrogen excitation measurements have been reported. In a critical survey of these efforts Moiseiwitsch and Smith [11] conclude that there needs to be additional work done to confirm the measurements now in the literature, and to extend the range of information available.

It is well known that atomic hydrogen offers relatively little resistance to theoretical analysis. Thus, much has been carried out. Clearly, it would be highly desirable and important to compare experimental results with these calculations. Considering how important such a comparison is, one may wonder why in the forty years since the first report of hydrogen excitation was made there has not been a significant number of successful measurements. The answer is that production and experimental investigation of atomic hydrogen has proven to be very difficult. The "successful" measurements that have been reported were obtained under severely limiting conditions. So limiting then were that others have been discouraged from pursuing the goal of obtaining these measurements. Moiseiwitsch and Smith [11] concluded that progress

has been impeded most by the technical problem of producing dissociated hydrogen in the laboratory in an adequately pure state and in sufficient concentration. But this is not the only problem. During the past forty years of experimental effort a number of equally important arguments have been proposed by experimentalists and theorists alike regarding the successful completion of an atomic hydrogen investigation.

In the most recent work on atomic hydrogen excitation, Walker [12,14] modified the Wood tube, improved on Ornstein and Lindeman's [13] cross beam design and took advantage of recent improvements in high vacuum technology in an effort to improve the atomic hydrogen concentration problem, but no effort was made with regard to the other questions. Walker [14] obtained data concerning atomic hydrogen excitation at high energies using his flow system. The present work was initiated for the purpose of conducting the difficult experiments necessary to evaluate these high energy measurements. In addition to accomplishing this goal we have obtained H_{α} , H_{β} , H_{γ} , H_{δ} Balmer optical excitation functions of atomic hydrogen from onset to 190 volts.

Basic Considerations in Atomic Hydrogen Measurement

Perhaps the most relevant concerns regarding experimental measurement of electron excitation cross sections of atomic hydrogen that have been proposed in the last forty years relate to:

- A. Pressure
- B. Molecular Background
- C. The Electron Gun Characteristics
- D. Stark Effects

These areas are discussed in the following sections. In order to examine

these areas of concern, some changes were made in Walker's [14] system. Although these changes were made, all of the arguments below apply to both systems.

A. Pressure. As described in Chapter II, we experimentally determined that excited atom-molecule cross sections on the order of 10^{-13}cm^2 caused non-linear pressure effects in molecular hydrogen. In helium such two body interactions severely distort excitation functions obtained at pressures greater than 5 mtorr of pressure. In addition resonance trapping of the n P states enhances this distortion. In helium, resonance trapping has been measured to be significant at pressures as low as .5 mtorr [58]. In our studies we have conducted investigations at pressures lower than 1 mtorr so that atom-molecule interaction reported in Chapter I insignificantly affect our excitation functions. In our hydrogen flow system resonance trapping is also negligible for two reasons. First, outside the particle beam the back ground gas is primarily molecular. Thus, atomic resonance trapping can only occur in the particle beam. This greatly decreases the likelihood of any noticeable experimental effect. Second, we have found that the atomic hydrogen density in the atomic beam is on the order of .1 mtorr. This is below the pressure we can expect resonance trapping to become significant.

Another pressure effect has to do with the particle beam coming from the Wood tube nozzle. We have not been able to determine definitely if the angular distribution of beam particles changes when the Wood tube is turned off and on. In the work reported here, the background pressure in the excitation chamber decreased approximately 2 per cent when the Wood tube was turned on. Since the Wood tube operated at

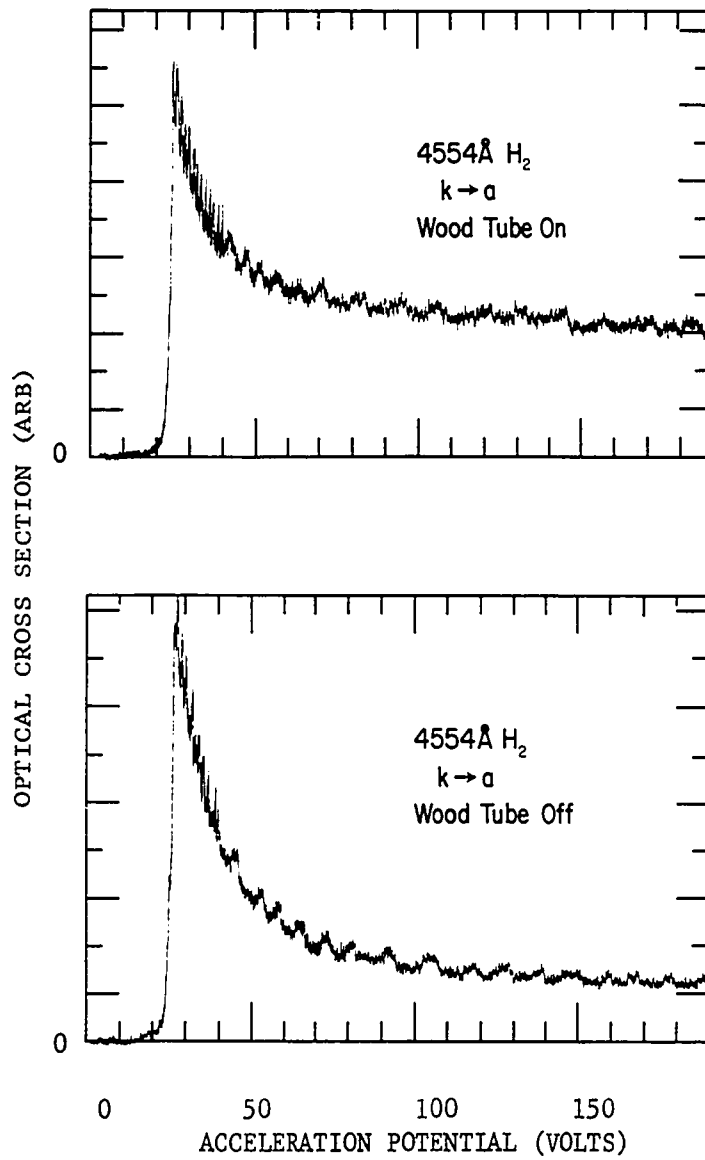


FIG. 20 Optical excitation functions of the 4554 Å k to a molecular transition with the Wood tube cathode close to the nozzle arm.

approximately 40° C above room temperature, we suspect that the angular distribution of particles is narrowed slightly with the Wood tube on.

Finally, we have found that the performance of the electron gun and consequently the shape of optical excitation functions are pressure dependent. This phenomena will be considered in the electron gun discussion.

B. Molecular Background. In Chapter II the molecular spectrum background problem was eliminated from Balmer excitation functions by closing down the slits on the monochromator and increasing the sensitivity of the phase sensitive detector. In the crossed beam investigation of atomic hydrogen molecular background radiation is experimentally eliminated when the difference of the excitation function, obtained when the Wood tube is on and off, is taken to find the electron-atom contribution to the excitation function obtained with the Wood tube on. Exceptions to this occur when secondary processes produce results when the Wood tube is on differing from those when it is off. This did happen when the power supply was connected to the Wood tube so that the cathode was nearest the nozzle arm. In Fig. 20 is the optical excitation functions of the 4554 Å k to a molecular transition. Note that the tail is higher with the Wood tube on. A change in the shape of the excitation function occurred in all other molecular transitions investigated. The change was different for each transition and was even different for different upper vibrational levels. It is interesting to note that of four molecular lines investigated only the 5055 Å N to B optical excitation cross section showed the decrease in intensity with the Wood tube on as predicted in Chapter III. The 5055 Å line was the line Walker [12,14]

used in his data analysis. To eliminate any question as to whether or not this phenomena occurred in his system, Fig. 21 shows the 4634 Å G to B taken on his system before any changes were made and were taken within four hours of time the excitation functions were taken in Ref. 14.

We found that the problem was negligible when we connected the power supply so that the Wood tube anode was the closest electrode to the nozzle arm. The atomic excitation functions reported herein were obtained with the electrodes connected in this manner.

C. Electron Gun Characteristics. An analysis of the electron gun characteristics was made in the flow system just as it had been made on the static system. See Fig 5 and the discussion in Chapter II. The composite of the electron gun characteristics for the flow system is shown in Fig. 22. The interpretation is the same as for Fig. 5. The dark lines are the upper limits of linearity for the three background pressures of .1 mtorr, .3 mtorr, and .5 mtorr. As in the static system the upper limit of linear operation increases if either the pressure or the electron energy is increased. Each pressure curve study was started at .5 eV or less from the onset of the H_β excitation function. The onset is indicated by a dotted vertical line and the graph shows that the onset of H_β varied with pressure. The onset potential is approximately 23.5, 22.5, 22.0 and 20.5 V for pressures of .1, .3, .5 mtorr with the Wood tube off and .5 mtorr with the Wood tube on respectively. We will designate the difference in the values of the acceleration potential and the electron energy, both measured relative to the cathode, as the potential shift. It is due to contact potentials, electronic

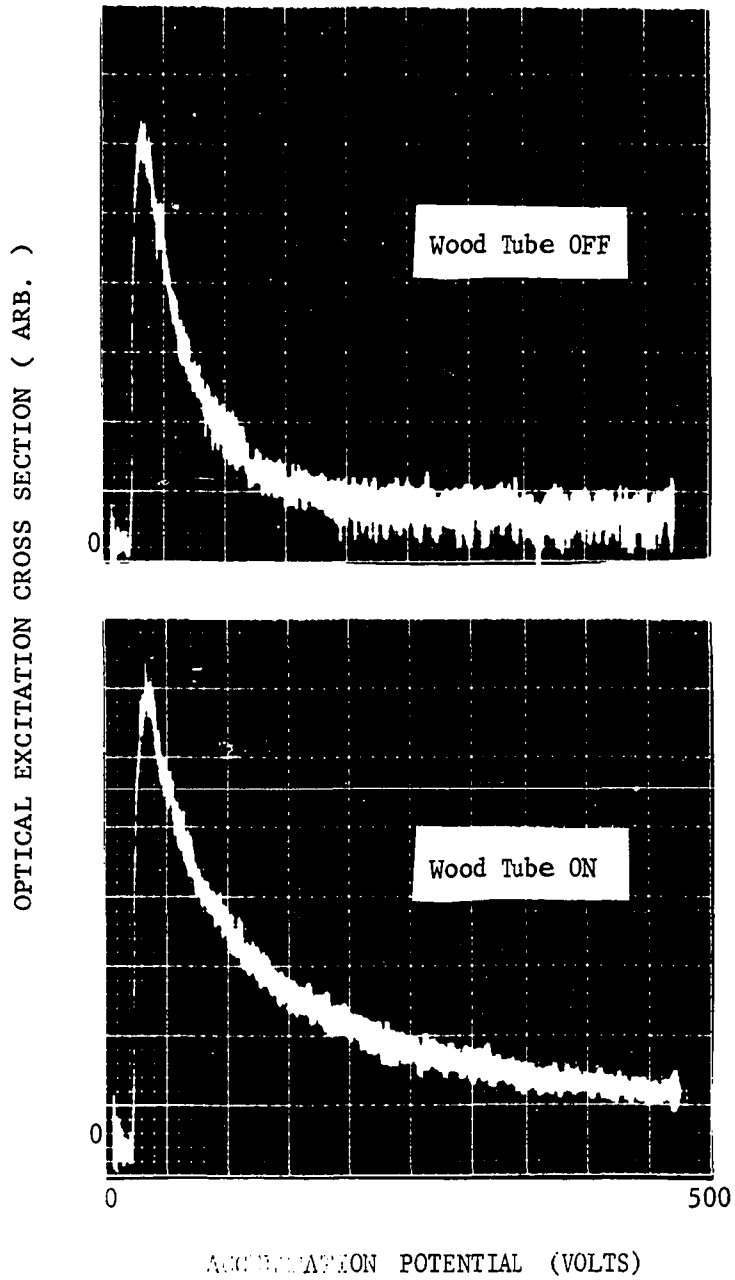
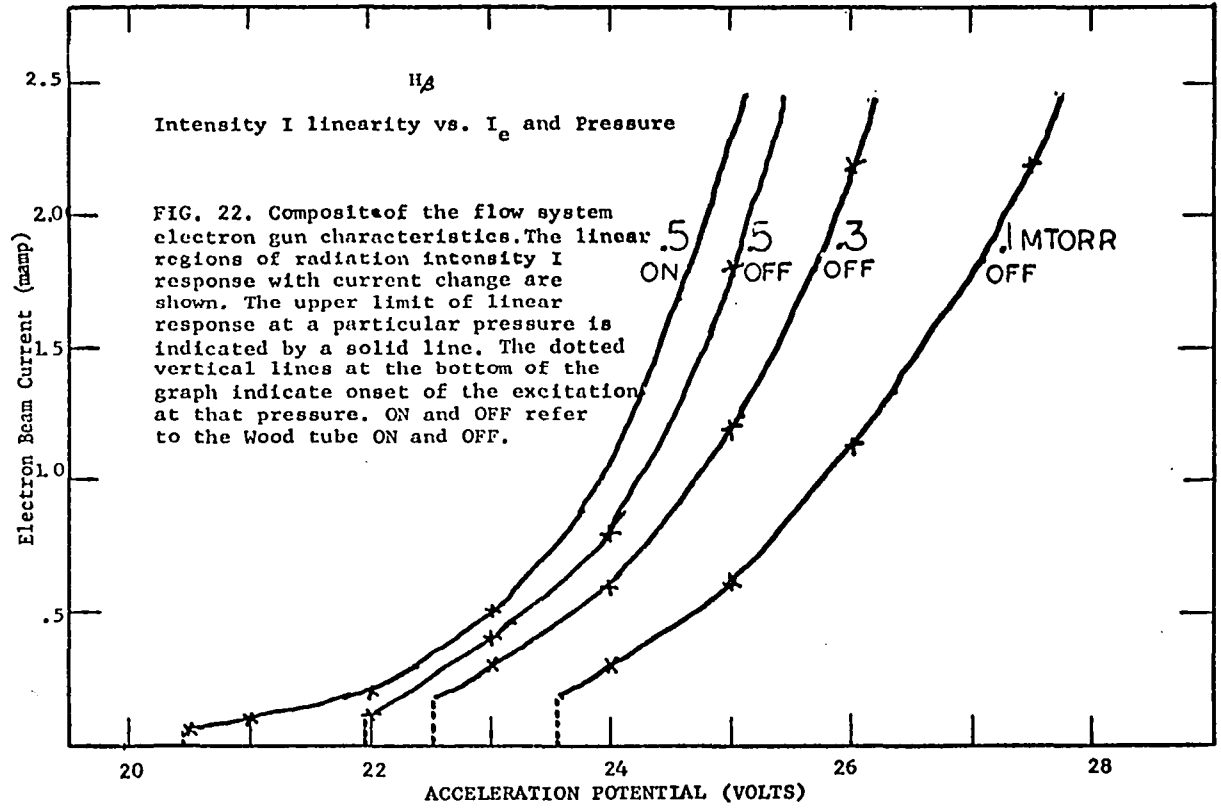


FIG. 21. Optical excitation cross sections of the 4634 Å G to B transition in molecular hydrogen. These functions were obtained on the same equipment in the same manner and at the same time as the data reported by Walker in Ref. 14.



space charge, positive ion space charge, and the penetration of fields from other electrodes.

Part of the shift in contact potential when the Wood tube is on is due to the excitation of atomic hydrogen as the energy required for excitation of $n = 3$ level of H is lower in H than in H_2 . Figures 23 and 24 show dramatic evidence of the presence of atomic hydrogen. In Fig. 23 the Wood tube current is from top to bottom, 200, 100, 50 and 0 ma. The onset energy of the electron-atom excitation function is 12 eV for the production of H_α and that of the electron-molecule excitation function is 16.5 eV. Clearly, there is not 4.5 V difference in the onsets with the Wood tube on and off. The spectroscopic evidence is too strong to suspect that theory is in error. Most likely the electron gun has a variable potential shift with electron energy. From Fig. 24 we add more strength to this argument. The upper excitation function with the Wood tube on was taken at .8 mtorr background pressure while the lower function was taken at .5 mtorr with the Wood tube on. Note that the molecular excitation function has shifted approximately 1.5 eV while the atomic hydrogen excitation function has shifted approximately 3.0 eV.

The change in the potential shift when the Wood tube is turned off and on and when the pressure is changed is totally due to the number density of ions around the grids of the electron gun. Also, the current drawing capabilities of the electron gun are largely affected by ions. When the pressure is changed in the system, the current drawing capabilities of the electron gun as well as the onset voltages of excitation functions changes. The same is true when different gases are introduced

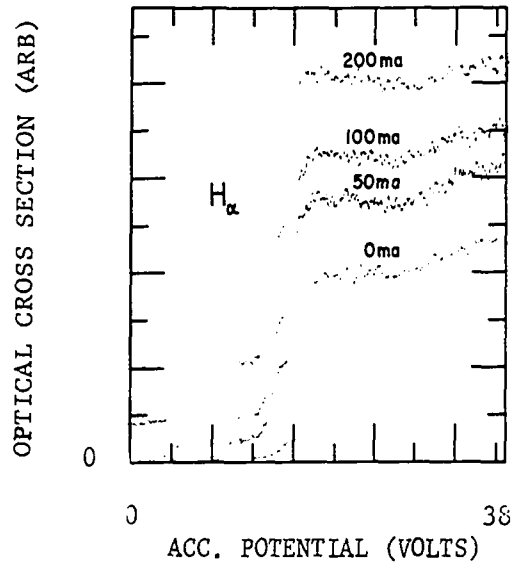


FIG. 23. Optical excitation functions change when Wood tube currents change.

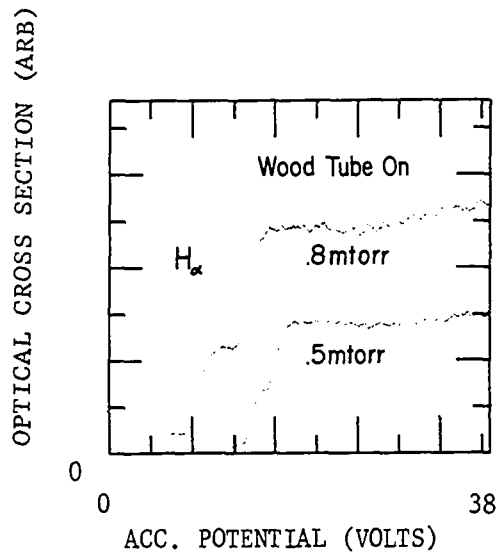


FIG. 24. Optical excitation functions change when the pressure is changed.

in the system. With hydrogen gas in the system, the electron gun produced over twice as much current as when nitrogen at an identical pressure was used.

In all our experiments with the Wood tube we found that the electron gun current increased when the Wood tube was turned on. In nitrogen the beam current increased as much as a factor of four. Clearly, a significant number density of ions reaches the electron gun from the Wood tube.

Although these non-linear electron gun characteristics exist in all such devices, to our knowledge such information as revealed in the electron gun characteristics composites Fig. 5 and 22 is not found in the literature. In other most experimental investigations it is not an important factor. Usually an excitation function is obtained from 0 to 500 eV as in Figs. 13 and 22. The distortion that occurs in the first few electron volts of the excitation function onset is not obvious from such data. Such experimental results are often compared with theory. Since the Born approximation and other theories are only good for higher electron energies, particular attention is not paid to the excitation onset. When excitation function onset obtained in such investigations show a shift, traditionally it is taken as a constant for all voltages. A correction is thus made by simply shifting the excitation over so its onset corresponds to the spectroscopically determined value. These shifts in a static system are on the order of 1 to 5 eV.

The potential shift observed in this investigation was on the order of 7 to 10 V. Although it is clear from Figs. 23 and 24 that the potential shift is not constant with electron energy, we made such an

assumption in order to analyze our data. This will be discussed later.

Fower [59] has proposed in an article:

"In most of the experiments it has been assumed that grids introduced in the gas discharge would influence the discharge by the laws of vacuum electrostatics, and hence that the accelerating potentials are accurately known. This may be doubted, owing to the well known impotence of control grids in gas discharges because of sheath formation. It is probably that the entire discharge has been controlled by a Langmuir sheath about the cathode in all cases in which thermionic cathodes were used, rather than by the grids. Hence it is unlikely that the electron velocities were known with true precision."

This work supports his conclusion.

The electron gun was operated as closely to steady state conditions as possible. The electron beam was not chopped. Instead the light coming from the collision area was chopped for phase sensitive detection purposes. By using this method of chopping, we were able to avoid overloading the photomultiplier tube and phase sensitive detector by suppressing the noise level. We also were able to watch for secondary effects that might originate from the nozzle arm. We saw no such effects.

We made no attempt to chop the atomic particle beam from the Wood tube nozzle arm as our investigations revealed that the potential shift changed when the Wood tube was turned on. Modulation of an atomic particle beam and electronic subtraction of the intensity when the Wood tube is off from intensity obtained when the Wood tube is on would clearly produce data that would not take this change in potential shift into account. The resulting shape of the excitation function would be somewhat inaccurate.

Kleinpoppen [60] has used the chopped atomic beam method in

investigating H_{α} excitation. Since he used a tungsten oven for his investigation, he was not as inclined to have additional ions introduced in the excitation chamber region when the atomic beam was turned on. But still, atomic hydrogen is a different gas than molecular hydrogen and could yield a different electron gun characteristics composite. More than likely his electron gun was not as sensitive to pressure and gas changes as the one used in this experiment. Thus, we suspect that his results to be shown and discussed later, are a realistic reflection of the H_{α} excitation function.

Figure 25 reveals another problem encountered with the electron gun. The onset of the 4634 Å G to B molecular hydrogen excitation function is shown. Grid number two voltage of the electron gun was set at its maximum value of 250 volts. Between zero and 10 volts below the onset of the excitation energy an electron beam existed that caused a non-zero amount of radiation to be recorded. This radiation ceased when the grid number two voltage was reduced. The deflection at approximately 1.5 eV is where this test was carried out. The dip in intensity starting at about 6 eV indicates that this below onset radiation is affected by the accelerator grid voltages and can not be taken as constant. This onset was taken under static conditions in the collision chamber and at 8.25 mtorr. When the pressure was decreased in the chamber, the below onset radiation became relatively less intense than the excitation function. Except for one case, under flow conditions this phenomena was undetectable with respect to the intensity of the excitation functions themselves. The exception occurred in an investigation involving the nitrogen molecular ion and will be discussed later.

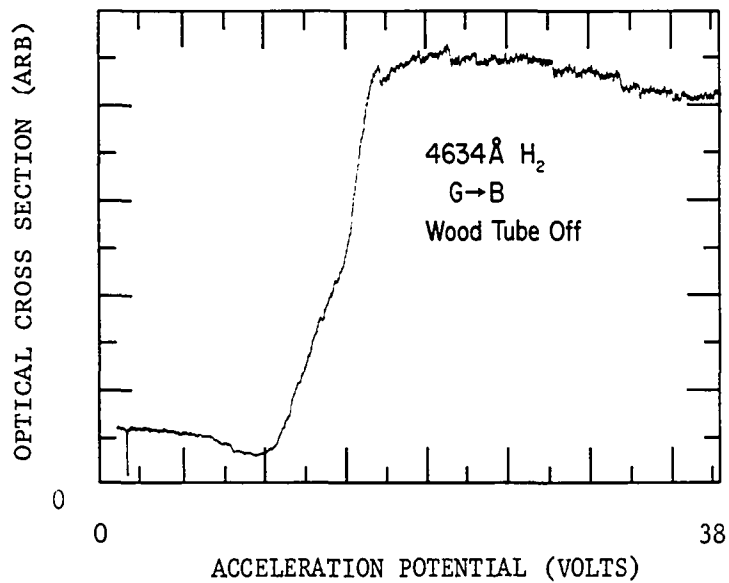


FIG. 25. Below onset an electron beam of high energy electrons exists in the collision chamber. It produces the non-zero below onset radiation shown. Its intensity is controlled by grid number two. This data was obtained under static conditions and at a pressure of 8 mtorr.

Finally, we viewed the electron beam at different pressures, electron energies, and current densities and could detect no change in beam shape.

D. Stark Effect. In the discussion on the electron gun characteristics we concluded that there is a significant number density of ions at the gun coming from the Wood tube when it is on. In Fig. 20 we have shown that the signal in the tail of the 4554 \AA k to a triplet excitation function increased absolutely when the discharge tube was turned on. By changing the power supply leads on the Wood tube so that the anode was closest to the nozzle arm we found we could eliminate most of this increase without significant reduction in the intensity due to electron-atom excitations. This perturbation in the molecular excitation functions can not be a pure pressure problem because the shape of the excitation functions change. It can not be an electron gun problem. If it were, every molecular excitation function produced would change in the same way. This was not observed. As stated before we found the intensity of the 5055 \AA N to B transition to decrease absolutely when the Wood tube was turned on. The only remaining explanations involve the atomic particles themselves and their pressure effects. Some or all of the following pressure effects could be responsible for this phenomena. They are

1. Excited atom-molecule interactions
2. Excited atom-atom interactions
3. Excited atom-ion interactions
4. Excited molecule-atom interactions
5. Excited molecule-ion interactions.

If these perturbations were ion dependent, then the ion number density from the Wood tube would probably be on the order of number density of the gas. From consideration of the Holtsmark theory in Chapter II there is evidence that these ions would create an electric field strong enough to mix the atomic hydrogen near degenerate ℓ -levels. The resulting atomic excitation cross sections obtained in the presence of such a field would not be directly comparable to present theoretical calculations.

Faced with this difficulty we inserted two thin 3 cm long probes in the middle of the Wood tube nozzle arm to determine if ions were responsible for the perturbation revealed in Fig. 20. By applying an electric field between the probes placed 1 cm apart, we hoped to collect all the ions and determine whether or not the ions were the perturbors. The probes were physically small so that significant atom recombination did not occur. Walker [12] surveys some of the work done on atomic hydrogen recombination and concludes that atomic hydrogen recombines much more swiftly on metallic surfaces than on glass.

The experiment met with limited success. Figure 26 shows that we were able to collect ions in the nozzle arm; however, the smoky pink-blue vapor - like hydrogen discharge that existed in the nozzle arm and originated from the Wood tube was not noticeably changed by the collection of these ions. We monitored the intensity of the 4554 \AA k to a triplet line in Fig. 20 and found only a very slight decrease in the perturbation effect when the power supply collecting ions was changed from zero to 450 volts. At higher voltages the gas between the probes would break down. In fact, that is what causes the spikes on the curve of

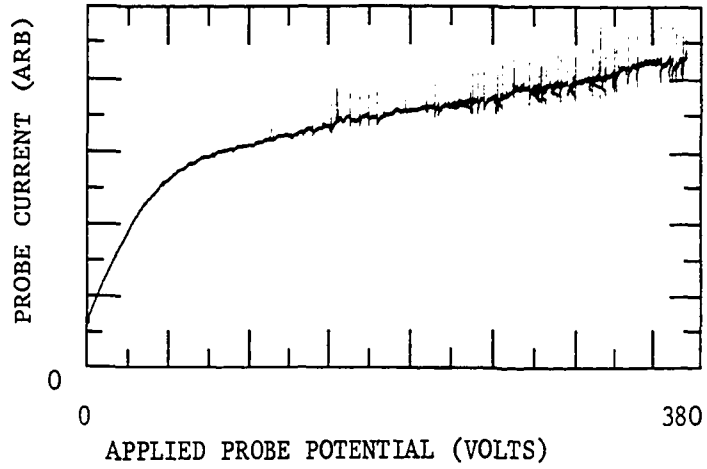


FIG. 26. Potential was applied to two 3cm long probes in the nozzle arm of the Wood tube. This current vs applied voltage curve resulted.

Fig. 26. We also noted that approximately an order of magnitude higher current was collected when the cathode of the Wood tube was placed nearest the nozzle arm.

We have concluded that ions are the interacting particles that cause the perturbation revealed in Fig. 20. And we also believe that our data is perhaps somewhat affected by fields produced by the ions. Whether the mechanism of the perturbation in Fig. 20 is due to excited atom-ion or excited molecule-ion interactions is still in question. Most likely it is excited molecule-ion interactions. In such processes there must be molecular states that gain energy and some that lose energy. Since the doubly excited 5055 Å N to B transition was found to decrease in intensity and the 4554 Å triplet line was found to increase, perhaps the doubly excited states are the feeders and the singly excited levels are the gainers. More work is required for a definite determination of the mechanism.

We feel that solution of the ion problem is a difficult but desirable step. If ions coming from the Wood tube are on the order of one-tenth the concentration of molecules and on the same order of concentration of hydrogen atoms, then their number density in this experiment would be on the order of 10^{12} ions/cm³. The upper limit of ion number densities that can be tolerated is between 10^8 and 10^9 ions/cm³ as we discussed in Chapter I. Thus, in order to claim field free atomic hydrogen H_α, H_β, H_γ and H_δ excitation functions we must eliminate 99.99% of the ions present in the nozzle arm. Atom-ion collisions in the flowing gas occur frequently enough to make this problem very difficult. Also, the method must not cause extensive recombination of hydrogen atoms.

The four areas just discussed are the ones that appear most in the literature. They are generally difficult to handle in a given experiment. So difficult are they that the experiments devised to determine their effects are generally far more difficult and extensive than those conducted to obtain the excitation function alone. Such was the case in this investigation. We have discussed the basic processes in atomic hydrogen measurement and our experimental results regarding them so that the reader would be better prepared to understand construction of the experimental system and the limitations of the results.

Throughout this entire research effort molecular hydrogen was used. In the next section information relating to the hydrogen molecule is discussed. In the following section, the experimental apparatus is presented. In the last section the experimental results are presented and discussed.

Molecular Hydrogen Studies

The helium atom has received the most attention in experimental electron impact excitation cross section work. The hydrogen molecule is much like a helium atom with a split nucleus but has received little. Brasefield [18] (1929) has shown that the singlet and triplet structure realized in helium excitation functions also appears in H₂ molecule excitation functions. Although there was some work done by Kruithoff and Ornstein [22] on the 4617 and 4634 Å transitions in the hydrogen molecule, no major study has been undertaken in electron impact excitation cross sections.

While conducting our atomic hydrogen studies in the static and

flow systems, we studied some of the transitions in the hydrogen molecule. Information on the molecular hydrogen is scattered and incomplete. Therefore, key aspects of the molecular hydrogen spectrum are discussed below for the benefit of those who may undertake a similar project in the future.

The spectrum of the hydrogen molecule is very complex. It is often referred to as the many line spectrum of hydrogen. When first encountering this spectrum, its comprehension appears impossible. In fact, historically, the spectrum defied analysis for many years. Today with the wavelength tables of Monk, Gale and Lee [39] or Kapuscinsk and Eymers [61] together with the monograph on molecular hydrogen by Richardson [40] the spectrum is at least attackable. The wavelength tables give the wavelength and wave numbers of thousands of lines of the secondary spectrum of hydrogen which were obtained with high resolution apparatus. Along with these lines the relative intensities are also listed. Richardson has arranged these lines in an internally consistent scheme such that most reported lines are identified with a specific transition. He compiles his scheme in tables and an energy level diagram. As expected, the energy level diagram is similar to atomic helium. Two major differences are the lack of high quantum number excited states in the molecule and the distinct presence of "double electron" excited states in the molecule. In Fig. 27 is the molecular hydrogen energy level diagram given by Dickie [62] with the triplet correction suggested by Sharp [41].

Although much is known about molecular hydrogen and its ions, a considerable amount of research remains to be done. Electron impact

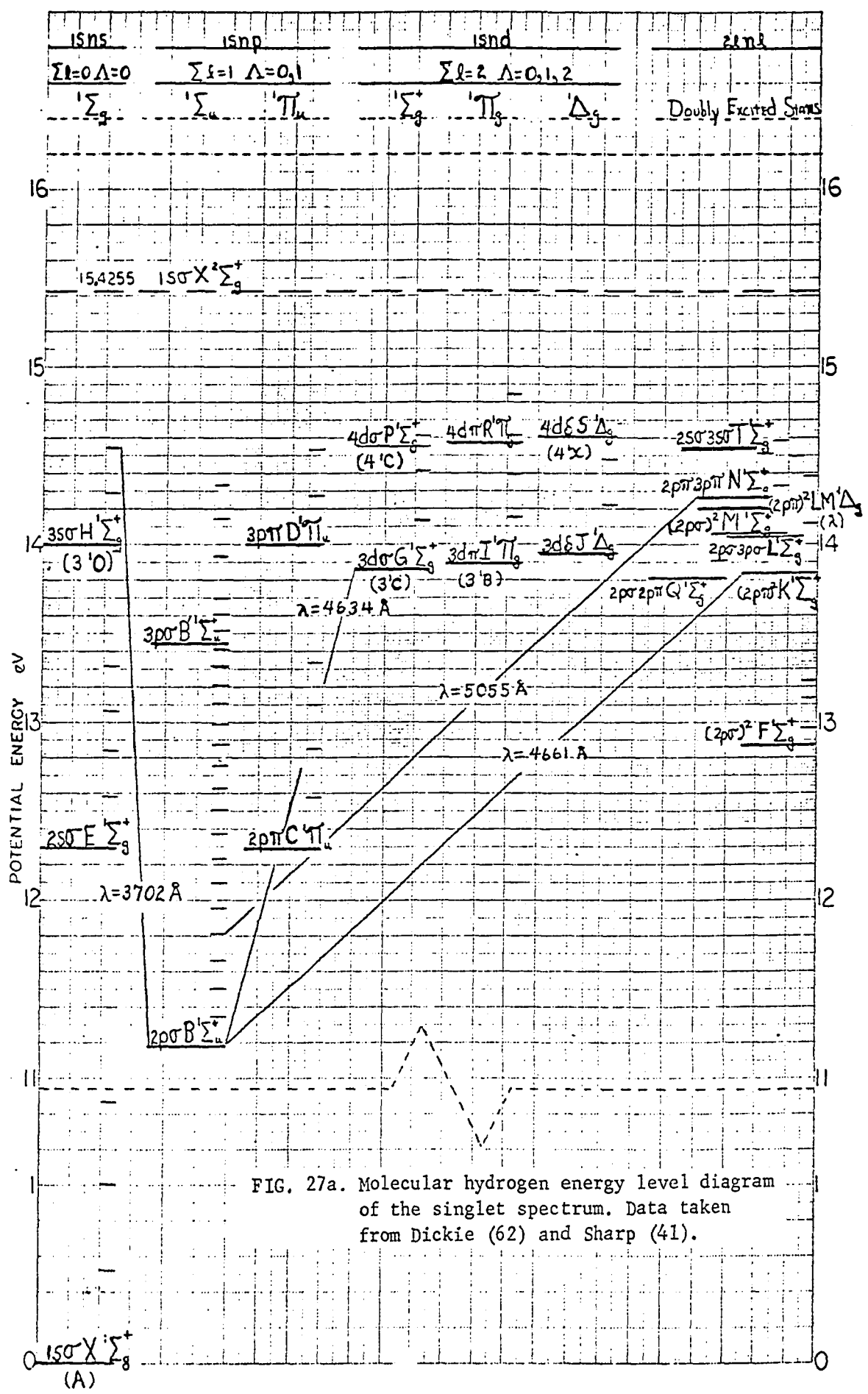


FIG. 27a. Molecular hydrogen energy level diagram of the singlet spectrum. Data taken from Dickie (62) and Sharp (41).

excitation cross sections of H_2 is one area that is essentially untouched. Possibly such cross section data will help answer some of the remaining questions about the hydrogen molecule.

Most of the H_2 visible spectrum results from transitions from quantum levels $(1s, n\ell)$ to $(1s, 2\ell)$ where n is 3 or greater. All published theoretical work has been done for excitation to lower quantum levels such as $B(1s, 2p)$, $C(1s, 2p)$, $D(1s, 3d)$ and $E(1s, 2s)$. Fajen [65] reviews some of the previous work as well as presents his own excitation cross sections for the B, C, and E levels.

Experimental Apparatus

The system that Walker [12] built and reported on in his dissertation suffered from phenomena that prohibited him from reporting optical excitation cross sections for electron energies less than 100 eV. Later he made the following modifications: (1) a high quality 4" Norton Model VHS4 Mexican hat diffusion pump was purchased to replace the 4" CVC 730 PMC, (2) Sanovac 5 replaced Dow Corning 704 silicone diffusion pump oil, (3) A 4" Norton Circular Chevron Cryo-Baffle cold trap was mounted just above the diffusion pump to limit backstreaming, (4) An Airco 4" valve was mounted immediately above the liquid nitrogen baffle so that the chamber could be closed off and used as a static system, (5) A stainless steel shield was nestled interior to the Pyrex chamber so as to reduce the stray electric fields due to charge build up on the glass, and (6) Finally the discharge tube nozzle was moved approximately 3 cm from the electron beam and was covered with aluminum foil and grounded to limit stray fields. Also an 80 per cent transparent fine nickle wire screen was placed over the nozzle outlet. After

these changes Walker obtained total optical excitation cross sections from 0 to 450 eV for H_{α} , H_{β} , H_{γ} , H_{δ} and H_{ϵ} [14].

This basic system was not changed when modifications were made to examine the questions discussed in the section, Basic Considerations in Atomic Hydrogen Measurement. His system, with modifications made for this research work, is presented in Fig. 28. A significant modification for this work is the addition of an MKS Baratron type 90 capacitance manometer to measure the background pressure in the collision chamber. For a limited time two probes were inserted in the Wood tube nozzle arm in an attempt to collect ions. A magnetic coil was also attached to the Wood tube outlet arm in an attempt to prohibit ions from flowing into the electron beam. Because of the random motion of the ions in the positive column of the glow discharge tube, the magnetic field has proven to have no effect as an ion flow control.

With the MKS Baratron we were able to continuously monitor the background pressure in the collision chamber and in the nozzle arm at a position midway between the Wood tube and the electron gun. The nozzle arm is approximately 30 cm in length. The Airco 4" valve can be closed and the system is then a static system. By comparing radiation intensity from the electron beam under static and flowing conditions we found that approximately 70 per cent of the gas particles in the electron beam are background particles and do not come directly from the nozzle. This high contribution of background particles is primarily hydrogen molecules. Because of this we always had a large contribution of molecular excitation radiation emerge from the collision chamber. We considered changing

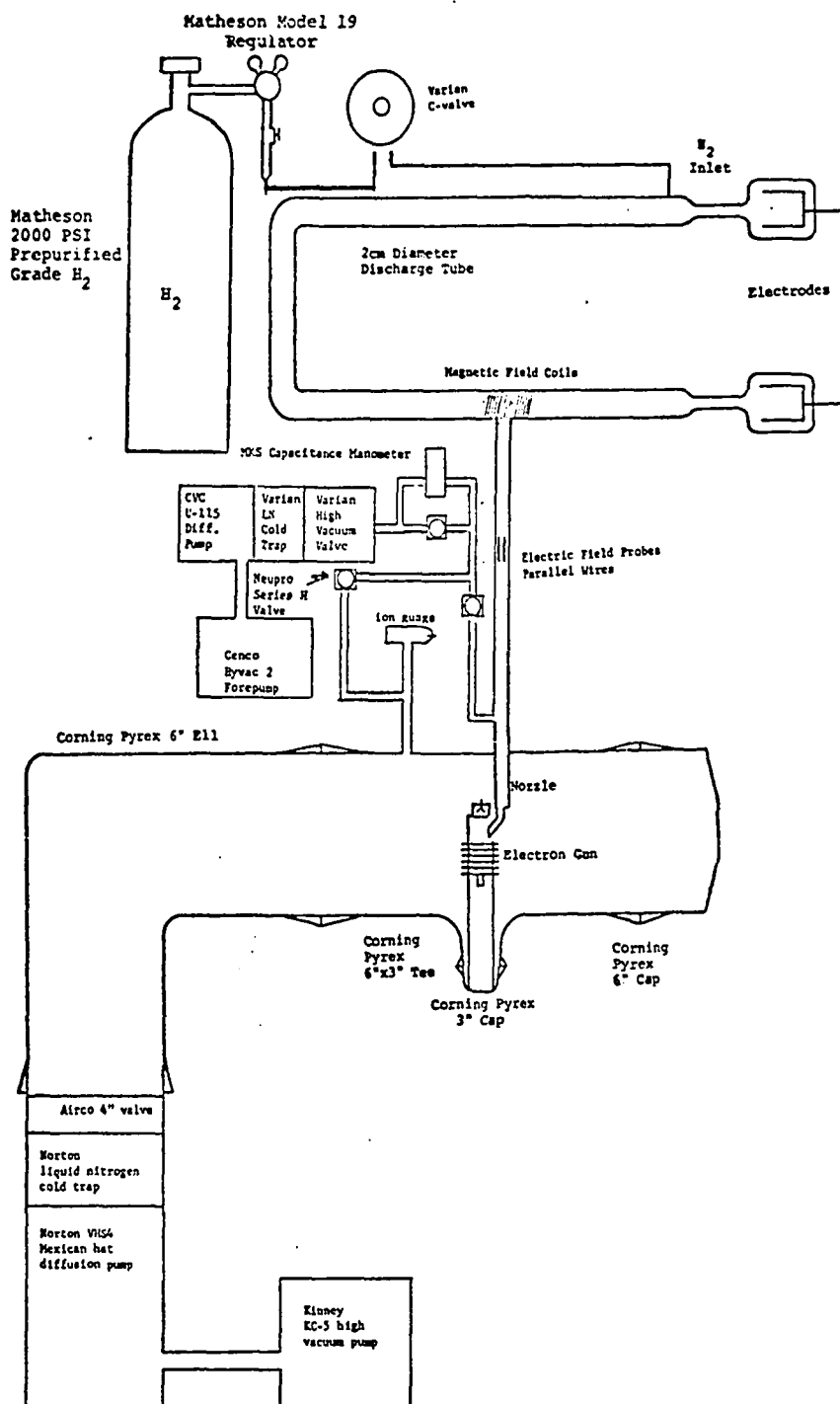


FIG. 28. Crossed beam flow system.

the system in an attempt to decrease this high background contribution, but we did not for continuity reasons.

We used pure hydrogen only in our investigations. Walker used a mixture of H_2 and H_2O in his dissertation research [12].

The Wood tube was modified by housing its cathode in quartz. In an attempt to get the Wood tube to operate at a variety of pressures and currents and not change the geometry used by Walker [12,14] we used quartz at the suggestion of Stermer [63]. In spite of this we were able to operate the system over only a small pressure range.

Two problems occurred that prevented us from having the pressure capabilities we desired. (1) At lower Wood tube pressures, electrons would be accelerated from the cathode straight into the housing wall. After a few moments of bombardment the housing would melt and a hole would develop in the system. (2) At higher pressures and current densities excessive sputtering of the Wood tube cathode would occur. After a significant layer of cathode material collected on the housing wall, the discharge from the cathode would again arc to the walls and melt the glass. This phenomena occurred with cathodes made of tantalum, stainless steel, and commercially alloyed aluminum.

In addition to the high and low pressure problems above we found that under normal operating conditions sputtered aluminum was swept down the Wood tube. Apparently in ionic form it collected on the barium coated cathode of the electron gun and deactivated it. This problem was eliminated by heating the aluminum almost to melting in air before putting it in the system.

The oxidized pure aluminum cathode was used in the investigations reported in this work. Bombardment of the cathode housing was minimized by crimping the edges of the Wood tube cathode inward so that the electrons would be focused inward toward the constriction in Walker's modified Wood tube. This suggestion was made by Fowler [64]. To dissipate some of the heat from the cathode extra layers of aluminum were wrapped around the single electrode used by Walker [12,14].

The electron gun was built by Jobe [66] and modified by Walker [12]. Its characteristics have already been discussed in the section, Basic Considerations in Atomic Hydrogen Measurement. Only grid number two was used to control beam current. With non-zero potential on grid number one we found less linearity than the composite in Fig. 22 reflects.

The data acquisition system is identical to the one used in the static system in Fig. 1. It differs only in what a Hewlett Packard 7004B X-Y recorder was used to monitor the excitation functions measured.

Although other investigators in this lab have used an analog divider circuit in their investigations, we found drift of the zero point of the divider and associated amplifier circuits to be as much as 10 per cent when one or the other of the divider input signals is small. We choose to hold the electron beam current constant in our investigations. The monochromator was positioned so that it viewed a section of the beam about .25 cm beyond the electron gun anode. By doing this we more than satisfy the condition for single electron collisions $n\Delta x Q \leq .01$ for the pressure range we used. Also this was established when we found that the intensity of the radiation was linear with respect to pressure for the 4634 Å line up to 10 mtorr of pressure in Chapter II. More

details about the equipment associated with radiation monitoring and electron gun operation can be found in Chapter II and in other works [12,15,23-26,66-68].

The 10,000 volt D.C. power supply of Walker was modified. By installing two large inductors and another large capacitor the ripple has been reduced to approximately 1 per cent. Voltage and current meters were installed on the power supply for a quantitative evaluation of the performance of the Wood tube. We found that once the Wood tube has warmed up it is fairly stable. Figure 29 shows the time dependence of the H_{β} excitation function. The first three runs were made approximately 10 minutes apart. The fourth was made an hour after initially turning the discharge tube on. After warming the discharge tube for 25 minutes the excitation functions obtained from the electron gun at the end of the nozzle arm do not change much, but they still change. The more the discharge tube is used the less atomic hydrogen reaches the electron gun.

We have also found that the flow system is extremely stable; however, due to eruptions in the oil diffusion pump, hydrogen data obtained at .5 mtorr background pressure fluctuated approximately 10 per cent. This severe fluctuation did not occur when nitrogen was observed. It is possible that the eruptions result from thermal gradients in the bottom of the diffusion pump where diffusion pump oil is baked on. When the diffusion pump was new the fluctuations were less severe.

Molecular Hydrogen Cross Sections

In Fig. 30 some molecular hydrogen optical excitation functions are presented. They were obtained when the Wood discharge tube was

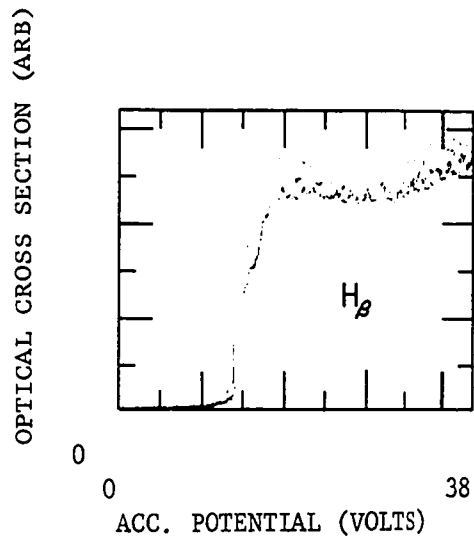


FIG. 29. The time dependence of the H_β excitation function with the Wood tube on.

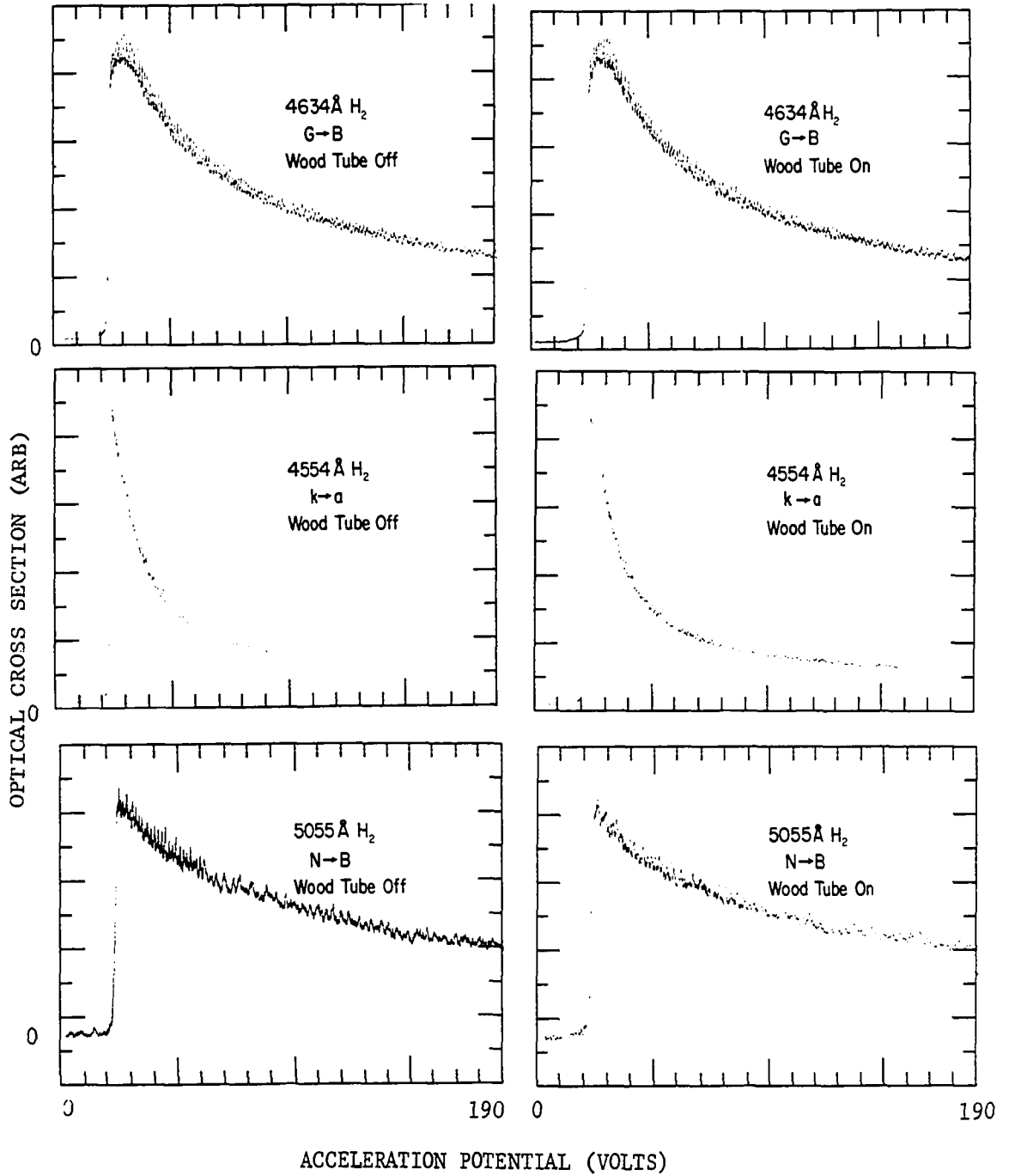


FIG. 30a. Molecular hydrogen optical excitation functions.

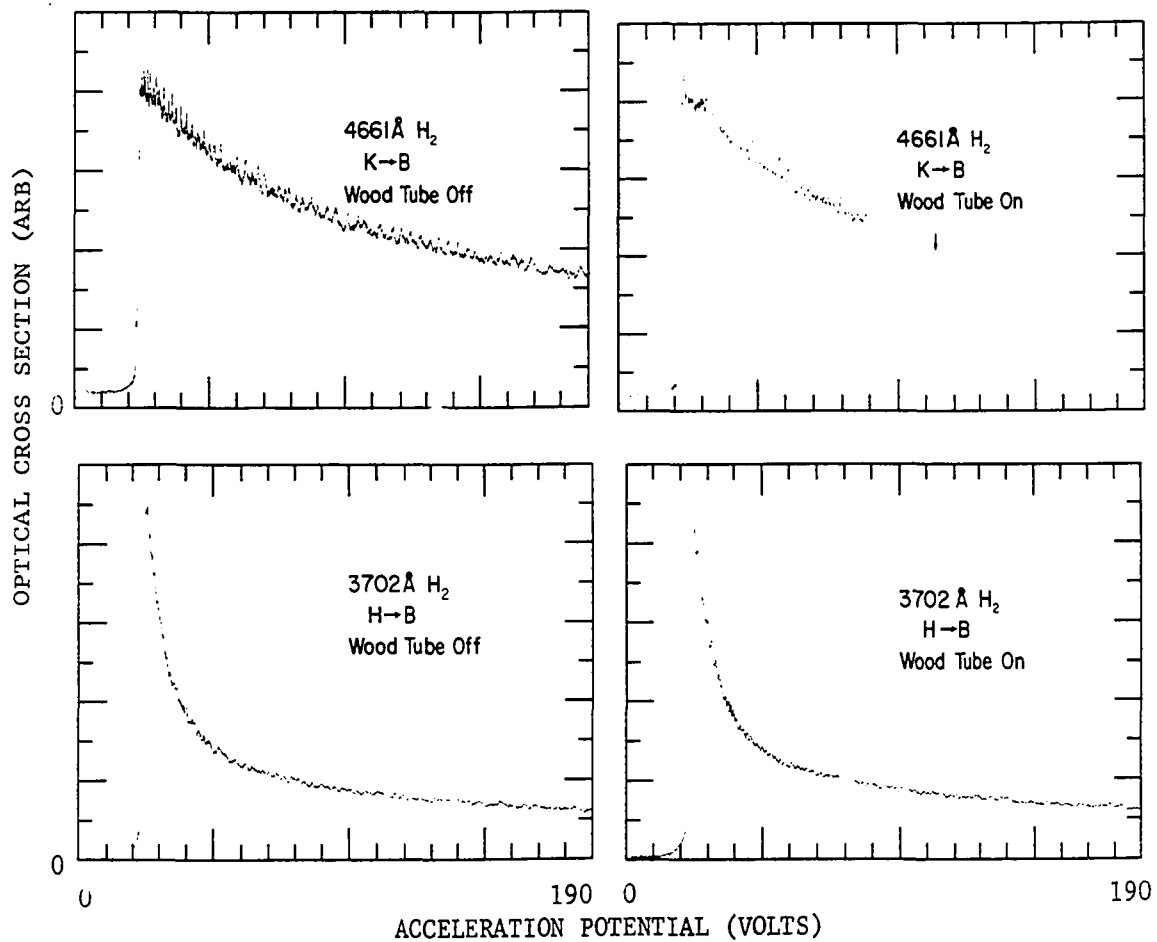


FIG. 30b. Molecular hydrogen optical excitation functions.

turned on and off. First is the 4634 Å G to B transition. This optical excitation function is the same one obtained with the static system which is pictured in Fig. 13. Next are the triplet 4554 Å k to a optical excitation functions. Then the optical excitation functions of the doubly excited singlet transitions 5055 Å N to B and 4611 Å K to B respectively. The last set of molecular data is the 3702 Å H to B singlet optical excitation functions.

These excitation functions are so near being identical when the Wood tube is on and off, that we must conclude from Eq. (51) that no more than a few per cent of the particles arriving in the collision chamber from the Wood tube are atomic hydrogen. Because we could not determine even approximately the atomic hydrogen number density, we were not able to obtain absolute Balmer optical excitation cross sections.

Atomic Hydrogen Cross Sections

In Fig. 31 hydrogen Balmer excitation functions from 0 to 38 eV and 0 to 190 eV are presented. The upper function was taken with the Wood tube on and the lower with the tube off. Because of the small number density of atomic hydrogen in the experiment $n_{H_2}^{on}/n_{H_2}^{off}$ may be taken as unity for use in the numerator of Eq. (52). Hence, the total hydrogen Balmer atomic optical excitation function is obtained by subtracting the lower functions from the upper.

In Figs. 32 to 35 the resulting total hydrogen Balmer optical excitation functions are compared with the Born approximation. For comparison the data was normalized at approximately 140 eV. We did not take enough data to justify a least squares analysis; however, a number of double checks were performed. We estimate the error in the relative

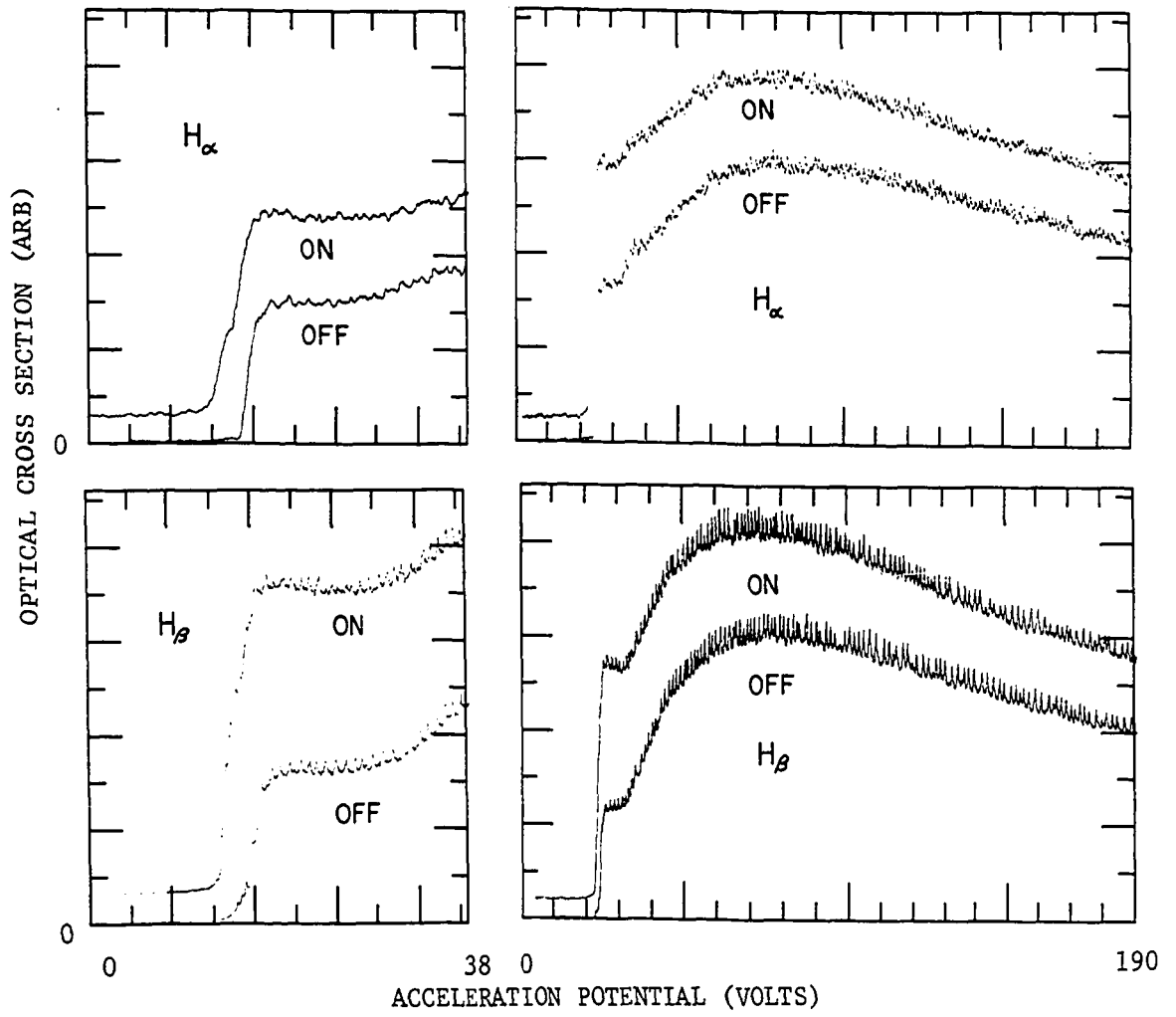


FIG. 31a. Hydrogen Balmer excitation functions.

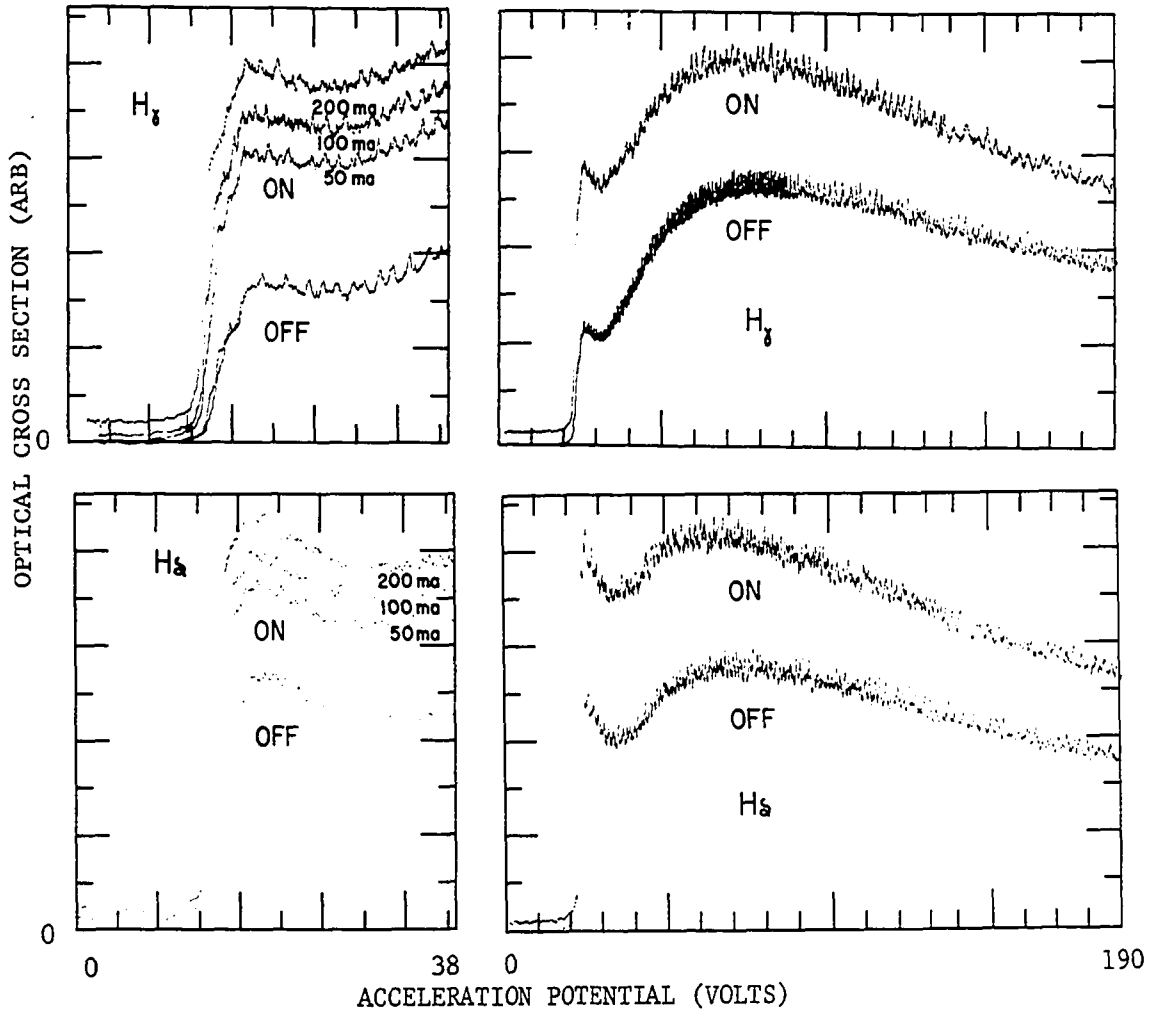
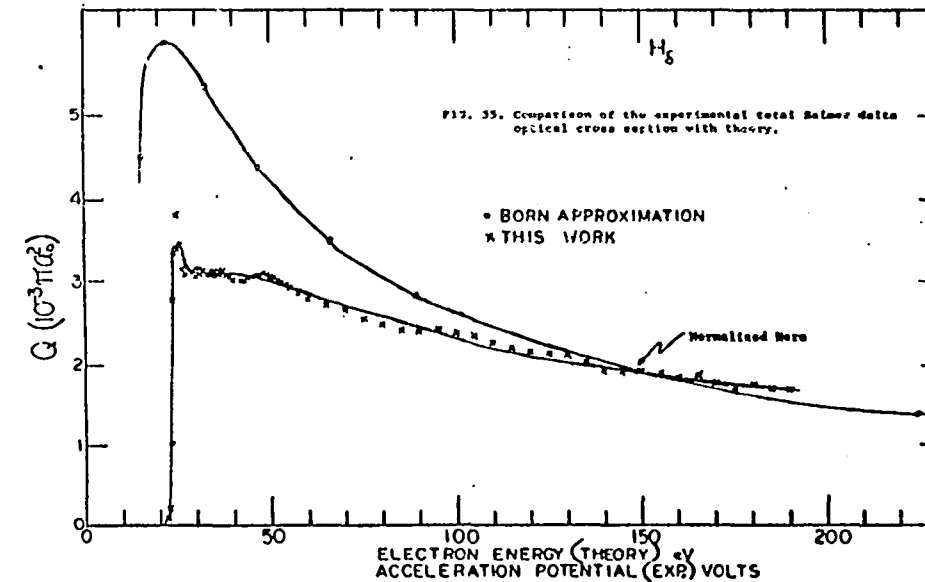
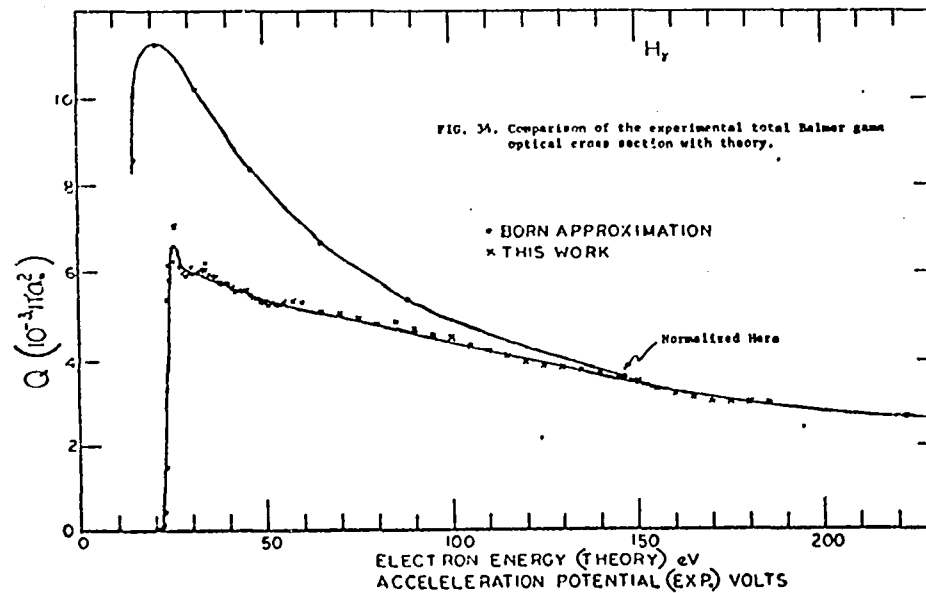
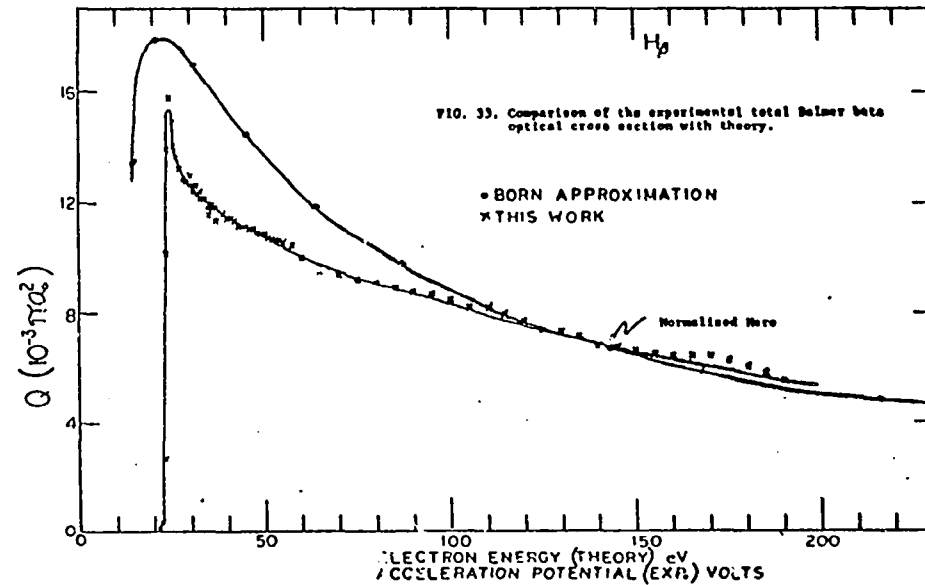
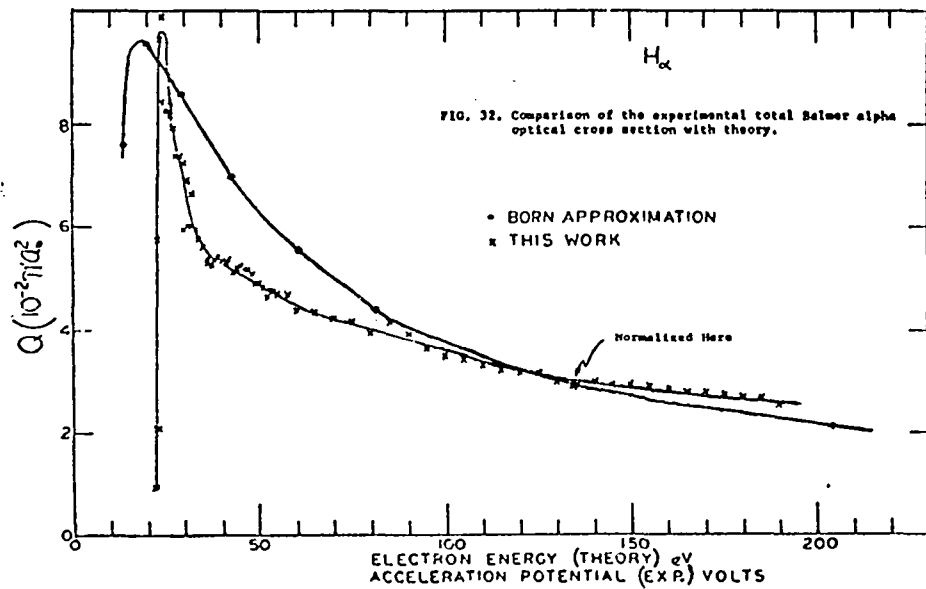


FIG. 31b. Hydrogen Balmer excitation functions.



values for the energies greater than 75 eV to be 20 per cent or less. For the values near the onset it is more difficult to estimate an error. Due to a variation in potential shift that occurred when the Wood tube was turned on, the lower excitation function was shifted to a lower voltage that corresponds with the onset of the upper function. Just a small error in this sort of correction can produce a large difference in the shape of the resulting excitation function and can even produce negative cross sections. We have examined carefully the various shifts in contact potential shifts and feel that the onsets plotted for H_α , H_β , H_γ and H_δ most closely represent the true excitation function shape. We estimate that the shapes of our excitation functions are approaching the ultimate limit of the system and will be within 50 per cent to 20 per cent of the true values obtained from onset to 75 eV respectively.

In Fig. 36 Kleinpoppen's [60] measurements of H_α are presented for comparison. His results were obtained by mechanically chopping an atomic beam from a tungsten oven. He then electronically subtracted the intensities resulting when the beam was open and closed. Our results would look very much like his if we did not consider a potential shift.

If the number density of ions coming from the Wood tube is on the order of 10^{12} ions/cm³ then from Eq. (7) we calculate that the Holtsmark field is approximately 40 volts per cm. Bethe and Salpeter [44] give the electric field strength at which the s and p $j = \frac{1}{2}$ hyperfine levels mix as 475, 58, 12 and 1.7 volts/cm for $n = 2, 3, 4$ and 6. For larger values of j smaller fields are necessary for mixing. Since these values are for complete mixing, we can suspect that all our data is to some extent affected by the fields. The H_β , H_γ and H_δ results

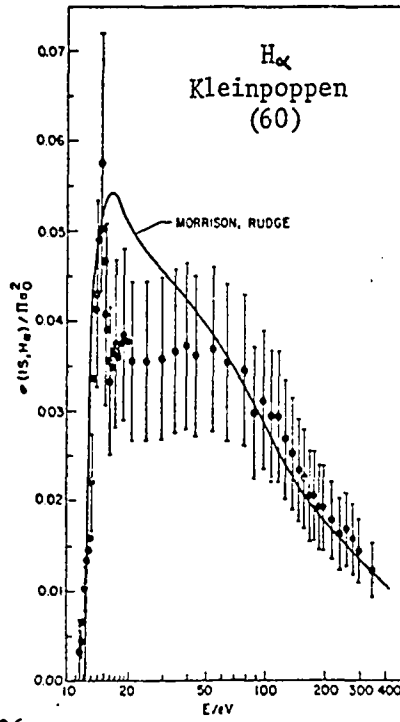


Fig. 36 Cross section $\sigma(1S, H_{\alpha})$ of atomic hydrogen as a function of the electron energy ($3 \times$ rms error plus estimated systematic error). The solid curve represents the theoretical results of Morrison and Rudge (Ref. 69)

should reflect completely mixed states and H_{α} almost completely mixed.

In spite of the mixing phenomena Walker [14] reports that the high energy portion of the Balmer excitation functions compare favorably with the Born approximation. From Figs. 16-19 we see that all three components of the Balmer optical excitation cross sections have close to the same slopes after 140 eV. Thus, although the near degenerate ℓ -levels are completely mixed they may not alter the shape of the higher energy portions of the excitation functions. The real test lies in the lower energy regions of the excitation function. Here is where a difference would show up if there were one. Perhaps Kleinpoppen's result is the field free shape of the H_{α} optical excitation function and the one present here is a consequence of mixing.

Molecular Nitrogen Excitation Functions

From lifetime studies the nitrogen molecular ion state $B^2\Sigma_u^+$ has been found to be cascade free and relatively insensitive to pressure effects [3]. The 3914 Å molecular band that originates from this state is so bright and unperturbable that it is ideal for experimental double checks.

We suspected if molecular ions originated from the Wood tube that we could obtain some sort of evidence of electron excitation of the ground state of the nitrogen molecular ion to the $B^2\Sigma_u^+$ state. In Fig. 37 we have such evidence. The top curve was obtained with the Wood tube off and the bottom curve with the tube on. The cross section for population of the $B^2\Sigma_u^+$ state by electron collision with neutral molecules is reduced by a constant factor. This reduction reflects a decrease in the number of neutral molecules in the particle beam with the Wood tube on.

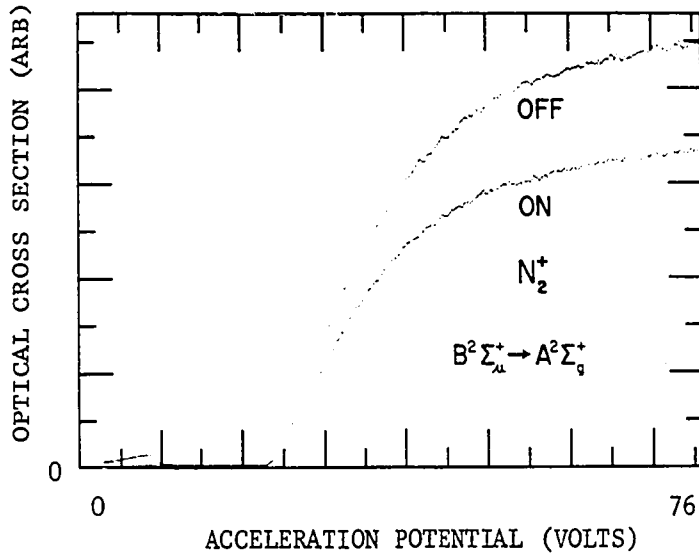


FIG. 37. The optical excitation cross section for population of the $B^2\Sigma_u^+$ state.

We would suspect that some of the resulting particles would be molecular ions, atomic ions, and neutral atoms.

In Fig. 37 the structure around 3 and 4 eV is most likely evidence of electron excitation of the N_2^+ molecule to the $B^2\Sigma_u^+$ state. We amplified that portion of the molecular excitation function that occurs only with the Wood tube on to confirm it was there. This experiment adds supporting evidence to the overwhelming evidence already presented that indicates a significant number density of ions survive the trip from the positive column of the Wood tube to the electron gun.

CHAPTER V

LIFETIME MEASURING SYSTEM

Introduction

Lifetime data analysis is time resolution analysis. In principle by experimentally time resolving hydrogen Balmer radiation, relative contributions of $ns \rightarrow 2p$, $np \rightarrow 2s$, and $nd \rightarrow 2p$ radiation is measurable. With both the absolute optical excitation cross section and the relative contributions of the l -levels to Balmer radiation, apparent and possible level cross sections can be derived from the flow system.

Also, if the near degenerate l -levels of the hydrogen atoms are populated differently from electron- H_2 molecule than from electron-H atom collisions, then in principle time resolution can ultimately be used as a method for measuring relative concentrations of hydrogen atoms and molecules in an electron beam.

A feasibility study for a lifetime system was made with such goals in mind. This Chapter is presented to help those who eventually undertake this or a similar project.

The Basic System

Since the early 1960's Fowler and others [2-8] have investigated lifetimes of excited atoms and molecules at the University of Oklahoma. In all these investigations a bright hollow cathode source was used. Atomic and molecular excitation is achieved by pulsing electrons radially

inward. These high energy electrons are not mono-energetic.

Lawrence [9] and Weaver and Hughes [10] have modified an electron gun for lifetime measurements. Data from this type of mono-energetic system complements information acquired by other means. Below, a discussion of the basic equipment needed to measure lifetimes with an electron gun is presented.

The basic system is drawn in Fig. 38. Only the components that are now now standard in the cross section data acquisition are indicated. The square wave pulse generator must cut off the electron beam in the order of one nanosecond. The E-H model 5112 pulse generator is ideal for cutting off the electron beam at grid two. This generator has one big advantage over charged coaxial cables described by Johnson [3]. It has a continuously variable pulse width and repetition rate. In general as the pulse widths are varied the lifetimes observed will vary also. This is due to cascades and in some cases electric fields caused by the beam itself. In order to use experimental and theoretical cross sections or branching ratios the losses by emission from an excited state must be equal to the population gain i.e., the radiation must have reached a steady state condition. In general the pulse width necessary to accomplish this is on the order of 1μ sec. This is equivalent to many meters of coaxial cable. As important as the pulse width is, it is best to have a convenient variable generator like the E-H model 5112.

Theoretically the onset of emitted radiation due to square pulse excitation could be used for extraction of lifetime information; however, the time dependence of ionization in most experimental systems make this

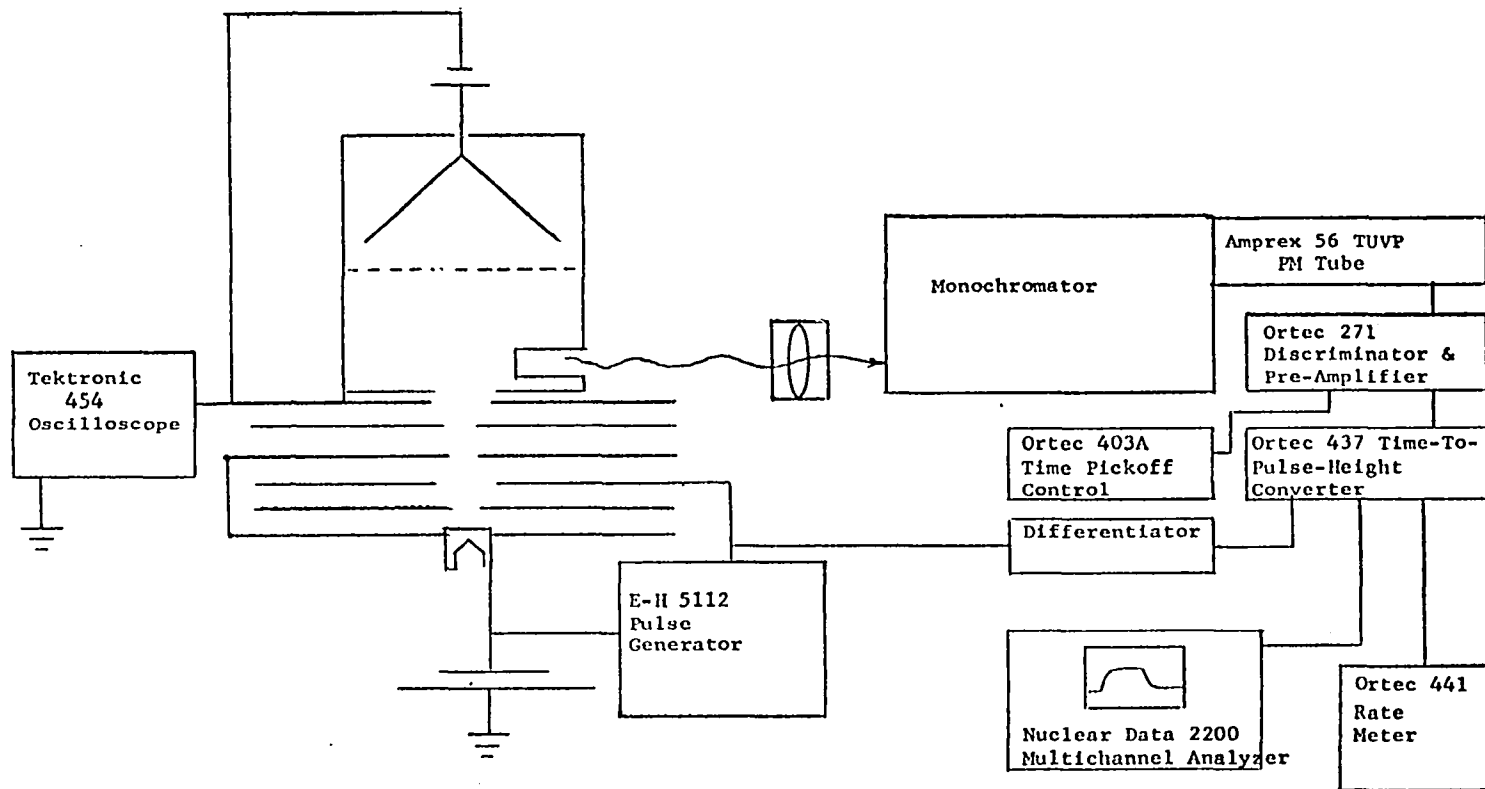


FIG. 38. Schematic of a system to be used for lifetime measurements in the 2000 Å to 7800 Å range.

approach impracticable. We feel the long excitation pulse and evaluation of the radiation after cutoff is the only feasible approach to this type of lifetime analysis.

The pulsed beam current and its cutoff should be monitored for completeness. The Tektronic 454 oscilloscope has a rise time fast enough time to be used as a current probe for this purpose.

There are three systems capable of sensing and monitoring the time dependency of the excited gas in the collision chamber that have been examined at the University of Oklahoma. Johnson [3] categorizes them by these titles : (1) Direct Observation, (2) Sampling Scope, and (3) Delayed Coincidence. He and others discuss them in their theses and dissertations [2-8]. So far, all evidence indicates that the delayed coincidence method is far superior to the others.

The delayed coincidence technique is a photon counting technique. Emitted photons from the collision chamber are selected by a monochromator and turned into current pulses by a photomultiplier tube. The time interval between cutoff of the excitation pulse and the formation of a current pulse in the photomultiplier tube is recorded by the rest of the sensing and readout equipment for each bombardment of the gas as follows:

- (1) Monochromator selects transition under study.

- (2) Differentiator. This device differentiates the square wave pulse applied to grid two of the electron gun. The resulting negative part of the differentiated signal is the input to the time-to-pulse height converter "start" terminal.

- (3) Ortec Model 437 Time-to-Pulse Height Converter.

The quarter-volt negative pulse from the TPHC differentiator triggers the

charging of a capacitor. The capacitor continues to charge until a quarter-volt negative pulse is received through the "stop" terminal or until an arbitrarily set time has elapsed. When charging is stopped, a voltage pulse proportional to the voltage on the capacitor appears at the two exit terminals of the time-to-pulse height converter. One exit terminal is hooked to a rate meter and the other is fed into a multichannel analyzer.

(4) Ortec Model 271 Discriminator and Pre-amplifier (PTDP).

The photomultiplier is an 56 TUVP Amperex with an S-20 spectral response cathode and a Corning Pyrex glass window. The discriminator and pre-amplifier transform the photon created current pulses of the photomultiplier into quarter volt negative pulses to be used to stop the charging capacitor in the time to pulse height converter. Thus, the voltage output of the time-to-pulse height converter is proportional to the time between the cutoff of the excitation pulse and the formation of a photon created pulse in the photomultiplier tube.

(5) Ortec Model 403A Time Pickoff Control. It serves as a power supply and bias control for the PTDP.

(6) Ortec Model 441 Rate Meter. A count of the number of stop pulses to reach the TPHC is continuously monitored by counting the voltage pulses coming out of the TPHC. This is very important since the number of stop pulses must be on the order of 1 per cent of the number of start pulses or the results will deviate from the true radiation time dependence. Mickish [7] discusses this more completely.

(7) Nuclear Data Model 2200 Multichannel Analyzer (MCA). The height of the voltage pulses from the TPHC are analyzed and stored in the MCA memory. An attached oscilloscope allows visual linear and semi-

log display of the frequency of a particular voltage vs the size of the voltage. These are effective time plots of the intensity of selected radiation originating in the collision chamber. A high speed paper tape printout allows retrieval of the data from the MCA memory.

The timing calibration of the TPHC and a simultaneous check for linearity is carried out by the use of several coaxial cables whose length in time (i.e., the time it takes an electric signal to travel the length of the cable) is determined by phase shift measurements. This procedure and analysis is described by Johnson [3].

A 1024 multichannel analyzer is recommended over smaller ones since determining how much noise exists in the decaying luminosity data obtained from the MCA is a different problem. Mickish [7] has suggested that the noise level appearing before the excitation onset in the MCA display should be taken as the noise level for all time. This is an acceptable assumption when photon counting. In order to monitor the entire excitation and decay of the atomic system in question and still have good resolution a large number of channels is needed. Such a system is expensive. The equipment described above presently costs on the order of \$20,000 and was not fundable.

BIBLIOGRAPHY

1. A. Corney. *Advances in Electronics and Electron Physics* 29, 115, Academic Press, New York (1970).
2. T. M. Holzberlein. Ph.D. Dissertation. University of Oklahoma (1963).
3. A. W. Johnson. Ph.D. Dissertation. University of Oklahoma (1968).
4. G. E. Copeland. Ph.D. Dissertation. University of Oklahoma (1970).
5. A. R. Schaefer. Ph.D. Dissertation. University of Oklahoma (1970).
6. P. R. Skwerski, Jr. Master's Thesis. University of Oklahoma (1969).
7. R. A. Mickish. Master's Thesis. University of Oklahoma (1970).
8. R. T. Thompson. Ph.D. Dissertation. University of Oklahoma (1972).
9. G. M. Lawrence. *Phys. Rev. A* 2, 397 (1970).
10. L. D. Weaver and R. H. Hughes. *J. Chem. Phys.* 52, 2299 (1970).
11. B. L. Moiseiwitch and S. J. Smith. *Rev. of Mod. Phys.* 40, No. 2 (1968).
12. J. D. Walker. Ph.D. Dissertation. University of Oklahoma (1970).
13. L. S. Ornstein and H. Lindeman. *Z. Physik* 80, 525 (1933).
14. J. D. Walker, R. M. St. John. To be published.
15. K. G. Walker. Ph.D. Dissertation. University of Oklahoma (1971).
16. F. A. Sharpton. Ph.D. Dissertation. University of Oklahoma (1968).
17. P.M.S. Blackett and J. Franck. *Z. Physik* 34, 389 (1925).
18. C. J. Brasefield. *Phys. Rev.* 34, 431 (1929).
19. E. R. Williams, J. V. Martinez, and G. H. Dunn. *Bull. Am. Phys. Soc.* 12, 233 (1967).
20. D. A. Vroom, F. J. de Heer. *J. Chem. Phys.* 50, 580 (1969).

21. L. R. Wilcox and W. E. Lamb. *Phys. Rev.* **119**, 1915 (1960).
22. A. A. Kruithof and L. S. Ornstein. *Physica* **2g** 611 (1935).
23. R. M. St. John, F. L. Miller and C. C. Lin. *Phys. Rev.* **134**, A888 (1964).
24. P. Stanton and R. M. St. John. *J. Opt. Soc. Am.* **59**, 252 (1969).
25. F. A. Sharpton, R. M. St. John, C. C. Lin and F. E. Fajen. *Phys. Rev.* **2A**, 1305 (1970).
26. J. Jobe and R. M. St. John. *Phys. Rev.* **164**, 117 (1967).
27. R. M. St. John. *Methods of Experimental Physics*. Academic Press, New York, **8**, 27 (1969).
28. M. Leventhal, R. T. Robiscoe and K. R. Lea. *Phys. Rev.* **158**, 49 (1967).
29. J. Holtzmark. *Ann. Physik (Leipzig)* **58**, 577 (1919); R. G. Breene. *Shape and Width of Spectral Lines*. Pergamon Press, London (1954).
30. H. R. Griem. *Plasma Spectroscopy*. McGraw-Hill, New York (1964).
31. H. Margenau and M. Lewis. *Rev. Mod. Phys.* **31**, 569 (1964).
32. M. Barranger. *Atomic and Molecular Processes*. D. R. Bates ed. *Ch. 13*. Academic Press, New York (1962).
33. J. W. Cooper. *Phys. Rev.* **128**, 681 (1962).
34. G. V. Marr. *Plasma Spectroscopy*. Elsevier Publishing Co., New York (1968).
35. N. F. Mott and H.S.W. Massey. *The Theory of Atomic Collisions*. Oxford at Clarendon Press, Third Edition (1965).
36. E. M. Purcell. *Astrophys. J.* **116**, 457 (1952).
37. H.S.W. Massey and E.H.S. Burhop. *Electronic and Ionic Impact Phenomena*, Oxford (1952).
38. L. J. Kieffer and G. H. Dunn. *Electron Impact Ionization Cross Section Data for Atoms, Atom Ions, and Diatomic Molecules: I Experimental Data*, *Rev. Mod. Phys.* **38**, 1 (1966).
39. H. G. Gale, G. S. Monk and K. O. Lee. *Astrophysical J.* **67**, 89 (1928).
40. O. Richardson. *Molecular Hydrogen and Its Spectrum*. New Haven, Yale University Press (1934).

41. T. E. Sharp. *Atomic Data* 2, 119 (1971).
42. G. W. Series. *Spectrum of Atomic Hydrogen*. Oxford: Oxford Press (1957).
43. H. Kohn. *Atomic Spectra*. Academic Press, New York (1962).
44. H. A. Bethe and E. E. Salpeter. *Quantum Mechanics of One-and-Two Electron Atoms*. Academic Press Inc. (1957).
45. G. Herzberg. *Molecular Spectra and Molecular Structure I*. Second Edition, D. Van Nostrand Co., Inc., New Jersey (1950).
46. G. Herzberg. *Atomic Spectra and Atomic Structure*. New York, Dover (1957).
47. H. E. White. *Introduction to Atomic Spectra*. McGraw-Hill Book Co., Inc. (1934).
48. L. Pauling and E. B. Wilson. *Introduction to Quantum Mechanics*. McGraw-Hill Book Co., Inc. (1935).
49. L. I. Schiff. *Quantum Mechanics*. McGraw-Hill Book Co., Inc. (1949).
50. E. V. Condon and G. H. Shortley. *The Theory of Atomic Spectra*. Cambridge Press (1953).
51. W. Heitler. *Quantum Theory of Radiation*. Third Ed. Oxford (1954).
52. P.A.M. Dirac. *Principles of Quantum Mechanics*. Oxford, Third edition (1947).
53. J. Von Neumann. *Mathematical Foundations of Quantum Mechanics*. Princeton, Princeton Press (1955).
54. R. W. Wood. *Proc. Roy. Soc.* 97A, 455 (1920).
55. L. A. Vainshtein. *Opt. Spectry*. USSR 18, 538 (1965).
56. H.S.W. Massey and E.H.S. Burhop. *Electronic and Ionic Impact Phenomena*. Oxford, Clarendon Press (1969).
57. E. N. McDaniel. *Collisional Phenomena in Ionized Gases*. John Wiley & Sons, Inc., New York (1964).
58. D.W.O. Heddle and C. B. Lucas, in Abstracts of *The Second International Conference on the Physics of Electronic and Atomic Collisions*, p. 119. W. A. Benjamin, Inc., New York (1961); Also in Ref. 11.
59. R. G. Fowler. *Handbuch Der Physik*, p. 220, Springer (1956).

60. H. Kleinpoppen. *Phys. Rev. Letters* 20, 8, 361 (1968).
61. W. Kapuscinsk and J. G. Eymers. *Roy Soc. Proc. A.* 122, 58 (1929).
62. G. H. Dieke. *J. Molec. Spectry.* 2, 494 (1958).
63. R. Stermer, Private Communication (1972).
64. R. G. Fowler, Private Communication (1972).
65. F. E. Fajen. Ph.D. Dissertation. University of Oklahoma (1968).
66. J. D. Jobe. Ph.D. Dissertation. University of Oklahoma (1968).
67. P. N. Stanton. Ph.D. Dissertation. University of Oklahoma (1968).
68. M. Lake. Master's Thesis, University of Oklahoma (1972).
69. D.T.J. Morrison and M.R.H. Rudge. *Proc. Phys. Soc. (London)* 89, 44 (1966).

APPENDIX I

MOLECULAR HYDROGEN SPECTRUM

RICHARDSON'S SCHEME

APPENDIX I

MOLECULAR HYDROGEN SPECTRUM RICHARDSON'S SCHEME

The following is a rearrangement of Richardson's Tables [40]. In his tables, Richardson has arranged spectral lines in an internally consistent scheme such that most reported lines are identified with a specific transition. His tables are arranged so that for a given transition particular wave number representing that transition can be found.

The following tables are arranged such that the transitions representing a particular wave number can be found. In the first column the spectrum and wave number is listed. In the next column is the visual estimate of the transition intensity given by Gale, Monk and Lee [39]. When the intensity estimates are followed by one of the letters A, B, C, D the mean error is estimated by Gale, Monk and Lee to be higher than usual, being between 0.01 and 0.02 Å for A, between 0.02 and 0.03 Å for B, and so on. The letter H indicates that the line is diffuse and possibly double. For a considerable number of lines which are not present in Gale, Monk and Lee's tables, the wave numbers and visual intensities are those given by other investigators discussed by Richardson. These lines are indicated by F, M, T, D and P.

A few lines whose status is doubtful are followed by a question mark. A bar after an intensity figure means that the value is for a blend of which the line forms part.

In the next columns is Richardson's designation of the transition that produces the particular line in the spectrum. First the

rotational levels K that the transition occurs between is given along with the standard notation P , Q and R . These three symbols represent rotational transitions such that P is $\Delta K = +1$, Q is $\Delta K = 0$, and R is $\Delta K = -1$ when $\Delta K = (K_{\text{lower}} - K_{\text{upper}})$.

Richardson's designations of the vibrational levels involved in the transition are listed in the next column. The upper vibrational level ν' is given first then the lower ν'' . They are written ν', ν'' .

The designations of the electronic levels involved are listed in the final columns. Some of Richardson's original symbols designating electronic states are no longer in use. The symbols used here are not standard but they are currently accepted.

If two letters such as IB represent a single electronic state the second is generally written as a subscript. For example $IB = I_b$. The upper electronic configuration is given first and the lower second. The transition from the singlet G to the B state is given by G^*B . In the last column S and T stand for singlet and triplet respectively.

-----	1	24789.58	1	14	2.1	G00	S	-----	0	25274.38	4	2R	1.0	H00	S
-----	0	24789.64	1	4H	0.2	H00	S	-----	0	25274.96	0	3P	2.1	L00	S
-----	0	24792.57	0F	30	2.1	H00	S	-----	0	25299.72	0F	5P	0.2	S00	S
-----	0	24791.10	9	2R	2.1	L00	S	-----	0	25299.20	0F	40	0.2	S00	S
-----	0	24791.46	9	0H	2.1	L00	S	-----	0	25188.73	1	1H	3.2	I00	S
-----	0	24790.27	1	40	1.0	J00	S	-----	0	25183.99	2F	60	3.2	I00	S
-----	0	24795.35	10	20	2.1	H00	S	-----	0	25151.59	3	1H	1.0	H00	S
-----	0	24793.84	2	3H	2.1	G00	S	-----	0	25138.56	3	50	3.2	I00	S
-----	0	24795.69	4	10	2.1	H00	S	-----	0	25176.92	1H	0F	3.2	I00	S
-----	0	24794.07	0	3R	0.2	H00	S	-----	0	25130.26	1	4P	2.1	L00	S
-----	0	24793.10	1	14	0.2	H00	S	-----	0	25102.47	4	40	3.2	I00	S
-----	0	24795.26	3	2R	0.2	H00	S	-----	0	25093.50	1	0R	1.0	H00	S
-----	0	24796.39	4	4R	2.1	G00	S	-----	0	25074.95	3	30	3.2	I00	S
-----	0	24795.26	0	04	2.2	H00	S	-----	0	25057.07	0F	30	0.2	S00	S
-----	0	24793.69	0F	4P	0.0	H00	T	-----	0	25055.40	0	20	3.2	I00	S
-----	0	24793.56	0F	110	1.0	H00	S	-----	0	25048.41	2	10	3.2	I00	S
-----	0	24793.47	1	10	1.1	H00	T	-----	0	25044.09	5	0R	3.2	G00	S
-----	0	24799.80	7	0H	2.1	H00	S	-----	0	25035.16	3	1R	3.2	G00	S
-----	0	24799.16	1H	50	2.1	G00	S	-----	0	25031.45	3	2P	3.2	I00	S
-----	0	24792.37	0	2P	0.2	H00	S	-----	0	25018.54	0F	3H	0.0	N00	T
-----	0	24790.05	0A	20	1.1	H00	T	-----	0	25015.71	0F	3R	0.0	H00	S
-----	0	24795.35	0F	1P	0.2	H00	S	-----	0	25013.66	2	3P	3.2	I00	S
-----	0	24794.03	2	6R	2.1	G00	S	-----	0	25012.10	0F	100	2.1	I00	S
-----	0	24798.63	5	1R	2.1	H00	S	-----	0	25010.82	7	2P	3.2	G00	S
-----	0	24799.17	1	30	1.0	J00	S	-----	0	24997.57	1	4R	2.1	I00	S
-----	0	24795.79	1-	2P	0.2	H00	S	-----	0	24993.35	0F	2R	0.0	H00	T
-----	0	24795.79	1-	30	1.1	H00	T	-----	0	24987.70	3	4P	3.2	I00	S
-----	0	24792.87	2	10	1.0	K00	T	-----	0	24977.38	4	2P	1.0	H00	S
-----	0	24771.46	3	2P	2.1	G00	S	-----	0	24974.33	2	3R	3.2	G00	S
-----	0	24795.47	9	2R	2.1	H00	S	-----	0	24971.92	1F	2H	0.2	H00	S
-----	0	24795.66	1	20	1.0	K00	T	-----	0	24969.36	0	2R	0.2	R00	S
-----	0	24449.75	0F	40	1.4	H00	S	-----	0	24965.00	1A	1R	0.0	H00	S
-----	0	24444.85	0	40	1.1	H00	T	-----	0	24959.26	1	3P	1.0	H00	S
-----	0	24442.38	0F	3P	2.2	H00	S	-----	0	24958.70	5	4P	1.0	H00	S
-----	0	24430.76	0	4P	2.2	H00	S	-----	0	24955.90	4	1R	0.0	H00	T
-----	0	24437.03	0F	5P	2.2	H00	S	-----	0	24954.84	1	4R	3.2	G00	S
-----	0	24436.62	0A	10	1.4	R00	S	-----	0	24938.63	2	2P	3.2	G00	S
-----	0	24433.30	0F	5P	0.0	H00	T	-----	0	24935.75	0A	5P	3.2	I00	S
-----	0	24429.62	0	2P	2.2	H00	S	-----	0	24933.37	2	3R	2.1	I00	S
-----	0	24420.29	0	10	6.4	K00	T	-----	0	24933.37	2-	0R	0.0	H00	S
-----	0	24417.87	1	30	1.0	K00	T	-----	0	24930.56	0	10	5.3	K00	T
-----	0	24414.65	0	30	1.4	R00	S	-----	0	24926.04	0	20	0.2	S00	S
-----	0	24409.98	3	3R	2.1	H00	S	-----	0	24922.03	0	3P	0.2	S00	S
-----	0	24407.51	1	20	1.4	R00	S	-----	0	24913.48	0	90	2.1	I00	S
-----	0	24406.78	1	3P	2.1	G00	S	-----	0	24911.08	1	0R	2.2	H00	S
-----	0	24406.78	1-	50	1.1	H00	T	-----	0	24907.10	0F	0R	0.0	H00	T
-----	0	24403.61	0	2P	1.1	H00	T	-----	0	24904.71	0	20	5.3	K00	T
-----	0	24398.66	3	20	1.0	J00	S	-----	0	24894.43	1	1R	2.2	H00	S
-----	0	24398.66	3	100	1.0	I00	S	-----	0	24897.49	0F	0R	0.2	D00	S
-----	0	24378.70	0AB	30	1.0	H00	T	-----	0	24876.07	0F	1P	2.2	H00	S
-----	0	24369.11	0F	4R	1.2	H00	S	-----	0	24868.64	0F	0R	0.2	R00	S
-----	0	21346.40	3	4R	2.1	H00	S	-----	0	24866.45	0	30	5.3	K00	T
-----	0	21327.15	2	4P	1.0	J00	S	-----	0	24867.68	1	2H	2.1	I00	S
-----	0	24328.22	2	4P	2.1	G00	S	-----	0	24860.33	2	3P	3.2	G00	S
-----	0	24327.05	0	3R	1.2	H00	S	-----	0	24860.33	2-	2R	2.2	H00	S
-----	0	24326.60	0F	3P	1.1	H00	T	-----	0	24857.55	2	1P	0.0	H00	S
-----	0	24323.37	2	2R	1.2	H00	S	-----	0	24852.40	0F	1P	0.2	D00	S
-----	0	24317.82	1A	1R	1.2	H00	S	-----	0	24848.61	0	4R	2.2	H00	S
-----	0	24303.27	2	0R	1.2	A00	S	-----	0	24839.38	4	10	0.0	H00	T
-----	0	24302.60	0F	4P	0.2	H00	S	-----	0	24830.20	2	60	1.0	J00	S
-----	0	24286.92	0	90	1.0	I00	S	-----	0	24827.81	3	80	2.1	I00	S
-----	0	24285.80	0A	5P	0.2	H00	S	-----	0	24823.07	3-	20	0.0	H00	T
-----	0	24282.95	1-	1P	1.2	H00	S	-----	0	24823.07	3-	3R	2.2	H00	S
-----	0	24249.95	1	3R	1.0	I00	S	-----	0	24816.94	0F	130	1.0	I00	S
-----	0	24242.02	0F	4P	1.1	H00	T	-----	0	24817.19	8	2P	0.0	H00	S
-----	0	24241.04	0	5P	2.1	G00	S	-----	0	24798.46	2	30	0.0	H00	T
-----	0	24198.83	0	10	2.2	H00	T	-----	0	24790.49	0	1R	2.1	I00	S
-----	0	24197.75	2	2P	1.2	H00	S	-----	0	24781.84	0	2P	0.2	C00	S
-----	0	24194.62	1	80	1.0	I00	S	-----	0	24772.69	4	3P	0.0	H00	S
-----	0	24182.88	3-	20	2.2	H00	T	-----	0	24768.00	1	4P	3.2	G00	S
-----	0	24182.88	3-	2R	1.0	I00	S	-----	0	24765.68	0	40	0.0	H00	T
-----	0	24160.22	0F	5P	1.1	H00	T	-----	0	24763.21	0F	2P	0.2	R00	S
-----	0	24158.36	0	30	2.2	H00	T	-----	0	24754.51	2	70	2.1	I00	S
-----	0	24143.04	0	3P	1.2	H00	S	-----	0	24750.65	1	10	0.2	R00	S
-----	0	24131.48	0	3	.0	L00	S	-----	0	24745.69	0	3R	2.2	H00	S
-----	0	24128.64	0	0R	2.2	L00	S	-----	0	24729.13	0F	4P	0.2	C00	S
-----	0	24125.31	0	40	2.2	H00	T	-----	0	24726.47	0A	4P	0.2	R00	S
-----	0	24116.66	0AB	50	1.0	H00	T	-----	0	24726.47	0A	40	0.2	R00	S
-----	0	24115.47	2	70	1.0	I00	S	-----	0	24724.90	0F	50	0.0	H00	T
-----	0	24111.46	2	1R	1.0	I00	S	-----	0	24723.72	5	4P	0.0	H00	S
-----	0	24107.55	0A	2P	2.2	L00	S	-----	0	24716.32	0	3R	1.1	H00	T
-----	0	24084.05	0F	50	2.2	H00	T	-----	0	24711.93	0	0R	2.1	I00	S
-----	0	24080.49	2	4P	1.2	H00	S	-----	0	24707.83	0F	2P	0.0	H00	T
-----	0	24077.06	0A	1P	2.2	L00	S	-----	0	24696.90	1	30	0.2	P00	S
-----	0	24074.32	2	10	5.1	D00	T	-----	0	24696.90	1	50	1.0	J00	S
-----	0	24055.98	2	0R	1.1	H00	S	-----	0	24694.77	1A	20	0.2	R00	S
-----	0	24051.24	4	60	1.0	I00	S	-----	0	24693.65	4	60	2.1	I00	S
-----	0	24049.86	4	.0	.0	L00	S	-----	0	24678.79	0F	2R	1.1	H00	T
-----	0	24048.05	1	1R	1.1	H00	S	-----	0	24676.58	2	5P	0.0	H00	S
-----	0	24038.10	0F	70	3.3	I00	S	-----	0	24663.71	1F	120	1.0	I00	S
-----	0	24035.74	5	10	2.1	K00	T	-----	0	24660.11	2	2H	0.2	T00	S
-----	0	24023.10	1	2P	2.2	L00	S	-----	0	24652.27	2	6P	2.1	I00	S
-----	0	24021.79	1	2R	1.1	H00	S	-----	0	24645.40	2	50	2.1	I00	S
-----	0	24020.51	5	0R	1.0	I00	S	-----	0	24640.91	0A	5R	0.2	P00	S
-----	0	24018.06	0A	5P	1.2	H00	S	-----	0	24640.91	0-	1R	1.1	H00	T
-----	0	24014.32	1	20	2.1	K00	T	-----	0	24624.94	0	3P	0.0	H00	T
-----	0	24012.12	2	5	.0	L00	S	-----	0	24617.47	0F	4P	2.2	H00	S
-----	0	24010.90	3	6	.0	L00	S	-----	0	24617.06	1	1R	2.2	H00	S
-----	0	24006.09	0A	3R	3.3	I00	S	-----	0	24615.73	0	1R	0.2	T00	S
-----	0	24001.74	3	50	1.0	I00	S	-----	0	24608.70	0A	6P	2.1	I00	S
-----	0	23998.08	2	2H	3.3	I00	S	-----	0	24608.70	0A	40	2.1	I00	S
-----	0	23984.06	0F	5P</											

00	0	22154.08	0	21	2.4	WAB	S	0.000000	0	22631.71	5	3R	0.0	MHC	T
00	0	22150.1R	OAB	30	2.2	MAAC	I	0.000000	0	22628.41	0	100	2.3	110R	S
00	0	22146.50	14	3M	1.2	MHA	T	4.000000	0	22624.42	1	50	0.0	MAAC	T
00	0	22143.41	6	3M	0.0	PAC	I	0.000000	0	22622.40	0	10	0.0	MHC	T
00	0	22143.81	6	24	2.3	IAAD	S	0.000000	0	22620.69	4	20	1.1	110R	S
00	0	22143.19	4	54	0.0	MAAC	T	0.000000	0	22619.03	1	4R	0.0	MHC	T
00	0	22140.01	OAB	40	2.2	RAAC	I	0.000000	0	22617.71	OF	10	7.3	DAA	T
00	0	22135.79	0	1P	1.1	PAC	T	0.000000	0	22616.55	4	4P	1.1	1A0	S
00	0	22133.48	1	OR	0.2	MAH	S	0.000000	0	22616.55	4	4P	2.2	RAAC	T
00	0	22133.24	1	2P	1.1	RHC	T	0.000000	0	22614.51	0	30	0.4	S10R	S
00	0	22129.79	5	OR	0.0	KHA	T	0.000000	0	22613.42	1	5P	1.1	1A0	S
00	0	22126.25	OAB	30	2.2	RAAC	T	0.000000	0	22613.42	1	10	1.1	110R	S
00	0	22125.17	OAH	50	0.0	RHC	T	0.000000	0	22612.15	2	3P	1.1	1A0	S
00	0	22120.24	3	40	3.3	S10C	T	0.000000	0	22608.47	OAB	60	0.0	MAAC	T
00	0	22116.21	1	10	0.1	MAA	T	0.000000	0	22604.45	1	1P	1.1	MAAC	T
00	0	22118.03	OAU	3P	1.1	RAAC	T	0.000000	0	22604.65	1	5R	0.0	RHC	T
00	0	22114.49	0	10	4.1	DAA	T	0.000000	0	22604.41	1	8R	1.1	G0C	S
00	0	22111.59	0	20	2.2	RAAC	T	0.000000	0	22604.07	1	20	3.4	110R	S
00	0	22111.57	0	2P	0.4	RAAC	S	0.000000	0	22602.82	2	1P	1.0	F0A	T
00	0	22108.89	2	30	0.0	JHP	S	0.000000	0	22601.50	3	20	1.1	SDAC	T
00	0	22108.49	2	20	0.1	MAA	T	0.000000	0	22591.76	2	2P	1.1	1A0	S
00	0	22106.34	OAB	30	1.1	RHC	T	0.000000	0	22587.92	2	3P	0.0	SDAC	T
00	0	22105.43	1	70	2.3	IRB	S	0.000000	0	22566.89	0	4P	0.0	MAAC	T
00	0	22104.85	1	30	3.3	SDC	T	0.000000	0	22564.34	1	0R	3.4	G0C	S
00	0	22104.85	1	3R	1.1	G0C	S	0.000000	0	22579.43	0	2P	3.4	1A0	S
00	0	22102.72	0	1P	1.1	K0P	S	0.000000	0	22576.51	0M	5P	0.0	S10C	T
00	0	22102.72	0	3R	2.4	M0P	S	0.000000	0	22570.83	0	3P	3.4	1A0	S
00	0	22099.80	0	60	1.2	JHP	S	0.000000	0	22559.44	1	2R	3.4	G0C	S
00	0	22099.80	0	2R	1.2	NUA	T	0.000000	0	22555.03	1M	110	0.0	LU0	S
00	0	22094.48	1	5P	0.0	JAC	S	0.000000	0	22555.03	1M	3R	2.2	RAAC	T
00	0	22094.48	1	1R	0.0	JAC	S	0.000000	0	22555.02	1M	4P	3.4	1A0	S
00	0	22093.22	0	10	0.4	ADP	S	0.000000	0	22553.90	0F	5R	0.0	1A0	S
00	0	22093.22	0	70	0.1	MAA	T	0.000000	0	22549.28	1	2P	0.0	RAAC	T
00	0	22093.02	0	10	2.2	RAAC	T	0.000000	0	22541.71	2	1R	2.2	SDAC	T
00	0	22087.71	0	2R	3.3	RAAC	T	0.000000	0	22537.10	1	20	0.0	RHC	T
00	0	22086.17	2	1R	1.1	PAC	T	0.000000	0	22526.29	OAB	3R	3.3	SDAC	T
00	0	22084.92	8	10	1.1	PAC	T	0.000000	0	22525.32	3	1P	0.0	PAC	T
00	0	22083.20	0F	20	4.1	DAA	T	0.000000	0	22523.16	2	2P	1.0	F0A	T
00	0	22079.29	OAB	3P	0.0	RAAC	T	0.000000	0	22521.98	0F	4R	3.4	G0C	S
00	0	22076.33	4	3P	2.4	M0P	S	0.000000	0	22519.12	1	7R	1.1	G0C	S
00	0	22073.84	1F	40	0.1	MAA	T	0.000000	0	22519.11	1	40	2.2	SDAC	T
00	0	22072.49	1	4P	2.2	SDC	T	0.000000	0	22509.10	2	0R	1.1	G0C	S
00	0	22069.39	1	3P	2.2	SDC	T	0.000000	0	22506.71	0	90	2.3	10R	S
00	0	22067.22	0	4P	1.1	RAAC	T	0.000000	0	22501.71	2	2P	0.0	ROAC	T
00	0	22063.25	9	10	0.0	KAA	T	0.000000	0	22498.80	0M	50	1.1	RAAC	T
00	0	22062.74	5X	90	0.0	IB0	S	0.000000	0	22498.28	0H	40	1.1	RAAC	T
00	0	22061.26	1A	1P	0.2	N0P	S	0.000000	0	22494.87	3	4R	0.2	N0P	S
00	0	22056.87	0A	20	3.3	SDC	T	0.000000	0	22489.66	7	20	1.1	RAAC	T
00	0	22056.27	0A	60	0.0	RHC	T	0.000000	0	22489.66	7	2R	2.2	RAAC	T
00	0	22055.49	1M	1R	1.2	NDAA	T	0.000000	0	22489.04	7	1R	1.1	RDAC	T
00	0	22053.41	0	5P	2.2	SDC	T	0.000000	0	22457.28	1	30	2.2	SDAC	T
00	0	22047.21	5	2P	1.1	KAD	S	0.000000	0	22447.68	1	1R	1.1	G0C	S
00	0	22047.21	5	20	0.0	KAA	T	0.000000	0	22431.73	0	10	1.1	RAAC	T
00	0	22039.17	1	40	1.1	RHC	T	0.000000	0	22427.97	9	1R	0.0	PAC	T
00	0	22037.62	0	5R	0.0	PAC	T	0.000000	0	22427.97	9	2R	1.1	RHC	T
00	0	22030.34	3	30	0.0	PAC	T	0.000000	0	22426.70	OAB	3P	0.0	RAAC	T
00	0	22030.34	3	2R	2.4	M0P	S	0.000000	0	22426.06	6	10	0.0	PAC	T
00	0	22027.58	3	2P	0.2	N0P	S	0.000000	0	22420.15	0	6R	1.1	G0C	S
00	0	22027.61	OAB	7P	0.0	RAAC	T	0.000000	0	22406.06	6	3R	1.1	RHC	T
00	0	22026.50	0	60	2.3	IB0	S	0.000000	0	22403.85	0	30	0.0	RHC	T
00	0	22025.84	OAB	4P	0.0	REAC	T	0.000000	0	22411.50	5	2R	1.1	G0C	S
00	0	22025.34	10	24	1.1	PAC	T	0.000000	0	22406.65	OAB	2R	3.3	SDAC	T
00	0	22025.34	10	1R	2.2	RBA	T	0.000000	0	22405.06	0	2R	0.0	JAB0	S
00	0	22023.30	4	30	0.0	KAA	T	0.000000	0	22401.67	3	4R	1.1	RHC	T
00	0	22019.64	0	2R	2.2	RHC	T	0.000000	0	22449.78	3	3R	0.0	KBA	T
00	0	22018.21	2	5P	1.1	RAAC	T	0.000000	0	22445.76	OAB	10	1.1	RHC	T
00	0	22016.21	2	3R	2.2	RHC	T	0.000000	0	22443.52	0D	5R	1.1	G0C	S
00	0	22013.99	OAB	4R	2.2	RHC	T	0.000000	0	22440.79	0	4R	3.3	RAAC	T
00	0	22008.13	1	1R	3.3	RAAC	T	0.000000	0	22436.69	1	3R	1.1	G0C	S
00	0	22008.13	1	5R	2.2	RHC	T	0.000000	0	22437.06	2	3P	0.2	N0P	S
00	0	22006.34	6	20	0.0	J0P	S	0.000000	0	22435.59	2	5R	1.1	RHC	T
00	0	22004.56	0F	0R	1.2	NGAA	T	0.000000	0	22432.41	1	4R	1.1	G0C	S
00	0	22003.18	2	3P	1.1	RHC	T	0.000000	0	22432.12	3	20	2.2	SDAC	T
00	0	22196.42	0	2	0.0	PAC	T	0.000000	0	22432.02	3	40	0.0	JBP	S
00	0	22193.99	2	3P	0.2	N0P	S	0.000000	0	22431.10	4	3P	1.0	F0A	T
00	0	22192.67	0F	2P	0.1	NDAA	T	0.000000	0	22430.19	3	3P	1.1	SDAC	T
00	0	22191.78	1	40	0.0	KAA	T	0.000000	0	22430.19	3	4P	1.1	SDAC	T
00	0	22188.25	6	4P	0.0	JAB	S	0.000000	0	22423.83	1	10	6.5	KAA	T
00	0	22188.23	6	50	3.3	RAAC	T	0.000000	0	22421.43	3	6P	0.0	JAB	S
00	0	22184.97	0F	4P	2.4	M0P	S	0.000000	0	22420.99	3	6R	1.1	RHC	T
00	0	22183.74	0	2P	2.2	RAAC	T	0.000000	0	22420.99	3	1R	2.2	RAAC	T
00	0	22179.91	OAB	10	2.2	RHC	T	0.000000	0	22419.49	2	5P	1.1	SDAC	T
00	0	22177.14	OAB	3P	0.0	PAC	T	0.000000	0	22419.49	2	2R	0.0	KBA	T
00	0	22172.89	1P	8P	0.0	IA0B	S	0.000000	0	22410.40	10	2R	0.0	PAC	T
00	0	22171.16	2	20	1.1	PAC	T	0.000000	0	22410.04	0U	4P	0.0	RAAC	T
00	0	22171.16	2	50	1.1	RHC	T	0.000000	0	22409.70	0F	0R	0.4	RA0B	S
00	0	22169.78	OAB	2P	1.1	PAC	T	0.000000	0	22401.26	0	2R	0.2	N0P	S
00	0	22167.05	OAB	6P	1.1	PAAC	T	0.000000	0	22399.20	0	80	2.3	10R	S
00	0	22163.07	OAB	40	3.3	PAAC	T	0.000000	0	22399.20	1F	100	0.0	1R0S	S
00	0	22162.31	5	3R	1.1	PAC	T	0.000000	0	22394.07	2	40	0.0	ROAC	T
00	0	22161.50	1U	50	2.4	IO0B	S	0.000000	0	22393.40	1	4P	1.2	M0P	S
00	0	22160.21	1	1R	2.4	M0P	S	0.000000	0	22386.03	0F	2P	1.2	M0P	S
00	0	22158.45	4	4P	0.2	N0P	S	0.000000	0	22390.49	0	3P	1.2	M0P	S
00	0	22147.75	3	50	1.2	JHP	S	0.000000	0	22379.40	8	1R	0.0	KBA	T
00	0	22147.95	3	0R	0.4	M0P	S	0.000000	0	22374.50	OAB	20	1.1	ROAC	T
00	0	22147.91	3	3P	2.2	RAAC	T								

00	0	21870.07	00	IR	1.4	NAB	S	00	0	22119.02	00	3P	0.1	NHAA	T
00	0	21873.10	0	IR	3.3	PAC	T	00	0	22119.07	00	7D	1.7	NABA	T
00	0	21878.34	1	AM	2.3	NAB	S	00	0	22119.51	0	7D	2.2	NHAC	T
-----		21877.03	8	3P	0.0	IAFU	S	00	0	22119.61	1	1P	2.2	PAC	T
00	0	21877.14	0	IR	8.0	EVA	T	-----		22110.74	3	4P	2.3	IAMP	S
00	0	21873.55	1H	10	3.3	PAC	T	-----		22110.43	3	4P	2.2	RAAC	T
00	0	21871.25	1	4P	2.2	NHAC	T	-----		22110.43	3	4D	2.3	IHHM	S
00	0	21871.27	1	2R	0.0	EVA	T	00	0	22106.39	0	30	1.2	NABA	T
00	0	21870.0	0AD	6P	1.1	RHAC	T	00	0	22105.74	1	4D	0.0	PAC	T
-----		21874.43	6	3D	0.0	IHAC	S	00	0	22105.74	1	2R	1.1	NHAA	T
00	0	21874.84	1	1P	0.0	NAB	S	00	0	22104.18	0	20	3.3	RAAC	T
-----		21870.56	5	10	0.0	IHHM	S	00	0	22103.87	1	6D	1.1	RHAC	T
00	0	21870.47	1A	4P	2.3	GAB	S	00	0	22102.13	2	3P	0.0	JAMP	S
-----		21877.99	10	20	0.0	IHHM	S	00	0	22102.12	2	3P	3.3	SUAC	T
00	0	21877.99	10x	90	1.2	INDM	S	00	0	22100.70	0	4P	3.3	SHAC	T
-----		21872.10	0AR	4P	1.1	PAC	T	-----		22099.47	0AD	5P	0.0	RHAC	T
00	0	21870.40	4	1R	3.3	RHAC	T	-----		22097.47	7	3P	2.3	IAMP	S
-----		21817.26	0A	10	1.1	PAC	T	00	0	22097.47	7	4H	1.1	PAC	T
00	0	21817.54	0A	2R	3.3	RHAC	T	00	0	22093.84	1	24	0.4	PAU	S
-----		21815.61	10	2P	0.0	IAMP	S	00	0	22086.00	0F	40	1.2	NABA	T
00	0	21813.40	0	3R	3.3	RHAC	T	00	0	22087.61	3H	7D	2.3	IAMP	S
-----		21812.07	0AB	5P	0.0	PAC	T	00	0	22081.00	0	1P	2.3	GAB	S
00	0	21809.48	2	20	1.2	JAMP	S	00	0	22081.00	0	7P	0.0	JAMP	S
-----		21806.87	0	3P	2.2	PAC	T	00	0	22079.60	2	4P	1.1	RHAC	T
00	0	21803.61	1	2R	3.3	PAC	T	-----		22079.72	2	1R	2.2	PAC	T
-----		21797.70	0AR	70	0.0	PAC	T	00	0	22073.37	5	10	2.2	PAC	T
00	0	21786.69	3	2P	0.0	NAB	S	00	0	22073.35	5	10	3.3	RAAC	T
-----		21785.95	0	1P	1.4	NAB	S	00	0	22072.56	2	5P	2.2	RAAC	T
00	0	21771.84	2	4P	1.2	JAMP	S	00	0	22072.46	2	30	2.3	IAMP	S
-----		21771.26	0-	10	3.4	NABA	T	00	0	22070.50	0	2P	2.2	RHAC	T
00	0	21771.26	0	10	3.3	RHAC	T	00	0	22068.24	0AB	5P	3.3	SHAC	T
-----		21760.46	0F	20	3.4	NABA	T	00	0	22064.55	1	1R	2.3	GAB	S
00	0	21757.96	0H	1R	0.1	LAE	S	00	0	22063.07	3	2R	2.3	GAB	S
-----		21755.92	1	0R	0.1	LAE	S	00	0	22063.07	3-	1R	1.1	KHAA	T
00	0	21751.56	0H	1R	2.2	KHAA	T	00	0	22056.15	0AB	30	2.2	RHAC	T
-----		21749.20	0	20	3.3	PAC	T	-----		22054.01	5U	30	1.1	PAC	T
00	0	21748.69	0-	3P	1.1	KHAA	T	00	0	22053.66	4	0R	2.3	GAB	S
-----		21748.69	0A	40	2.2	PAC	T	00	0	22053.66	4	3R	2.3	GAB	S
00	0	21746.27	4	2P	1.4	NAB	S	00	0	22048.66	7	3P	0.0	KHAA	T
-----		21746.27	4-	2R	0.1	LAE	S	00	0	22047.14	1	70	0.0	IBAS	S
00	0	21744.19	0F	30	3.4	NABA	T	00	0	22046.37	6	20	2.3	IBAS	S
-----		21739.06	0AD	2P	3.3	PAC	T	00	0	22040.16	2H	70	1.1	RHAC	T
00	0	21736.08	0AB	5P	2.2	RHAC	T	00	0	22040.15	2H	4R	2.3	GAB	S
-----		21729.01	1	3P	0.0	PAB	S	00	0	22040.15	2H	1R	0.0	IAMP	S
00	0	21723.3	0AB	7P	1.1	RHAC	T	00	0	22038.48	0F	1P	0.4	TAB	S
-----		21723.06	0F	40	3.4	NABA	T	00	0	22034.53	0AB	6P	2.2	RAAC	T
00	0	21716.11	0AB	20	3.3	RHAC	T	00	0	22034.53	2	10	2.3	IBAS	S
-----		21699.61	1-	3P	1.4	NAB	S	-----		22025.24	0F	2P	1.2	NHAA	T
00	0	21699.61	1-	1P	0.1	LAE	S	00	0	22024.35	5	2R	2.2	PAC	T
-----		21689.41	0H	10	5.2	DAFA	T	00	0	22014.85	2	40	1.2	JAMP	S
00	0	21689.41	4	2R	0.1	NAB	S	00	0	22014.85	2	2R	1.2	JAMP	S
-----		21688.62	0-	4P	1.1	KHAA	T	00	0	22005.06	1	4P	2.4	NAB	S
00	0	21688.62	0-	0R	2.4	LAR	S	00	0	22002.19	5	6P	0.0	IAMP	S
-----		21667.31	0AD	2P	3.3	RHAC	T	00	0	22001.89	0AB	40	2.2	RHAC	T
00	0	21664.36	3	4P	0.0	NAB	S	00	0	21999.45	0AB	3P	1.1	PAC	T
-----		21664.36	3	6R	0.0	GAB	S	00	0	21992.65	0AB	4D	0.0	PAC	T
00	0	21661.76	0AR	30	3.3	RHAC	T	00	0	21991.63	0	50	0.0	PAC	T
-----		21658.70	0F	20	5.2	DAFA	T	00	0	21981.71	5	0R	2.3	KAB	S
00	0	21655.75	0AB	5P	1.1	PAC	T	00	0	21978.40	0F	2P	2.4	NAB	S
-----		21650.56	10	10	2.2	KHAA	T	00	0	21976.78	0AR	6P	0.0	RHAC	T
00	0	21648.95	0	30	3.3	PAC	T	00	0	21972.38	3	6P	0.0	IAMP	S
-----		21647.76	1	4P	1.4	NAB	S	00	0	21970.34	1	20	2.2	PAC	T
00	0	21646.92	5	7R	0.0	GAB	S	00	0	21969.00	0AB	2P	3.3	RAAC	T
-----		21645.54	2	2P	0.1	LAE	S	00	0	21967.13	5	60	0.0	IBAS	S
00	0	21645.12	0AB	4P	2.2	PAC	T	00	0	21963.56	3	2P	2.2	PAC	T
-----		21644.05	0AD	6P	0.0	PAC	T	00	0	21963.56	3	3R	2.2	PAC	T
00	0	21636.35	1A	2P	6.0	EVA	T	00	0	21963.56	3-	1R	2.3	KAB	S
-----		21635.44	5	20	2.2	KHAA	T	00	0	21960.18	2	4P	0.0	KHAA	T
00	0	21632.10	0AB	6P	2.2	RHAC	T	00	0	21959.22	0AB	5P	1.1	PHAC	T
-----		21631.16	0AR	50	2.2	PAC	T	00	0	21952.20	1H	3P	2.2	RHAC	T
00	0	21628.20	0A	3R	3.5	JAMP	S	00	0	21952.60	0F	2P	2.3	GAB	S
-----		21627.98	0F	5P	0.5	SAB	S	-----		21951.80	10	10	1.1	KHAA	T
00	0	21623.82	2F	60	3.5	IBAS	S	00	0	21948.45	0AB	3P	3.3	RAAC	T
-----		21619.80	1	1P	2.4	LAE	S	00	0	21946.45	0AB	50	2.2	RHAC	T
00	0	21615.69	0F	30	5.2	DAFA	T	00	0	21946.11	0F	10	2.3	NABA	T
-----		21614.14	5	5R	0.0	GAB	S	00	0	21937.52	4	2R	2.3	KAB	S
00	0	21612.85	3-	30	2.2	KHAA	T	00	0	21936.14	5-	20	2.3	NABA	T
-----		21607.34	0H	40	3.3	RHAC	T	00	0	21936.14	5-	20	1.1	KHAA	T
00	0	21607.27	1F	70	1.2	IBAS	S	00	0	21931.77	4	0R	0.0	IAMP	S
-----		21601.63	10	0R	0.0	GAB	S	00	0	21930.40	4	5P	0.0	IAMP	S
00	0	21598.27	1-	5P	0.0	NAB	S	00	0	21927.12	0AB	4P	3.3	RAAC	T
-----		21596.27	1-	5P	1.4	NAB	S	00	0	21920.84	0-	30	2.3	NABA	T
00	0	21593.77	2	2R	1.2	IAMP	S	00	0	21920.84	0-	3R	0.6	NAB	S
-----		21593.39	0AB	3P	3.3	PAC	T	00	0	21918.18	1	2R	0.0	NAB	S
00	0	21591.65	1	6P	1.4	NAB	S	00	0	21913.02	4	30	1.1	KHAA	T
-----		21595.48	8	1R	0.0	GAB	S	00	0	21911.91	1	1R	0.0	NAB	S
00	0	21593.67	9-	5P	1.1	KHAA	T	00	0	21909.00	0AB	5P	3.3	RAAC	T
-----		21593.67	9-	40	2.2	PAFA	T	00	0	21905.79	3	50	0.0	IBAS	S
00	0	21593.62	9	4R	0.0	GAB	S	00	0	21901.17	1	30	1.2	JHAC	S
-----		21575.44	0	1R	0.1	NAB	S	00	0	21900.12	0-	40	2.3	NABA	T
00	0	21575.04	0	3P	0.1	LAE	S	00	0	21900.12	0A	3R	2.3	KAB	S
-----		21573.86	10	2R	0.0	GAB	S	00	0	21897.08	3	3P	2.3	GAB	S
00	0	21570.83	5	3R	0.0	GAB	S	00	0	21897.08	3	0R	0.0	NAB	S
-----		21570.31	2	1P	0.0	GAB	S	00	0	21896.92	3	4R	2.2	PAC	T
00	0	21561.31	0AR	3P	3.3	RHAC	T	00	0	21891.54	0AB	40	2.2	RHAC	T
-----		21556.52	1P	50	3.5	IAMP	S	00	0	21890.22	0AB	60	0.0	PAC	T
00	0	21552.64	1H	3	1.2	LAMP	S	00	0	21886.46	0	4R	0.0	NAB	S
-----		21552.04	1H	1R	3.5	IAMP	S	-----		21884.68	10	4P	0.0	IAMP	S
00	0	21530.0	0AR	7P	2.2	RHAC	T	00	0	21882.35	1A	40	1.1	KHAA	T
-----		21527.04	1	0R	1.3	NHAC	T	00	0	21876.81	0	1P	3.3	PAC	T
00	0	21527.06	0A	1R	1.3	NHAC	T	00	0	21873.50	0P	50	2.3	NABA	T
-----		21520.92	3	60	1.2	IBAS	S	00	0	21871.90	0	2R	1.4		

00	0	20070.07	0-	1P	0.1	KAP	S	0--	0	20470.90	1	34	2.4	LHP	S
00	0	20070.07	0	7M	1.1	GPH	S	0--	0	20670.90	1	40	0.2	HAP	S
00	0	20081.93	0	4R	0.4	NHP	S	0--	0	20815.78	9	14	0.0	FSA	T
-----		20093.41	4-	2P	2.6	NHP	S	0--	0	20814.00	0	50	0.1	IHPH	S
-----		20093.91	4-	0Q	1.4	NHP	S	0--	0	20813.46	1	0R	0.1	IAPH	S
-----		20097.09	7	2P	0.1	KAP	S	0--	0	20807.12	1	1P	1.5	NHP	S
-----		20008.60	7	2P	1.1	FSA	T	0--	0	20595.01	0	4P	0.1	IAPH	S
-----		20007.03	3	4P	0.1	GPH	S	0--	0	20570.67	3	0R	0.0	FSA	T
-----		20002.69	5	6R	1.3	GPH	S	0--	0	20569.45	2	2P	1.5	NHP	S
-----		19493.55	1	3R	0.4	NHP	S	0--	0	20568.99	0	2P	1.3	JHPH	S
-----		19490.86	9	0R	1.3	GPH	S	0--	0	20561.05	3	4P	0.1	IHPH	S
-----		19462.54	8	1R	1.3	GPH	S	0--	0	20554.94	1	1P	0.2	NHP	S
-----		19460.91	0	1P	1.3	GPH	S	0--	0	20553.99	0	1D	0.6	KAPA	T
-----		19359.86	1	5R	1.3	GPH	S	0--	0	20540.65	3	3P	0.1	IAPH	S
-----		19349.79	8	2R	0.4	NHP	S	0--	0	20530.48	4-	5P	2.0	DHPA	T
-----		19342.45	10	2R	1.3	GPH	S	0--	0	20530.48	4	3D	0.1	IHPH	S
-----		19336.73	4	2P	1.4	HHP	S	0--	0	20526.44	1	3P	1.5	NHP	S
-----		19334.35	8	4R	1.3	GPH	S	0--	0	20514.48	8	2D	0.1	IHPH	S
-----		19329.31	1	1D	4.2	DAPA	T	0--	0	20514.19	2	1D	0.1	IHPH	S
-----		19328.69	6	3R	1.3	GPH	S	0--	0	20510.10	4	2P	0.2	NHP	S
-----		19326.18	5	3P	1.1	FSA	T	0--	0	20508.15	0	0P	1.3	IHPH	S
-----		19319.73	0	1D	8.5	DAPA	T	0--	0	20503.04	6	2P	0.1	IAPH	S
-----		19315.90	0	1R	2.2	FSA	T	0--	0	20493.95	3	1Q	7.4	DAPA	T
-----		19311.82	4	1R	0.4	NHP	S	0--	0	20479.72	7	4P	1.5	NHP	S
-----		19304.16	0	2Q	4.2	DAPA	T	0--	0	20478.13	0	1R	0.2	LHP	S
-----		19305.10	1	6P	0.1	GPH	S	0--	0	20474.44	1	0R	0.2	LHP	S
-----		19305.10	1	6D	1.4	JHPH	S	0--	0	20469.77	1A	24	0.2	LHP	S
-----		19301.49	0A	6P	0.2	JHPH	S	0--	0	20459.24	2P	2P	1.0	RHC	S
-----		19304.78	1	6D	2.5	IHPH	S	0--	0	20459.24	2-	1P	0.0	FSA	T
-----		19379.73	2	2P	1.3	GPH	S	0--	0	20457.15	0	3P	0.2	NHP	S
-----		19373.74	9	0R	0.4	NHP	S	0--	0	20438.89	4	1D	3.1	DAPA	T
-----		19366.70	1	4D	0.2	JHPH	S	0--	0	20436.09	1	6P	1.5	NHP	S
-----		19366.70	1-	3D	4.2	DAPA	T	0--	0	20436.09	1	5P	1.5	NHP	S
-----		19358.39	1	1R	0.1	KAPA	T	0--	0	20419.64	0-	1P	0.2	LHP	S
-----		19336.46	9	1R	1.3	KAP	S	0--	0	20419.64	0	3D	7.4	DAPA	T
-----		19316.46	9	2R	1.3	KAP	S	0--	0	20412.95	1	2D	3.1	DAPA	T
-----		19329.35	8	0R	1.3	KAP	S	0--	0	20398.78	2	4P	0.2	NHP	S
-----		19305.44	0A	5D	2.5	IHPH	S	0--	0	20396.79	0	7D	1.3	IHPH	S
-----		19305.44	0-	0R	0.1	KAPA	T	0--	0	20394.70	2	24	0.2	NHP	S
-----		19304.30	5	1P	0.4	NHP	S	0--	0	20376.15	4	2P	0.0	FSA	T
-----		19300.96	1M	6P	2.5	IAPH	S	0--	0	20374.25	1	3D	3.1	DAPA	T
-----		19304.83	0	3P	1.3	GPH	S	0--	0	20368.97	3	2P	0.2	LHP	S
-----		19377.54	2A	1P	1.3	KAP	S	0--	0	20365.97	5	7P	0.1	GPH	S
-----		19376.54	9	2P	0.4	NHP	S	0--	0	20351.33	1	2R	1.3	IAPH	S
-----		19365.11	0M	1R	1.0	JHPH	T	0--	0	20340.22	0	5P	0.2	NHP	S
-----		19350.59	4	3P	0.4	NHP	S	0--	0	20334.94	0	3P	2.5	LHP	S
-----		19342.75	1	4P	2.5	IAPH	S	0--	0	20323.15	5-	4D	3.1	DAPA	T
-----		19342.22	6	4D	2.5	IHPH	S	0--	0	20323.15	5	5R	0.1	GPH	S
-----		19342.22	6-	1D	0.1	KAPA	T	0--	0	20318.18	1	3D	3.6	IHPH	S
-----		19332.69	0	2D	0.1	KAPA	T	0--	0	20314.59	2-	3	.3	LHPH	S
-----		19320.21	5	2P	1.3	KAP	S	0--	0	20314.59	2-	3P	1.0	RHC	S
-----		19326.71	5	5D	1.4	JHPH	S	0--	0	20314.59	2-	2P	3.1	DHPA	T
-----		19325.70	7	6P	0.4	NHP	S	0--	0	20302.96	3	6D	1.3	IHPH	S
-----		19319.71	1	3P	2.5	IAPH	S	0--	0	20295.69	0	1R	0.2	NHP	S
-----		19318.44	0	3D	0.1	KAPA	T	0--	0	20293.69	1A	2D	1.4	NHP	S
-----		19317.24	1	6P	0.4	NHP	S	0--	0	20285.06	4	3D	0.0	FSA	T
-----		19309.41	2	4P	1.3	GPH	S	0--	0	20283.93	9	2D	3.6	IHPH	S
-----		19308.20	1	5D	0.4	NHP	S	0--	0	20283.93	9	4R	0.1	GPH	S
-----		19307.24	4	2P	2.5	IAPH	S	0--	0	20283.29	8	2D	3.6	IHPH	S
-----		19304.55	1	3D	2.5	IHPH	S	0--	0	20283.29	8-	0R	0.1	GPH	S
-----		19300.44	1	1P	2.5	GPH	S	0--	0	20269.03	7	1R	0.1	GPH	S
-----		19304.29	0M	6R	2.5	GPH	S	0--	0	20263.88	4	3R	0.1	GPH	S
-----		19377.66	7	2R	2.5	GPH	S	0--	0	20262.54	0	6	.3	LHPH	S
-----		19375.87	1	3R	2.5	GPH	S	0--	0	20260.90	10	2R	0.1	GPH	S
-----		19374.02	2	1R	2.5	GPH	S	0--	0	20259.51	1	2P	3.6	IAPH	S
-----		19372.11	2	4R	2.5	GPH	S	0--	0	20259.51	1-	5D	3.1	DAPA	T
-----		19368.85	1-	3P	1.3	KAP	S	0--	0	20256.79	3	3P	3.6	IAPH	S
-----		19368.85	1	5R	2.5	GPH	S	0--	0	20256.79	3	0R	3.6	GPH	S
-----		19360.83	9	2D	2.5	IHPH	S	0--	0	20253.93	1	1P	0.1	GPH	S
-----		19360.83	9-	0R	2.5	GPH	S	0--	0	20253.11	1A	1R	3.6	GPH	S
-----		19358.29	0M	2P	2.6	HHP	S	0--	0	20251.93	1A	4	.3	LHPH	S
-----		19344.35	0	2D	1.0	JHPH	T	0--	0	20250.78	2	4P	3.6	IAPH	S
-----		19340.06	1	1D	2.5	IHPH	S	0--	0	20248.48	0	6P	0.2	NHP	S
-----		19332.10	1	5P	1.3	GPH	S	0--	0	20240.71	5	1R	1.1	FSA	T
-----		19332.10	1-	4R	0.6	NHP	S	0--	0	20238.91	4	2R	3.6	GPH	S
-----		19327.77	1	4P	0.2	JHPH	S	0--	0	20237.22	1	5	.3	LHPH	S
-----		19316.95	1M	3P	2.2	FSA	T	0--	0	20229.13	2	3P	3.1	DHPA	T
-----		12475.8	0	2R	2.2	RHC	S	0--	0	20226.66	3	5D	1.3	IHPH	S
-----		19303.36	2	4P	1.3	KAP	S	0--	0	20222.49	0	5P	3.6	IAPH	S
-----		19308.70	4	0R	2.5	KAP	S	0--	0	20217.55	2	2P	1.4	NHP	S
-----		19376.33	1	6P	1.3	GPH	S	0--	0	20217.55	2-	3P	3.6	GPH	S
-----		19373.06	3	1R	2.5	KAP	S	0--	0	20213.54	0	0R	0.2	NHP	S
-----		19370.32	0A	3R	0.6	NHP	S	0--	0	20198.29	3	0R	1.1	FSA	T
-----		19366.76	4	1D	1.2	KAPA	T	0--	0	20185.85	3	4P	0.0	FSA	T
-----		19357.39	1	2D	1.2	KAPA	T	0--	0	20176.00	1	8R	1.3	GPH	S
-----		19352.08	7	2R	2.5	KAP	S	0--	0	20174.02	1	0R	1.3	IAPH	S
-----		19351.47	0	2P	0.6	NHP	S	0--	0	20172.92	6	2P	0.1	GPH	S
-----		19343.59	2M	3P	0.1	KAPA	T	0--	0	20168.72	5	4D	1.3	IHPH	S
-----		19343.59	2M	3D	1.2	KAPA	T	0--	0	20151.83	2	4P	0.2	NHP	S
-----		19335.78	1	1R	0.6	NHP	S	0--	0	20135.01	2	1R	0.1	KAP	S
-----		19325.33	0A	6D	1.2	KAPA	T	0--	0	20128.48	1	0R	0.1	RHP	S
-----		19323.42	0	3D	0.2	JHPH	S	0--	0	20127.64	6	3D	1.3	IHPH	S
-----		19322.09	1	3R	2.5	KAP	S	0--	0	20127.64	6-	2R	0.1	KAP	S
-----		19315.98	4	0R	0.6	NHP	S	0--	0	20123.80	0	0R	2.6	NHP	S
-----		19440.80	1M	1R	2.1	JHPH	T	0--	0	20120.69	0	3P	0.2	NHP	S
-----		19440.07	2	4R	2.5	KAP	S	0--	0	20118.28	5	4P	1.3	IAPH	S
-----		19432.12	1	6P	0.2	JHPH	S	0--	0	20112.75	0	1R	2.6	NHP	S
-----		19440.79	2	1P	0.6	NHP	S	0--	0	20107.99	1	2P	0.2	NHP	S
-----		19436.91	0	6D	0.2	IHPH	S	0--	0	20101.74	8	2D	1.3	IHPH	S
-----		19436.36	3	1D	5.3	DAPA	T	0--	0	20098.31	0A	1R	1.4	NHP	S
-----		19427.89	5	2P	0.6	NHP	S	0--	0	20096.33	3	1D	1.3	IHPH	S
-----		19417.96	0	3P	2.5	KAP	S	0--	0	20088.33	3-	2D	2.6	NHP	S
-----		19411.89	0	2D	5.3	DAPA	T	0--	0	20084.15	1	3P	0.1	GPH	S
-----		19379.80	0A	2R	0.3	HHP	S	0--	0	20081.77	4	1P			

17084-56	2	30	1-1	JHC	1	0	17087-13	6	20	0-0	JHC	1	20	0-0
17074-54	0AN	1	0-0	JHC	1	0	17084-67	1	20	2-8	JHC	1	20	2-8
17068-60	1	30	0-0	JHC	1	0	17084-68	1	50	1-1	JHC	1	50	1-1
17056-30	0	40	1-1	JHC	1	0	17057-57	0	50	0-3	GES	5	50	0-3
17056-20	0	21	2-8	JHC	1	0	17466-16	3	20	0-0	JHC	1	20	0-0
17054-50	1	50	1-1	JHC	1	0	17451-59	10	20	0-0	JHC	1	20	0-0
17048-15	5	30	1-1	JHC	1	0	17449-52	1	18	3-0	CEA	1	18	3-0
17040-75	1	40	3-2	JHC	1	0	17441-22	0	2-2	JHC	1	2-2	JHC	1
17036-21	0AN	50	3-3	JHC	1	0	17437-27	1A	60	0-0	JHC	1	60	0-0
17031-64	0AN	40	3-3	JHC	1	0	17433-50	1A	30	0-0	JHC	1	30	0-0
17030-60	1	70	1-1	JHC	1	0	17430-26	1M	00	1-5	JHC	1	00	1-5
17030-19	1	30	3-3	JHC	1	0	17431-57	6	1R	1-1	JHC	1	1R	1-1
17028-36	2	20	3-3	JHC	1	0	17428-63	6	4R	2-7	GEB	5	6	4R
17025-81	6	20	3-3	JHC	1	0	17426-23	10	1R	1-1	JHC	1	1R	1-1
17023-67	1	40	0-0	JHC	1	0	17421-59	2	40	0-0	JHC	1	40	0-0
17022-60	0AD	20	0-0	JHC	1	0	17416-51	3	2R	2-2	JHC	1	2R	2-2
17013-50	1	2R	0-5	JHC	1	0	17415-21	1	50	0-0	JHC	1	50	0-0
17007-59	1	30	2-2	JHC	1	0	17413-62	0	1R	2-7	GEB	5	0	1R
17006-43	10	30	2-2	JHC	1	0	17411-21	5	60	1-1	JHC	1	60	1-1
17004-60	3A	20	0-0	JHC	1	0	17407-51	1	40	1-1	JHC	1	40	1-1
16996-32	1A	1R	0-5	JHC	1	0	17404-90	2	20	2-7	GEB	5	2	20
16990-71	6	3R	1-1	JHC	1	0	17421-59	1	3R	2-7	GEB	5	1	3R
16985-72	8	10	1-1	JHC	1	0	17386-47	2	50	1-1	JHC	1	50	1-1
16980-72	1A	4R	1-1	JHC	1	0	17387-14	1	10	1-5	JHC	1	10	1-5
16978-32	10	1R	1-1	JHC	1	0	17370-38	0	10	2-7	JHC	1	10	2-7
16976-53	5	40	2-2	JHC	1	0	17375-75	1	40	0-3	JHC	1	40	0-3
16976-03	5	0R	0-5	JHC	1	0	17369-32	5	1R	0-0	JHC	1	1R	0-0
16969-59	1	40	2-2	JHC	1	0	17365-20	5	10	1-1	JHC	1	10	1-1
16968-63	1	10	0-5	JHC	1	0	17364-64	6	20	1-1	JHC	1	20	1-1
16962-69	0M	3R	2-2	JHC	1	0	17358-18	9	2R	2-2	JHC	1	2R	2-2
16961-69	0A	20	0-5	JHC	1	0	17356-18	9	2R	2-2	JHC	1	2R	2-2
16959-24	0	1R	0-5	JHC	1	0	17342-82	7	20	1-5	JHC	1	20	1-5
16952-24	0AD	50	2-3	JHC	1	0	17341-28	1	40	1-5	JHC	1	40	1-5
16948-94	1	50	2-3	JHC	1	0	17337-30	3	30	1-1	JHC	1	30	1-1
16945-99	0	30	6-5	JHC	1	0	17335-25	2	4R	1-1	JHC	1	4R	1-1
16940-99	0A8	60	0-0	JHC	1	0	17325-27	1	60	0-3	JHC	1	60	0-3
16939-26	0	10	1-1	JHC	1	0	17316-92	1	50	0-3	JHC	1	50	0-3
16937-70	0AD	50	0-0	JHC	1	0	17316-56	5	20	1-1	JHC	1	20	1-1
16935-24	0	1R	2-0	JHC	1	0	17312-48	3	10	5-4	JHC	1	10	5-4
16932-40	1	70	2-2	JHC	1	0	17311-88	0	20	1-1	JHC	1	20	1-1
16930-40	0	4R	0-0	JHC	1	0	17299-30	4	40	0-0	JHC	1	40	0-0
16927-66	9	20	1-1	JHC	1	0	17296-19	2M	2R	2-7	JHC	1	2R	2-7
16927-70	2	30	3-3	JHC	1	0	17294-13	1	20	5-4	JHC	1	20	5-4
16926-40	1	40	0-4	JHC	1	0	17287-27	2	30	0-0	JHC	1	30	0-0
16926-14	0	4R	0-0	JHC	1	0	17282-98	1	3R	1-1	JHC	1	3R	1-1
16925-61	1M	30	0-0	JHC	1	0	17280-68	3	1R	2-2	JHC	1	1R	2-2
16925-64	0	4R	0-0	JHC	1	0	17279-01	7	1R	2-2	JHC	1	1R	2-2
16925-65	2	50	0-0	JHC	1	0	17273-61	0	10	2-4	JHC	1	10	2-4
16925-66	1M	30	0-0	JHC	1	0	17271-56	4	30	0-0	JHC	1	30	0-0
16925-67	1M	30	0-0	JHC	1	0	17266-62	2	30	5-4	JHC	1	30	5-4
16925-68	1M	30	0-0	JHC	1	0	17261-34	4	40	0-0	JHC	1	40	0-0
16925-69	1M	30	0-0	JHC	1	0	17252-65	2	50	0-0	JHC	1	50	0-0
16925-70	1M	30	0-0	JHC	1	0	17251-99	0A	40	0-0	JHC	1	40	0-0
16925-71	1M	30	0-0	JHC	1	0	17248-35	1	20	3-0	JHC	1	20	3-0
16925-72	1M	30	0-0	JHC	1	0	17245-71	0	2R	3-0	JHC	1	2R	3-0
16925-73	1M	30	0-0	JHC	1	0	17244-91	0	3R	3-3	JHC	1	3R	3-3
16925-74	1M	30	0-0	JHC	1	0	17239-70	2	3R	3-3	JHC	1	3R	3-3
16925-75	1M	30	0-0	JHC	1	0	17239-70	2	4R	2-7	JHC	1	4R	2-7
16925-76	1M	30	0-0	JHC	1	0	17233-16	2M	50	0-0	JHC	1	50	0-0
16925-77	1M	30	0-0	JHC	1	0	17233-16	2M	60	0-0	JHC	1	60	0-0
16925-78	1M	30	0-0	JHC	1	0	17233-16	2M	60	0-0	JHC	1	60	0-0
16925-79	1M	30	0-0	JHC	1	0	17230-99	1M	40	5-4	JHC	1	40	5-4
16925-80	1M	30	0-0	JHC	1	0	17228-24	0	20	3-0	JHC	1	20	3-0
16925-81	1M	30	0-0	JHC	1	0	17228-94	1	60	2-2	JHC	1	60	2-2
16925-82	1M	30	0-0	JHC	1	0	17218-50	6	40	2-2	JHC	1	40	2-2
16925-83	1M	30	0-0	JHC	1	0	17218-50	6	2R	1-1	JHC	1	2R	1-1
16925-84	1M	30	0-0	JHC	1	0	17218-50	6	2R	2-2	JHC	1	2R	2-2
16925-85	1M	30	0-0	JHC	1	0	17213-05	0U	50	2-2	JHC	1	50	2-2
16925-86	1M	30	0-0	JHC	1	0	17213-05	0U	50	2-2	JHC	1	50	2-2
16925-87	1M	30	0-0	JHC	1	0	17212-01	1	10	0-0	JHC	1	10	0-0
16925-88	1M	30	0-0	JHC	1	0	17212-01	1	10	0-0	JHC	1	10	0-0
16925-89	1M	30	0-0	JHC	1	0	17212-01	1	10	0-0	JHC	1	10	0-0
16925-90	1M	30	0-0	JHC	1	0	17212-01	1	10	0-0	JHC	1	10	0-0
16925-91	1M	30	0-0	JHC	1	0	17212-01	1	10	0-0	JHC	1	10	0-0
16925-92	1M	30	0-0	JHC	1	0	17212-01	1	10	0-0	JHC	1	10	0-0
16925-93	1M	30	0-0	JHC	1	0	17212-01	1	10	0-0	JHC	1	10	0-0
16925-94	1M	30	0-0	JHC	1	0	17212-01	1	10	0-0	JHC	1	10	0-0
16925-95	1M	30	0-0	JHC	1	0	17212-01	1	10	0-0	JHC	1	10	0-0
16925-96	1M	30	0-0	JHC	1	0	17212-01	1	10	0-0	JHC	1	10	0-0
16925-97	1M	30	0-0	JHC	1	0	17212-01	1	10	0-0	JHC	1	10	0-0
16925-98	1M	30	0-0	JHC	1	0	17212-01	1	10	0-0	JHC	1	10	0-0
16925-99	1M	30	0-0	JHC	1	0	17212-01	1	10	0-0	JHC	1	10	0-0
16926-00	1M	30	0-0	JHC	1	0	17212-01	1	10	0-0	JHC	1	10	0-0
16926-01	1M	30	0-0	JHC	1	0	17212-01	1	10	0-0	JHC	1	10	0-0
16926-02	1M	30	0-0	JHC	1	0	17212-01	1	10	0-0	JHC	1	10	0-0
16926-03	1M	30	0-0	JHC	1	0	17212-01	1	10	0-0	JHC	1	10	0-0
16926-04	1M	30	0-0	JHC	1	0	17212-01	1	10	0-0	JHC	1	10	0-0
16926-05	1M	30	0-0	JHC	1	0	17212-01	1	10	0-0	JHC	1	10	0-0
16926-06	1M	30	0-0	JHC	1	0	17212-01	1	10	0-0	JHC	1	10	0-0
16926-07	1M	30	0-0	JHC	1	0	17212-01	1	10	0-0	JHC	1	10	0-0
16926-08	1M	30	0-0	JHC	1	0	17212-01	1	10	0-0				

00	0	16270.11	0AH	40	3.3	IUC	T	0	0	16084.88	1	10	2.2	IAC	T
0-----	0	16270.75	1	40	1.1	DAA	T	0-----	0	16076.77	10-	0H	0.0	DHAA	T
00	0	16270.9	0AH	7P	1.1	IH	T	0-----	0	16076.77	10	4H	3.3	IAC	T
000	0	16270.3.07	1	4H	2.2	DHAA	T	0	0	16067.11	1	5P	0.0	IHAC	T
0000	0	16270.9.53	1	2H	3.3	IHAC	T	0-----	0	16056.76	9	30	0.0	GC	T
0-----	0	16271.1.79	4	3P	3.3	IAC	T	0-----	0	16046.40	2	10	2.2	IHAC	T
0-----	0	16271.1.79	4	3P	4.1	E	T	0	0	16045.3V	0AH	60	1.1	IHAC	T
0-----	0	16271.1.79	2	3H	2.2	GC	T	0	0	16041.0P	1	5H	0.0	GC	T
0-----	0	16270.41	5	3R	2.2	DHAA	T	0-----	0	16042.14	2	3P	6.2	E	T
0-----	0	16270.41	2	50	1.1	DAA	T	0	0	16035.48	0	0R	1.6	IAC	T
0-----	0	16270.06	8	5P	0.0	DHAA	T	0	0	16033.03	0	3R	3.3	IAC	T
0-----	0	16272.72	2	70	2.2	GC	T	0-----	0	16030.47	3	1R	1.1	GC	T
000	0	16218.24	1H	4P	3.3	IAC	T	0	0	16027.24	1	10	7.6	DAA	T
0000	0	16214.41	0A	2R	2.6	GC	S	0	0	16014.02	0	4P	1.6	IAC	T
0-----	0	16204.42	4	2R	2.2	DHAA	T	0-----	0	16111.43	10	10	0.0	DAA	T
0-----	0	16203.73	7	2P	1.1	DHAA	T	0-----	0	16A05.44	1	1P	1.1	GC	T
0-----	0	16197.25	6	4R	2.2	GC	T	0-----	0	16003.20	9	10	1.1	GC	T
0-----	0	16190.17	3	50	1.1	GC	T	0-----	0	16096.37	10	20	0.0	DAA	T
000	0	16187.50	1	2P	2.2	GC	T	0	0	16070.70	1	4P	1.1	IHAC	T
0-----	0	16176.63	3	3P	1.1	IAC	T	0-----	0	16064.71	10	2R	1.1	GC	T
000	0	16186.46	0	4P	1.1	GC	T	0-----	0	16079.03	2	2R	3.3	IAC	T
000	0	16175.0	0AH	5P	3.3	IAC	T	0-----	0	16075.12	5	2P	2.2	IAC	T
000	0	16170.95	0AH	6P	2.2	IAC	T	0-----	0	16071.34	10	30	0.0	DAA	T
0-----	0	16164.45	10	1R	2.2	DHAA	T	0	0	16071.34	2	4R	0.0	GC	T
0-----	0	16132.09	5	30	2.2	GC	T	0	0	16072.35	0	20	1.6	IAC	T
0000	0	16130.47	2-	4P	4.1	E	T	0	0	16040.20	0AH	6P	0.0	IHAC	T
0000	0	16130.47	2-	6P	0.0	DHAA	T	0-----	0	16040.20	3	3P	2.2	IAC	T
000	0	16129.0	0AH	6P	3.3	IAC	T	0	0	16045.00	3	3R	0.4	IAC	T
0-----	0	16126.19	10	3P	1.1	DHAA	T	0	0	16044.31	2	40	0.0	DAA	T
0-----	0	16121.52	8	CR	2.2	DHAA	T	0	0	16038.06	2	2P	2.2	IAC	T
000	0	16105.59	1	4P	3.3	IAC	T	0	0	16030.63	1	40	0.0	GC	T
000	0	16099.13	0	4P	1.6	K+E	S	0	0	16032.07	0A	3P	6.2	E	T
000	0	16074.39	0	60	1.1	GC	T	0	0	16032.67	0A	2R	0.4	GC	T
000	0	16068.78	0	6P	0.0	GC	T	0-----	0	16030.23	5	3R	1.1	GC	T
0000	0	16068.21	2	7P	2.2	IAC	T	0-----	0	16017.04	6	4P	2.2	IAC	T
0-----	0	16060.31	10	10	2.2	DAA	T	0-----	0	16015.45	5	20	1.1	GC	T
0-----	0	16046.26	7	20	2.2	DHAA	T	0	0	16011.46	1	1R	3.3	IAC	T
0-----	0	16039.1E	5	4P	1.1	DHAA	T	0-----	0	16007.71	2	50	0.0	DAA	T
000	0	16032.26	1A	40	2.2	GC	T	0	0	16004.37	0	2P	1.7	IAC	T
0000	0	16031.77	2A	7P	0.0	DHAA	T	0	0	16001.07	0	3R	1.1	DHAA	T
0-----	0	16025.36	10	30	2.2	DAA	T	0	0	16000.15	8	2P	1.1	GC	T
000	0	16018.16	1	5P	3.3	IAC	T	0	0	16005.14	0AH	50	2.2	IAC	T
0000	0	15997.73	2	40	2.2	DAA	T	0	0	16004.00	1	5P	1.1	IHAC	T
000	0	15976.14	0	1R	3.3	GC	T	0	0	16004.00	1-	10	3.1	IAC	T
000	0	15973.65	00	3R	3.3	DHAA	T	0-----	0	16079.06	7	2P	0.0	DHAA	T
0000	0	15963.63	2	50	2.2	DAA	T	0	0	16078.43	0AH	5P	2.2	IAC	T
000	0	15957.57	0AH	70	1.1	GC	T	0-----	0	16076.10	7-	2R	1.1	DHAA	T
0-----	0	15949.72	3	2R	3.3	GC	T	0-----	0	16076.10	7	3R	3.3	IAC	T
000	0	15946.21	00	5P	1.1	DHAA	T	0	0	16069.93	6	4R	1.1	GC	T
0-----	0	15943.20	3	2R	3.3	DHAA	T	0-----	0	16065.55	2	2R	3.3	IAC	T
0-----	0	15941.22	5	2P	2.2	DHAA	T	0	0	16064.49	0	60	0.0	DAA	T
000	0	15933.16	0A	2R	3.1	EP+B	S	0-----	0	16058.03	5	3P	2.2	IAC	T
0000	0	15921.94	2	10	3.3	GC	T	0-----	0	16045.00	3	1R	7.3	IHAC	T
000	0	15927.60	1-	10	0.1	PAC	S	0-----	0	16040.72	10	1R	1.1	DHAA	T
000	0	15927.60	1-	0R	3.1	EP+B	S	0-----	0	16040.72	10A	0R	1.6	GC	T
0000	0	15926.52	3H	50	2.2	GC	T	0	0	16031.36	0	6P	2.2	IAC	T
000	0	15913.37	0	1P	3.3	GC	T	0	0	16031.36	0	7P	0.0	IAC	T
000	0	15910.77	0	3R	3.3	GC	T	0	0	16030.10	0	40	2.6	IAC	T
0-----	0	15905.53	10	1R	3.3	DHAA	T	0	0	16030.10	0	4R	1.6	GC	T
000	0	15877.20	1	20	3.3	GC	T	0	0	16020.00	0AH	60	2.2	IAC	T
0-----	0	15870.10	10	3P	2.2	DHAA	T	0	0	16028.77	0	40	3.3	IAC	T
0000	0	15862.06	1H	4R	3.3	GC	T	0	0	16026.79	0	50	3.3	IAC	T
0-----	0	15858.66	5	0R	3.3	DHAA	T	0	0	16026.79	0-	10	1.6	GC	T
000	0	15858.30	0	6P	1.1	GC	T	0	0	16025.72	0	1R	1.6	GC	T
0000	0	15827.48	1	2P	3.3	GC	T	0	0	16024.30	0	30	3.3	IAC	T
0-----	0	15817.47	3-	2P	3.1	EP+B	S	0-----	0	16016.55	0	4P	0.0	GC	T
0-----	0	15817.43	3-	3R	0.1	PAC	S	0-----	0	16016.35	2	50	0.0	GC	T
0-----	0	15800.76	10	10	3.3	DAA	T	0-----	0	16016.35	2-	1R	3.1	GC	T
0000	0	15795.05	2	30	3.3	GC	T	0	0	16014.03	0	70	0.0	DAA	T
0-----	0	15793.09	5	4P	2.2	DHAA	T	0-----	0	16013.37	7	30	1.1	GC	T
0-----	0	15787.23	5	20	3.3	DAA	T	0-----	0	16013.37	7	2R	1.6	GC	T
0-----	0	15767.10	7	30	3.3	DAA	T	0	0	16010.14	0	3R	1.6	GC	T
0000	0	15740.49	1-	3P	3.1	EP+B	S	0	0	16007.51	0AH	20	3.3	IAC	T
0000	0	15740.49	1-	40	3.3	DAA	T	0	0	16005.53	0A	5R	1.1	GC	T
000	0	15716.4	0	3P	3.3	GC	T	0-----	0	16000.79	10-	3P	0.0	DHAA	T
0-----	0	15712.79	6	5P	2.2	DHAA	T	0-----	0	16000.79	9	0R	1.1	DHAA	T
000	0	15707.53	1	50	3.3	DAA	T	0	0	16000.32	1	10	3.3	IAC	T
0000	0	15706.57	1	40	3.3	GC	T	0	0	16000.32	0AH	6P	1.1	IAC	T
0-----	0	15688.01	5	2P	3.3	DHAA	T	0	0	16000.32	1	4P	2.2	IAC	T
000	0	15679.24	1	4P	3.1	EP+B	S	0-----	0	16000.32	1	10	3.3	IAC	T
0000	0	15676.02	1	2R	2.0	E	T	0	0	16000.00	0	2P	2.8	IAC	T
0-----	0	15669.39	4	1R	2.0	E	T	0	0	16000.00	0H	2P	4.1	F	T
0-----	0	15662.53	2	3R	2.0	E	T	0	0	16000.00	1	2P	0.7	IAC	T
0000	0	15650.27	1-	10	1.1	NAC	S	0	0	16000.00	0	3P	1.1	GC	T
0000	0	15650.27	1-	1R	5.2	E	T	0	0	16000.00	0	20	3.3	IAC	T
0000	0	15642.48	1	0R	2.0	E	T	0	0	16000.00	1	6R	1.1	GC	T
000	0	15629.10	0	4R	2.0	E	T	0	0	16000.00	1	1R	2.2	GC	T
000	0	15626.94	1	6P	2.2	DHAA	T	0-----	0	16000.00	10	10	1.1	DAA	T
0000	0	15621.96	10	3P	3.3	DHAA	T	0	0	16000.00	0	3P	0.7	IAC	T
0000	0	15610.91	1	50	3.3	GC	T	0	0	16000.00	0	20	2.8	IAC	T
0000	0	15610.91	1	20	0.5	IHAC	S	0	0	16000.00	0A	4P	0.7	IAC	T
000	0	15589.01	0	4P	3.3	GC	T	0-----	0	16000.00	6	40	1.1	DAA	T
0000	0	15576.06	0A	5R	2.0	E	T	0-----	0	16000.00	4	4P	0.0	DHAA	T
0-----	0	15552.37	10	10	4.4	DAA	T	0	0	16000.00	0A	4P	0.4	GC	T
0-----	0	15549.47	3	4P	3.3	DAA	T	0	0	16000.00	0	10	8.7	DAA	T
0-----	0	15539.36	3	20	4.4	DAA	T	0	0	16000.00	0A	2R	1.6	K+E	T
0-----	0	15526.92	3	1P	2.0	E	T	0	0	16000.00	1	40	1.1	GC	T
0000	0	15520.05	3	30	4.4	DAA	T	0-----	0	16000.00	5	10	2.2	GC	T
000	0	15494.05	0	40	4.4	DAA	T	0-----	0	16000.00	1	60	0.0	GC	T
000	0	15473.43	00	5P	3.1	DHAA	T	0-----	0	16000.00	3	2R	2.2	GC	T
000	0	15463.17	0	50	4.4	DAA	T	0-----	0	16000.00	10				

13709.4	2	20	2:3	DAAA T	15,485.11	7	20	5:3	DAAA T
13709.5	2A	20	2:1	DAAA T	15,485.22	2	20	5:3	FFAC S
13709.6	10	20	2:1	DAAA T	15,485.33	2	20	5:3	FFAC S
13709.7	3	14	3:4	UNDA S	...	15,485.44	1	28	0:5	UNDA S
13709.8	0	40	2:3	DAAA T	15,485.55	0A	40	2:0	LFAC S
13709.9	1	28	1:0	LAA T	...	15,486.06	0	28	0:5	LAA S
13710.0	1A	38	1:0	FBA T	...	15,486.17	0	38	1:7	LAA S
13710.1	2A	38	1:0	FBA T	...	15,486.28	0	38	1:7	LAA S
13710.2	00	50	2:3	DAAA T	15,486.39	2	50	2:0	FFAC S
13710.3	7	14	1:0	FBA T	...	15,486.50	7	14	1:0	FBA T
13710.4	00	48	1:0	EAA T	...	15,486.61	0A	48	1:0	EAA S
13710.5	0	20	0:0	MFC S	15,486.72	0	20	0:0	MFC S
13710.6	1	04	1:4	DAAA T	15,486.83	1	04	1:4	DAAA T
13710.7	2A	30	2:1	FFAC S	15,486.94	2A	30	2:1	FFAC S
13710.8	0	20	1:1	FBA T	15,487.05	0	20	1:1	FBA T
13710.9	2	08	1:0	FBA T	15,487.16	2	08	1:0	FBA T
13711.0	3	28	0:2	MFC S	15,487.27	3	28	0:2	MFC S
13711.1	1	10	2:2	MFC S	15,487.38	1	10	2:2	MFC S
13711.2	0A	20	2:3	DAAA T	15,487.49	0A	20	2:3	DAAA T
13711.3	0C	40	1:2	DAAA T	15,487.60	0C	40	1:2	DAAA T
13711.4	5	10	0:1	LAA S	15,487.71	5	10	0:1	LAA S
13711.5	0	30	0:0	DAAA T	15,487.82	0	30	0:0	DAAA T
13711.6	2	40	2:1	FFAC S	15,487.93	2	40	2:1	FFAC S
13711.7	1A	30	3:4	DAAA T	15,488.04	1A	30	3:4	DAAA T
13711.8	0	20	3:4	DAAA T	15,488.15	0	20	3:4	DAAA T
13711.9	4	18	1:0	FFAC S	15,488.26	4	18	1:0	FFAC S
13712.0	4	20	1:0	FFAC S	15,488.37	4	20	1:0	FFAC S
13712.1	1	20	2:1	DAAA T	15,488.48	1	20	2:1	DAAA T
13712.2	0A	40	2:1	FFAC S	15,488.59	0A	40	2:1	FFAC S
13712.3	0A	40	2:1	FFAC S	15,489.10	0A	40	2:1	FFAC S
13712.4	0A	30	0:1	JABC S	15,489.21	0A	30	0:1	JABC S
13712.5	0A	30	0:1	JABC S	15,489.32	0A	30	0:1	JABC S
13712.6	0A	30	0:1	JABC S	15,489.43	0A	30	0:1	JABC S
13712.7	0	10	4:5	DAAA T	15,489.54	0	10	4:5	DAAA T
13712.8	0	20	4:5	DAAA T	15,489.65	0	20	4:5	DAAA T
13712.9	1	30	4:5	DAAA T	15,489.76	1	30	4:5	DAAA T
13713.0	3	20	1:0	FBA T	15,489.87	3	20	1:0	FBA T
13713.1	1	50	2:3	DAAA T	15,489.98	1	50	2:3	DAAA T
13713.2	0	50	2:3	DAAA T	15,490.09	0	50	2:3	DAAA T
13713.3	1A	28	0:0	JABC S	15,490.20	1A	28	0:0	JABC S
13713.4	1	28	1:0	FFAC S	15,490.31	1	28	1:0	FFAC S
13713.5	0	40	2:2	MFC S	15,490.42	0	40	2:2	MFC S
13713.6	2A	18	1:0	FFAC S	15,490.53	2A	18	1:0	FFAC S
13713.7	1	10	5:6	DAAA T	15,490.64	1	10	5:6	DAAA T
13713.8	0	20	5:6	DAAA T	15,490.75	0	20	5:6	DAAA T
13713.9	0	30	5:6	DAAA T	15,490.86	0	30	5:6	DAAA T
13714.0	4	30	1:0	FBA T	15,490.97	4	30	1:0	FBA T
13714.1	4	30	1:0	FBA T	15,491.08	4	30	1:0	FBA T
13714.2	0	50	3:4	DAAA T	15,491.19	0	50	3:4	DAAA T
13714.3	1A	28	0:0	JABC S	15,491.30	1A	28	0:0	JABC S
13714.4	1	28	1:0	FFAC S	15,491.41	1	28	1:0	FFAC S
13714.5	0	40	2:2	MFC S	15,491.52	0	40	2:2	MFC S
13714.6	2A	18	1:0	FFAC S	15,491.63	2A	18	1:0	FFAC S
13714.7	1	10	5:6	DAAA T	15,491.74	1	10	5:6	DAAA T
13714.8	0	20	5:6	DAAA T	15,491.85	0	20	5:6	DAAA T
13714.9	0	30	5:6	DAAA T	15,491.96	0	30	5:6	DAAA T
13715.0	4	30	1:0	FBA T	15,492.07	4	30	1:0	FBA T
13715.1	4	30	1:0	FBA T	15,492.18	4	30	1:0	FBA T
13715.2	1	30	0:0	JABC S	15,492.29	1	30	0:0	JABC S
13715.3	3	18	1:0	FFAC S	15,492.40	3	18	1:0	FFAC S
13715.4	1B	40	0:0	JABC S	15,492.51	1B	40	0:0	JABC S
13715.5	0	20	3:3	FFAC S	15,492.62	0	20	3:3	FFAC S
13715.6	0	28	2:2	FFAC S	15,492.73	0	28	2:2	FFAC S
13715.7	9	20	1:0	FFAC S	15,492.84	9	20	1:0	FFAC S
13715.8	1P	30	0:0	JABC S	15,492.95	1P	30	0:0	JABC S
13715.9	0	10	7:8	DAAA T	15,493.06	0	10	7:8	DAAA T
13716.0	0	20	0:0	JABC S	15,493.17	0	20	0:0	JABC S
13716.1	1	40	0:0	JABC S	15,493.28	1	40	0:0	JABC S
13716.2	1	40	0:0	JABC S	15,493.39	1	40	0:0	JABC S
13716.3	1	40	0:0	JABC S	15,493.50	1	40	0:0	JABC S
13716.4	1	40	0:0	JABC S	15,493.61	1	40	0:0	JABC S
13716.5	2A	30	1:0	FFAC S	15,493.72	2A	30	1:0	FFAC S
13716.6	2A	30	1:0	FFAC S	15,493.83	2A	30	1:0	FFAC S
13716.7	1A	40	1:0	FFAC S	15,493.94	1A	40	1:0	FFAC S
13716.8	1A	40	1:0	FFAC S	15,494.05	1A	40	1:0	FFAC S
13716.9	1	20	0:0	JABC S	15,494.16	1	20	0:0	JABC S
13717.0	1	38	0:0	JABC S	15,494.27	1	38	0:0	JABC S
13717.1	0	10	0:0	JABC S	15,494.38	0	10	0:0	JABC S
13717.2	1A	10	1:1	JABC S	15,494.49	1A	10	1:1	JABC S
13717.3	1A	70	3:3	FFAC S	15,494.60	1A	70	3:3	FFAC S
13717.4	1A	70	3:3	FFAC S	15,494.71	1A	70	3:3	FFAC S
13717.5	7	70	3:3	FFAC S	15,494.82	7	70	3:3	FFAC S
13717.6	7	70	3:3	FFAC S	15,494.93	7	70	3:3	FFAC S